UNIVERSITY OF CALIFORNIA SAN DIEGO

Phylogenetic and Mitogenomic Insights of Acrocirridae (Cirratuliformia; Annelida): A Trans-Pacific Range Extension, New Genus, and Four New Species

A Thesis submitted in partial satisfaction of the requirements
for the degree Master of Science

in

Marine Biology

by

Paul Proctor

Committee in charge:

Professor Greg Rouse, Chair
Professor Ron Burton
Professor Moira Decima

2023

The Thesis of Paul Proctor is approved, and it is acceptable in quality and form for publication on microfilm and electronically.

University of California San Diego

2023

DEDICATION

This thesis is dedicated to my partner, Ethan Quick, for his unwavering source of support and love. Your belief in me and constant encouragement have been the driving force behind the completion of this thesis. Your patience and understanding have carried me through many challenges, and I am eternally grateful.

To my parents and sisters, your belief in my abilities and relentless support have helped me along my journey. Thank you for instilling in me the values of hard work and perseverance, and for pushing me to pursue academic endeavors.

To my incredible lab mates, Eesha Rangani, Kiirah Green, Gabriella Burman, Sonja Huč, Tiffany Wong, Marina McCowin, and Avery Hiley whose camaraderie, guidance, and friendship have been invaluable. Your expertise, collaboration, and support have fueled my passion for research. Together, we faced challenges, celebrated breakthroughs, and formed a bond extending outside the lab.

This thesis is dedicated to each of you for your belief in my capabilities, your encouragement, and endless support in my pursuit of a master's degree. Your presence in my life has been a constant reminder of the power of love, friendship, and family. I am truly grateful for all the contributions which have shaped the person and researcher I have become.

TABLE OF CONTENTS

LIST OF FIGURES

LIST OF TABLES

ACKNOWLEDGEMENTS

I would like to acknowledge my advisor and chair of my committee, Professor Greg Rouse, for his guidance and expert knowledge and passion for pelagic acrocirrids.

I would also like to acknowledge my committee: Professor Ron Burton and Professor Moira Decima for their guidance.

Thanks to all my co-authors and lab members who collected and sequenced samples and helped write and edit the publications that will come out of my thesis: Greg Rouse, Avery Hiley, Nerida Wilson, Andrew Hosie, and Ana Hara.

Thank you to Charlotte Seid for helping me to access specimens from the Benthic Invertebrate Collection, as well as being a constant resource to exchange ideas.

Many thanks to Avery Hiley, Marina McCowin, and Sonja Huč for training me on lab logistics, sequencing techniques, and bioinformatics.

Thank you to my partner, Ethan Quick, and my parents for supporting me through graduate school.

Finally, thank you to the members of the Rouse Lab for their advice and friendship through the graduate process.

Chapter 1 is currently being prepared for submission for publication of the material. Proctor, Paul P.; Wilson, Nerida; Hara, Ana; Hosie, Andrew; Rouse, Greg W. The thesis author was the primary investigator and author of this material.

Chapter 2 is currently being prepared for submission for publication of the material. Proctor, Paul P.; Hiley, Avery S.; Rouse, Greg W. The thesis author was the primary investigator and author of this material.

VITA

2019 Bachelor of Science in Biology, Indiana University

2019 Bachelor of Science in Animal Behavior, Indiana University

2023 Master of Science in Marine Biology, University of California San Diego

ABSTRACT OF THE THESIS

Phylogenetic and Mitogenomic Insights of Acrocirridae (Cirratuliformia; Annelida): A Trans-Pacific Range Extension, New Genus, and Four New Species

by

Paul Proctor

Master of Science in Marine Biology

University of California San Diego, 2023

Professor Greg Rouse, Chair

Understanding the diversity, phylogenetic relationships, and evolutionary transitions within Acrocirridae, a clade of polychaete worms, is crucial for unraveling the complexities of benthic-pelagic evolutionary transitions in marine ecosystems. In this study, we describe four new species, erect a new genus to accommodate two of these species, and provide an updated phylogeny for Acrocirridae. Additionally, we assemble complete mitogenomes and present the

first mitogenome phylogeny for the broader Cirratuliformia, offering valuable insights into the genetic characteristics and evolutionary history of benthic and pelagic species. The new species described in this study significantly contribute to the known diversity within Acrocirridae. Furthermore, the establishment of a new genus highlights the importance of taxonomic revisions in capturing the true evolutionary relationships and diversification patterns within this clade. Our updated phylogeny for Acrocirridae incorporates both morphological and molecular data, providing a comprehensive understanding of relationships. By assembling complete mitogenomes, we unravel the genetic composition and mitochondrial gene arrangement of key taxa within Cirratuliformia. This dataset serves as a valuable resource for future studies investigating the genomic features and evolutionary dynamics within this group of polychaetes. Importantly, our mitogenome-based phylogeny reveals variation in gene arrangements and codon usage. Overall, this study provides a comprehensive investigation of the diversity, phylogeny, and evolutionary transitions within Acrocirridae. Our findings enhance our understanding of the genetic and ecological factors driving benthic-pelagic transitions in polychaete evolution and provides a framework for future research.

CHAPTER 1: Phylogenetics and New Species Descriptions

INTRODUCTION

Acrocirridae Banse 1969 is a clade of polychaete worms comprising 10 genera with just over 40 known species (Rouse 2022). Cirratuliformia, a clade comprising Acrocirridae, Flabelligeridae de Saint-Joseph 1894, and Cirratulidae Ryckholt 1851, has limited DNA data. While a phylogenetic analysis of Acrocirridae and Flabelligeridae has provided support for their sister relationship, adding new DNA data aids in the phylogenetic resolution within Cirratuliformia and improves evolutionary hypotheses that can be drawn from cirratuliforms (Osborn & Rouse 2011). Some deep-sea genera within Acrocirridae lack DNA data and species with DNA data have had only five or fewer genes sequenced.

The ten current accepted genera of Acrocirridae are as follows: (1) *Acrocirrus* Grube, 1873 and (2) *Macrochaeta* Grube, 1850 introduced in 1969 followed by the transfer of (3) *Flabelligella* Hartman, 1965*,* (4) *Chauvinelia* Laubier, 1974*,* and (5) *Helmetophorus* Hartman, 1978 into Acrocirridae (Orensanz 1974; Averincev 1980; Glasby & Fauchald 1991). Then, (6) *Flabelligena* Gillet, 2001 was split from *Flabelligella,* and Salazar-Vallejo et al. 2007 transferred (7) *Flabelliseta* Hartman, 1965 into Acrocirridae. The newest member is (8) *Actaedrilus* Jimi, Fujimoto, & Imura 2020, collected off the coast of Japan. While all taxa mentioned up to this point are benthic, two deep-sea taxa noted above, *Chauvinelia* collected by epibenthic dredge from the Gulf of Biscay (Spain) at 4455 meters and *Helmetophorus* collected by anchor dredge from the Weddell Sea (Antarctica) at 3111 meters (Laubier 1974; Hartman 1978), have been speculated to be pelagic due to their overall body plan and distinct chaetae with potential swimming capability (Averincev 1980; Kirkegaard 1982; Salazar-Vallejo et al. 2007). These putative swimmers have morphological descriptions, but the dredging method of collection

provided specimens in suboptimal condition. Pelagic organisms are often fragile, so key features may have been lost or rendered difficult to recognize. Additionally, *Chauvinelia* and *Helmetophorus* lack genetic data that could support their phylogenetic relationship within Acrocirridae (Osborn et al. 2011b).

In recent years, expeditions off California (USA) and the Philippines collected deep-sea, swimming acrocirrids later shown to represent a clade consisting of (9) *Swima* Osborn, Haddock, Pleijel, Madin, & Rouse 2009, (10) *Teuthidodrilus* Osborn, Madin, & Rouse 2011, and two yet-to-be-described genera. Remotely operated vehicle (ROV) recordings of these animals *in situ* have revealed a peculiar swimming behavior through a form of chaetae undulation providing direct evidence of pelagic members in Acrocirridae, the central focus of this thesis (Osborn et al. 2009; Osborn et al. 2011b).

Teuthidodrilus, a monotypic swimming genus collected from the Celebes Sea (Philippines), is slightly larger than *Swima* with a darkly pigmented body surrounded by a thin gelatinous sheath penetrated by clavate papillae. Their head possess a pair of grooved palps longer than the body, eight filamentous branchiae equal to the body length, and branched nuchal organs between the palps and branchiae (Osborn et al. 2011a). *Teuthidodrilus* swims with paddle-like chaetae and is found ~100 meters from the seafloor. *Teuthidodrilus samae* Osborn, Madin, & Rouse 2011 is the only described species of this genus.

Swima, the other pelagic genus, has a transparent body surrounded by a thick gelatinous sheath penetrated by long, clavate papillae (Osborn et al. 2011b). Additionally, they possess four pairs of elliptical "bomb" organs that can be dropped to release green bioluminescence and are homologous to the segmental branchiae of their benthic relatives (Osborn et al. 2011b). *Swima bombiviridis* Osborn, Haddock, Pleijel, Madin, & Rouse 2009 is the first described species of

this genus from Monterey Canyon (Monterey Bay, CA, USA), followed by *Swima fulgida* Osborn, Haddock, & Rouse 2011 and *Swima tawitawiensis* Osborn, Haddock, & Rouse 2011, collected from Monterey Canyon (CA, USA) and Celebes Sea (Philippines), respectively (Osborn et al. 2009; Osborn et al. 2011b). *Swima* is found neutrally buoyant or actively swimming in the mesopelagic more than 400 meters above the seafloor propelling their bodies with fans of long chaetae (Osborn et al. 2011b). Additional swimming species, such as the Tiburon Bomber, Horned Bomber, and Juanita Worm, were scored for morphology and had DNA sequenced but remained undescribed (Osborn & Rouse 2011). *Swima* is not rare in the deep, seen on more than half the MBARI ROV dives to sufficient depth since 2001 (Osborn et al. 2011b). This point is further underscored by the discovery and collection of new species of *Swima* and other swimming acrocirrids from Western Australia presented in this study.

Recent expeditions to the Galápagos Rift and the deep-sea canyons off the West Coast of Australia led to the collection of fourteen additional swimming acrocirrid specimens. This provides an opportunity to extend the geographical range of existing species and improve the resolution of relationships within Acrocirridae by sequencing new species' nuclear and mitochondrial genes and describing their morphology. Further, this study adds to the known diversity of acrocirrids, specifically pelagic acrocirrids, and builds on the ecological diversity of understudied deep-sea annelids.

MATERIALS AND METHODS

Sample Collection

Sample collection took place in the deep-sea canyons of Western Australia during research cruises using R/V *Falkor* with ROV *SuBastian* in 2020, while additional samples were

collected from a research cruise to the Galapagos Rift using E/V *Nautilus* with ROV *Little Hercules* in 2015 (Table 1.1). Samples were fixed and stored in 95% ethanol or 10% formalin in seawater and rinsed and preserved in 50% ethanol. Live specimens were photographed with a Canon EOS M5, Olympus Corporation TG-5, or Olympus Corporation E-M5MarkII digital camera. Acrocirrid specimens were collected from the Galápagos Rift off Ecuador and the following canyons off Western Australia: Hood Canyon, Perth Canyon, Cape Range Canyon, and Cloates Canyon, shown in Figure 1.1. Holotypes, paratypes, and additional material were deposited at the Western Australia Museum Worms Collection (WAM:VER) Welshpool DC, Western Australia, Australia and the Museum of Comparative Zoology, Department of Invertebrate Zoology (MCZ:IZ) at Harvard University, Cambridge, MA, USA.

Morphological Analyses

Preserved specimens were observed and imaged using stereomicroscopy (Leica MZ12.5 and Canon RebelT6s camera), compound light microscopy (Leica DMR and Canon RebelT5i), and scanning electron microscopy (SEM) using Zeiss EVO10. Parapodia were mounted on slides permanently using 'Aquamount'® Thermo Fisher Scientific (Waltham, MA). For SEM preparation, specimens were dehydrated through an ethanol series, transferred to Hexamethyldisilazane (HMDS), and air-dried for at least 12 hours. Dried specimens were mounted on aluminum stubs with double-sided carbon adhesive tape and sputter-coated with gold-palladium (Au-Pd). A 28-character morphology matrix was used to compare the relationships of the new taxa to acrocirrids and flabelligerids with and without published DNA data (Table 1.2). These characters, listed in Table 1.3, were modified from Osborn & Rouse

2011, and they were coded from the type material when possible or from paratypes, original descriptions, or revisions.

DNA Extraction and Amplification

DNA was extracted from subsampled tissues in 95% ethanol with the Zymo Research DNA-Tissue Miniprep or Microprep kits (Irvine, California, USA), depending on tissue size, using the manufacturer's protocol. All specimens collected were sequenced for *cytochrome c oxidase subunit I* (*COI*), except WAM:VER:9621, which was fixed in formalin only. One representative of each new species was sequenced for four other genes, mitochondrial *cytochrome b* (*CYTB*) and *16S rRNA* (*16S*) and nuclear *18S rRNA* (*18S*) and *28S rRNA* (*28S*).

DNA sequences for *COI*, *CYTB*, *16S*, *18S*, and *28S* were amplified using primers as shown in Table 1.4. PCR amplification was carried out with 12.5 µl Apex 2.0 Taq Red DNA Polymerase Master Mix (Genesee Scientific, San Diego, California, USA) or 12.5 µl Conquest PCR 2.0x Master Mix 1 (Lamda Biotech, Ballwin, Missouri, USA), 1 µl each of the appropriate forward and reverse primers (10 µM), 8.5 µl ddH_2O, and 2 µl eluted DNA.

Amplification was performed using thermal cyclers (Eppendorf, Hamburg, Germany) under the following thermal profiles (Table 1.4): *COI* was amplified up to 683 base pairs using polyLCO/polyHCO (Carr et al. 2011) by initial denaturation at 95°C (3 minutes), followed by 40 cycles of denaturation at 95°C (40 seconds), annealing at 42°C (45 seconds), elongation at 72°C (50 seconds), and final extension at 72°C (5 minutes) or using LCO1490/HCO2198 (Folmer et al. 1994) by initial denaturation at 94°C (3 minutes), followed by 5 cycles of denaturation at 94°C (30 seconds), annealing at 47°C (45 seconds), elongation at 72°C (60 seconds), followed by 30 cycles of denaturation at 94°C (30 seconds), annealing at 52°C (45 seconds), elongation at

72°C (60 seconds), and final extension at 72°C (5 minutes). *CYTB* was amplified up to 394 base pairs using CytB424F/CytB876R (present study) by initial denaturation at 94°C (2 minutes), followed by 35 cycles of denaturation at 94°C (30 seconds), annealing at 45°C (1 minute), elongation at 68°C (1 minute), and final extension at 68°C (7 minutes). Up to 512 base pairs were amplified for *16S* was amplified using 16SarL/16SbrH (Palumbi et al. 1996) by initial denaturation at 95°C (3 minutes), followed by 35 cycles of denaturation at 95°C (40 seconds), annealing at 50°C (40 seconds), elongation at 72°C (50 seconds), and final extension at 72°C (5 minutes). *18S* was amplified up to 1,850 base pairs using three primer pairs: 18S-1F/18S-5R (Giribet et al. 1996) and 18S-a2.0/18S-9R (Giribet et al. 1996; Whiting et al. 1997) by initial denaturation at 95°C (3 minutes), followed by 40 cycles of denaturation at 95°C (30 seconds), annealing at 50°C (30 seconds), elongation at 72°C (90 seconds), and final extension at 72°C (8 minutes); 18S-3F/18S-bi (Giribet et al. 1996; Whiting et al. 1997) by initial denaturation at 95°C (3 minutes), followed by 40 cycles of denaturation at 95°C (30 seconds), annealing at 52°C (30 seconds), elongation at 72°C (90 seconds), and final extension at 72°C (8 minutes). *28S* was amplified up to 1,106 base pairs using Po28F1/Po28R4 (Struck et al. 2006) by initial denaturation at 95°C (3 minutes), followed by 40 cycles of denaturation at 95°C (30 seconds), annealing at 55°C (40 seconds), elongation at 72°C (75 seconds), and final extension at 72°C (5 minutes). PCR products were purified using Exo-SAP-IT with the manufacturer's protocol (USB, Affymetrix, Ohio, USA).

Sanger Sequencing

Sanger sequencing was performed by Eurofins Genomics (Louisville, KY, USA). Consensus sequences were assembled using the "De Novo Assembly" option under default

settings using Geneious v.11.0.14 (Kearse et al. 2012). Complete *COI*, *CYTB*, and *16S* sequences from assembled mitogenomes, see Chapter 2: Materials and Methods, were used when available for a complete evidence approach. Nuclear genes for *Acrocirrus validus* (*28S*)*, Macrochaeta pege* (*18S, 28S*)*, Macrochaeta* cf. *westheidei* (*28S*)*, Flabesymbios commensalis* (*28S*), and *Flabelligella macrochaeta* (*18S, 28S*) were assembled in Geneious using genome skimming data from Chapter 2. MitoBIM v.1.9.1 (Hahn et al. 2013) was used to interleave forward and reverse reads, then minimap2 (Li 2018) and samtools (Danecek et al. 2021) were used to align, and map reads to a list of reference *18S* or *28S* genes from close relatives to assemble a high-quality consensus sequence in Geneious. All sequences generated for this study were deposited in GenBank (Bethesda, Maryland, USA) (Table 1.5).

Phylogenetic analyses

A representative sequence for all published swimming acrocirrids, the new species of acrocirrids, and closely related benthic genera were included in the analysis (Table 1.5). Four members of Flabelligeridae, the sister family to Acrocirridae, were chosen as outgroup representatives (Osborn & Rouse 2011). Individual genes were aligned in Mesquite v.3.8 (Maddison & Maddison 2023) using Muscle (Edgar 2004) with default settings for *COI* and *CYTB* and MAFFT (Katoh & Standley 2013) with default settings for the rRNA genes. Two concatenations were performed using SequenceMatrix (Vaidya et al. 2011): one with the five gene partitions and one with the five genes and 28-character morphology matrix. A maximum likelihood (ML) analysis was run with RAxML-NG (Kozlov et al. 2019) using RAxML GUI v.2.0 (Edler et al. 2020) on the five gene concatenated dataset. Optimal models were chosen for each partition using the RAxML GUI interface as follows based on Akaike Information Criterion

corrected (AICc): *COI* = TIM2+G4, *CYTB* = GTR+I+G4, *16S* = TIM2+I+G4, *18S* = GTR+I+G4, and *28S* = TIM3+G4. Node support was assessed through bootstrapping with 1000 pseudoreplicates.

Bayesian analyses were conducted on both the five gene concatenated dataset and the five gene with morphological characters dataset using mrBayes v.3.2.7 (Ronquist et al. 2012) with models chosen using jModelTest v.2.1.10 (Darriba et al. 2012; Guindon & Gascuel 2003) according to AIC criterion. GTR+I+G was the optimal model for all genes. Morphological characters were given a variable rate of evolution under the gamma model. Partitions were unlinked in the analysis. Each Markov Chain, three heated and one cold, was started from a random tree and ran simultaneously for 40000000 generations with trees sampled every 1000 generations. Tracer v.1.7.2 (Rambaut et al. 2018) was used to check for convergence, stationarity, and decide the burnin of 10%. Support was assessed through posterior probabilities generated through the Markov chain Monte Carlo (MCMC) method.

Maximum parsimony (MP) analyses were run on the morphological character matrix and the two concatenated datasets with PAUP* v.4.0a168 (Swofford 2002) using an equally weighted character matrix, heuristic search option, branch swapping algorithm, and 100 random addition replicates. Bootstrap values were obtained with the same settings and 100 replicates. All trees generated by these analyses were visualized using FigTree (Rambaut 2009) and enhanced in Adobe Illustrator (Adobe Inc. 2019). Interspecific and intraspecific pairwise distances were calculated in PAUP* v.4.0a168 (Swofford 2002) using untrimmed *COI* alignments (Table 1.6). TCS haplotype networks (Clement et al. 2000) were constructed using PopArt (Leigh & Bryant 2015) using untrimmed *COI* alignments.

RESULTS

Range Extensions

Teuthidodrilus samae Osborn, Madin, & Rouse 2011

Type Locality.

Specimens known only from the Celebes Sea, Philippines between 2000-2800 meters (Osborn et al. 2011a). Holotype NMA:04342 (GenBank Accession# FJ944537).

New Specimens.

Galápagos Rift, Ecuador at 2555 meters. Paratypes MCZ:IZ:70186 (GenBank# OQ716777) and MCZ:IZ:70357 (GenBank# OQ716778).

Remarks.

A new Eastern Pacific record indicating a trans-Pacific distribution with a distance just over 17000 kilometers. Specimens were found at a depth range consistent with holotype and previous paratype depths. Specimens found within ~100 meters of the seafloor and had four pairs of elongate branchiae, a pair of body length palps, and branched nuchal organs consistent with the diagnosis of *Teuthidodrilus samae* (Figure 1.2A-B). *COI* sequences revealed two unique haplotypes, including the holotype, with a maximum intraspecific pairwise distance of 0.01% (Table 1.6, Figure 1.3).

Swima tawitawiensis Osborn, Haddock, & Rouse 2011

Type Locality.

Specimens known only from the Celebes Sea, Philippines at ~2800 meters (Osborn et al. 2011b). Holotype NMA:04327 (GenBank# FJ944533).

New Specimens.

Cloates and Cape Range Canyon, Western Australia at ~2500 meters. Paratypes WAM:VER:V9874 (GenBank# OQ716775) and WAM:VER:V9829 (GenBank# OQ716776).

Remarks. A new Northwest Australia record indicating a range extension from the Pacific Ocean in the Philippines to the Indian Ocean off Australia, just over 3,000 kilometers. Specimens found actively swimming over 400 meters above the seafloor. Each had three subulate branchiae, with one positioned medially, in a single row behind a U-shaped nuchal organ. Specimens had four pairs of elliptical branchiae with two pairs located on the achaetonous region consistent with the diagnosis of *Swima tawitawiensis* (Figure 1.2C-D). *COI* sequences revealed three unique haplotypes, including the holotype, with a maximum intraspecific pairwise distance of 0.00% (Table 1.6, Figure 1.4).

Systematics

Teuthidodrilus Osborn, Madin, & Rouse 2011

Type species: *Teuthidodrilus samae* Osborn, Madin, & Rouse 2011

Diagnosis (emended).

A member of Acrocirridae having a pair of grooved palps longer than body length. Branchial membrane dorsal, with four pairs of elongate, tapered branchiae equal in length to the body. Nuchal organs as ciliated ridge continuous on five to six pairs of free-standing, oppositely branched structures. Neuropodia contain two to four simple chaetae, which are flattened in the distal three-quarters. Prominent notopodial lobes contain 50 or more simple, flattened, concavo-convex chaetae that taper abruptly at the tip forming a fine point. All chaetae with fine rings of tiny spines, most obvious at distal tips. First chaetiger with reduced number of chaetae, and no

obvious achaetonous anterior segments. Adults with 25 or more chaetigers. Papillae small, clavate, reduced to a small longitudinal row between noto- and neuropodial lobes and possibly a single lateral row on ventrum of each segment. Gonopores as broad or digitate papillae immediately ventral to neuropodia on the second, third, and possibly fourth chaetigers. Body wall darkly pigmented and gelatinous sheath thin

Remarks.

Changes to the diagnosis involve including five pairs of nuchal organs as a variant to the number of pairs of nuchal organs. Individual branching is difficult to determine in this genus and more care should be taken into understanding the variability of these structures. Additionally, rows of papillae on the ventrum are variable as they are not found in *Teuthidodrilus australis* n. sp. as the papillae are restricted to the parapodial lobes only. Finally, gonopores are digitate papillae and found on chaetigers 2-4 in *Teuthidodrilus australis* n. sp.; *Teuthidodrilus* diagnosis is emended to reflect this change.

Teuthidodrilus australis n. sp.

Figure 1.5

Material examined.

Holotype: WAM:VER:V9804 (GenBank# OQ784049 (*COI*), OQ807205 (Whole mitochondrion), OQ724829 (*18S*), OQ724825 (*28S*). Paratypes: WAM:VER:V9805 (GenBank# OQ784048 (*COI*)), WAM:VER:V9831 (GenBank# OQ784047 (*COI*)), and WAM:VER:V9662 (GenBank# OQ784046 (*COI*)). Photographs of WAM:VER:V9831 and WAM:VER:V9662 not shown. All specimens fixed in 95% ethanol.

Diagnosis and description.

Teuthidodrilus australis n. sp. is between 72-100 mm long and has 28-29 chaetigers in adults, while the juvenile has 16 chaetigers and is about 21 mm in length. Body brownish purple in life with a thin gelatinous sheath showing clear distinct parapodia. Palps approximately body length located antero-dorsal to a dark buccal organ. Branchial membrane posterior to palps supports: five to six pairs of branched nuchal organs on a continuous, ciliated ridge, four pairs elongate branchiae in two rows, and a pair of nephridiopores as dark papillae lateral to anterior pair of branchiae (Figure 1.5D). Branchiae easily lost leaving large, circular scars, while palps not easily lost leaving jagged, elliptical scars (Figure 1.5B-D). Gonopores present as broad, digitate papillae on the neuropodia of chaetigers 2-4 and rows of papillae lacking on ventrum of segments as is present for *Teuthidodrilus samae* (Figure 1.5C, E). Biramous parapodia with a small bundle of simple neurochaetae (2 to 3) and a notochaetal fan consisting of broad, flat, notochaetae with a spinous distal tip (Figure 1.5F).

Distribution.

The holotype, WAM:VER:V9804, and two paratypes, WAM:VER:V9805 and WAM:VER:V9831, were collected between 2175-2525 meters in Cape Range Canyon of the northerly Ningaloo canyon system (Western Australia) (Figure 1.1). A single paratype, WAM:VER:V9662, was collected by ROV *SuBastian* at 1925 meters in Perth Canyon of the southerly Bremer canyon system (Western Australia) (Figure 1.1).

Etymology.

From the Latin root “auster” meaning “south” in the third-declension two-termination adjective in the singular genitive to mean “of the South” or may refer to “of Australia.”

Remarks.

Teuthidodrilus australis n. sp. belongs to the swimming clade of Acrocirridae with elongated branchiae and branched nuchal organs. Live specimens were observed and photographed following collection by ROV *SuBastian* (Figure 1.5B-C). The holotype, WAM:VER:V9804, was sequenced for *18S*, *28S*, *COI*, and the whole mitochondrial genome and each paratype was sequenced for *COI* only. *Teuthidodrilus australis* n. sp. had a 0.00% maximum intraspecific pairwise distance among the four sequences available (Table 1.6). The haplotype network for *Teuthidodrilus australis* n. sp. had two unique haplotypes, one of which is shared between the northern Cape Range Canyon and southern Perth canyon (Figure 1.6). *Teuthidodrilus australis* n. sp. was recovered as the sister species to *Teuthidodrilus samae* with 100% bootstrap support in the ML analysis and a posterior probability of 1.0 in the Bayesian analysis (Figure 1.7-1.8). *Teuthidodrilus australis* shares most morphological features with *Teuthidodrilus samae* including branchiae structure, nuchal organ position, and general body plan, but they differ by two observations. *Teuthidodrilus australis* lacks rows of papillae on the ventrum of anterior segments and has three finger-like gonopores on the neuropodia of chaetigers 2-4 (Figure 1.5C, E). Even with few morphological differences between the two, there is sufficient evidence supporting the designation as separate species as their minimum pairwise interspecific distance is 14.85% and the lowest observed interspecific distance between acrocirrids is approximately 13% (Table 1.6). Specimen WAM:VER:V9831 is the first juvenile of this genus to be collected. ROV *SuBastian* footage has offered key insight into the benthopelagic natural history of *Teuthidodrilus*. Footage from paratype, WAM:VER:V9662, in Perth Canyon showed *Teuthidodrilus australis* n. sp. actively swimming in the water column, while video evidence collected from Cape Range Canyon showed the worm hovering near the

seafloor with its palps full of sediment providing direct evidence for deposit feeding that had been suggested previously from sediment gut contents (Figure 1.5A) (Osborn et al. 2011a, supplement).

Swima osbornae n. sp.

Figure 1.9

Material examined.

Holotype: WAM:VER:V9872 (GenBank# OQ713623 (*COI*)). Paratypes: WAM:VER:V9873 (GenBank# OQ713622 (*COI*)) and WAM:VER:V9876 (GenBank# OQ713624 (*COI*), OQ718583 (*CYTB*), OQ722175 (*16S*), OQ724827 (*18S*), and OQ724823 (*28S*)). All specimens preserved in 95% ethanol.

Diagnosis and description.

Swima osbornae n. sp. holotype is approximately 20 mm in length. Body is transparent with a thick gelatinous sheath. There is a pair of grooved palps antero-dorsal to a muscular buccal organ (Figure 1.9C). Only two pairs of elliptical branchiae noted with one shown as a circular scar (Figure 1.9C). A single, medial subulate branchiae is present immediately posterior to palps on a simple nuchal organ (Figure 1.9B). Anterior and mid-gut darkly pigmented with the former appearing black in both the fixed and live specimens and the latter reddish-brown in live specimens (Figure 1.9B). Notopodia and neuropodia smooth and continuous with lollipop-shaped papillae between lobes (Figure 1.9D) with long (5 mm), simple chaetae with dehiscent scales found on neuro- and notochaetae distal tips in organized rows (Figure 1.9E-F).

Distribution.

The holotype, WAM:VER:V9872, and both paratypes, WAM:VER:V9873 and WAM:VER:V9876, were collected by ROV *SuBastian* at 2600 meters known only from Cloates Canyon (North Ningaloo canyon system, Western Australia) (Figure 1.1).

Etymology.

Swima osbornae n. sp. is named in appreciation for Dr. Karen Osborn, an invertebrate zoologist and curator at the National Museum of Natural History, whose postdoctoral work at Scripps Institution of Oceanography describing *Swima* laid the groundwork for the study of pelagic acrocirrids. Latin feminine ending -ae.

Remarks.

Swima osbornae n. sp. is a part of the *Swima* clade of pelagic acrocirrids which have at least one subulate branchiae positioned medially. The paratype, WAM:VER:V9876, was sequenced for *16S*, *18S*, *28S*, *COI*, and *CYTB* and the others were sequenced for *COI* only. All three available *Swima osbornae* n. sp. *COI* sequences were identical, a 0.00% maximum pairwise intraspecific distance (Table 1.6). The nearest relative was *Swima fulgida*, a bomber worm collected from 3300 meters in Monterey Canyon (Monterey Bay, CA, USA) with which it shares a dark anterior gut, although the dark gut may extend further in *Swima osbornae* n. sp. The minimum pairwise interspecific distance between these two was 13.45% (Table 1.6), which is just above the minimum interspecific distance observed within acrocirrids (13%). Large clutches of oocytes were present in all three specimens (Figure 1.9B). All specimens showed artifacts of fixation or damage upon collection making some key morphological features of *Swima* difficult to distinguish such as the positions of the elliptical, bioluminescent branchiae. Two pairs were located on the achaetonous region, but the presence of the two segmental pairs

found in neighboring species were not confirmed. Although key morphological features of *Swima* were difficult to confirm and no obvious apomorphies were found, DNA evidence supported its inclusion in *Swima* and delineation as a separate species from both *Swima fulgida* and *Swima bombiviridis* as well as the more distantly related *Swima tawitawiensis* (Table 1.6; Figure 1.7-1.8). Additionally, ROV *SuBastian* footage showed an identical body plan to *Swima* and the same form of chaetae undulation swimming and neutral buoyancy behavior of *Swima* (Figure 1.9A).

Paraswima n. gen.

Type species: *Paraswima sonjae* n. gen. n. sp.

Diagnosis.

Swimming acrocirrids with more than 30 chaetae per parapodium. Eyes absent and head not retractable. Thin gelatinous sheath penetrated by clavate papillae. Two pairs of grooved palps with nuchal organs immediately posterior as convoluted, ciliated ridges. Subulate branchiae found in pairs and positioned in rows on head. Anterior achaetonous segments support four pairs of bioluminescent, elliptical branchiae or large branchiae more than half body length at widest. Subulate branchiae not easily lost, while main branchiae are lost easily leaving circular scars. Parapodial lobes obvious with two or more lollipop-shaped interramal papillae. Notochaetae simple, while neurochaetae are compound with a simple, 'blade-like' distal element.

Etymology.

Paraswima is a Latin combination of the preposition "para" meaning near and "swima" an arbitrary combination of letters with the feminine ending -a. Named for the sister relationship and morphological similarity to *Swima.*

Remarks.

Paraswima n. gen. shared achaetonous anterior segments, prostomium shape, four pairs of dehiscent branchiae, and simple, spinous notochaetae with Acrocirridae. *Paraswima* n. gen. differed from benthic acrocirrids by overall body form, lack of eyes, large bundles of chaetae, and presence of notochaetae. The genus was most like *Swima* with which it shares swimming behavior, structure of the buccal organ, and lollipop-shaped interramal papillae and potentially *Helmetophorus* and *Chauvinelia* with which it shares a similar structure to the buccal organ and potentially the ability to swim. *Paraswima* n. gen. differed from these three genera by having subulate branchiae in pairs and main branchiae only present on achaetonous segments. *Paraswima* n. gen. further differed from *Helmetophorus* and *Chauvinelia* by possessing over 30 chaetae per parapodium and a larger body size. *Paraswima* n. gen. formed a well-supported clade distinct from all other acrocirrids (Figure 1.7-1.8). Analyses excluding species with no genetic data (Figure 1.7) placed *Paraswima* sister to *Swima* with high bootstrap support 79% (1.0 in Bayesian analysis).

Paraswima sonjae n. gen. n. sp.

Figure 1.10

Material examined.

Holotype: WAM:VER V9877 (GenBank# OQ713620 (*COI*), OQ718584 (*CYTB*), OQ722174 (*16S*), OQ724828 (*18S*), OQ724824 (*28S*)). Paratype: WAM:VER:V9878 (GenBank# OQ713621 (*COI*)). Photos of paratype WAM:VER:V9878 are not shown. Both specimens preserved in 95% ethanol.

Diagnosis and description.

Paraswima sonjae n. gen. n. sp. is 55 mm long and has 33 chaetigers. Body light beige *in situ* with a thin gelatinous sheath that obscures internal features (Figure 1.10C). Mid-body enlarged and tapers narrowly at both ends. Pair of grooved palps antero-dorsal to buccal organ, which has a reddish-brown color (Figure 1.10A). Brachial membrane posterior to palps supports digitiform branchiae laterally, a single pair of subulate branchiae evenly spaced in a row behind a convoluted, ciliated nuchal organ (Figure 1.10D). Achaetonous anterior region narrow and muscular supporting four pairs of small, elliptical branchiae (Figure 1.10A-B). A distinct red color is obvious throughout the digestive tract including the buccal organ, pharynx, midgut, anus, and possibly outside the digestive tract on the branchial membrane as well, although the color may be slightly different here appearing browner (Figure 1.10A-B). Biramous parapodia with fans of numerous, 30 or more, long chaetae with three or more lollipop-shaped papillae between lobes (Figure 1.10E). Notochaetae simple, broad, and flat, and neurochaetae compound with a simple, "blade-like" distal tip (Figure 1.10E-F).

Distribution.

Known only from Cloates Canyon (North Ningaloo canyon system, Western Australia) at 3400 meters (Figure 1.1).

Etymology.

Paraswima sonjae n. gen. n. sp. was named for Sonja Huč, a master's graduate of the Rouse lab, with the Latin feminine ending -ae.

Remarks.

Paraswima sonjae n. gen. n. sp. belonged to a clade sister to *Swima* with paired subulate branchiae arranged in rows and main branchiae located only on the achaetonous region. The

holotype, WAM:VER:V9877, was sequenced for *16S*, *18S*, *28S*, *COI*, and *CYTB* and the paratype, WAM:VER:V9878, was sequenced for *COI* only. The maximum pairwise intraspecific distance between the holotype and paratype was 0.00% (Table 1.6). *Paraswima sonjae* n. gen. n. sp. was recovered as the sister species of the undescribed Tiburon bomber, a bomber worm with paired subulate branchiae collected from Juan de Fuca Ridge (USA) at 2400 meters, with high bootstrap support of 80% and posterior probability of 1.0 (Figure 1.7). The minimum pairwise interspecific distance between the Tiburon bomber and *Paraswima sonjae* n. gen. n. sp. was 15.83% (Table 1.6) which is above the minimum interspecific distance we observe in Acrocirridae (13%). The main branchiae of this species was more like *Swima* than the other members of the *Paraswima* clade in that they were small and elliptical, though it cannot be ruled out that these "bomb" organs may have been in the middle of regenerating. *Paraswima sonjae* n. gen. n. sp. differed from *Swima* in that all four pairs of main branchiae were positioned in the achaetonous region and the subulate branchiae were arranged in pairs. ROV *SuBastian* footage showed the benthopelagic lifestyle of this species swimming within a couple hundred meters from the seafloor unlike *Swima* which is more mesopelagic found more than 400 meters above the seafloor (Figure 1.10C).

Paraswima ethanquicki n. gen. n. sp.

Figure 1.11

Material examined.

Holotype: WAM:VER:V9620 (GenBank# OQ713618 (*COI*), OQ718582 (*CYTB*), OQ722173 (*16S*), OQ724826 (*18S*), OQ724822 (*28S*)). Paratypes: WAM:VER:V9621 (no DNA)

and WAM:VER:V9663 (GenBank# OQ713619 (*COI*)). Specimens fixed in 95% ethanol except WAM:VER:V9621 fixed in formalin.

Diagnosis and description.

Paraswima ethanquicki n. gen. n. sp. holotype is 25 mm long and has 29 chaetigers. Body transparent with a thin gelatinous sheath obscuring internal features (Figure 1.11A-B). Two pairs of grooved palps antero-dorsal to a buccal organ that is darker than the surrounding body (Figure 1.11A-B, D). Branchial membrane supports three pairs of subulate branchiae in two rows behind a convoluted nuchal organ (Figure 1.11B, D). Muscular achaetonous region truncated or fused supporting four pairs of large, elliptical branchiae with length at least half body width at widest part (Figure 1.11D). Parapodia biramous with fans of numerous, more than 30, long chaetae and 3 or more lollipop-shaped papillae in between the lobes (Figure 1.11E). Notochaetae simple, broad, and flat, while neurochaetae are compound with a simple, "blade-like" distal tip (Figure 1.11E-F).

Distribution.

Known only from Hood Canyon (South Bremer canyon system, Western Australia) at 1550 meters (Figure 1.1).

Etymology.

Paraswima ethanquicki n. gen. n. sp. was named for Mr. Proctor's partner, Ethan Quick, with the Latin masculine ending -i.

Remarks.

Paraswima ethanquicki n. gen. n. sp. belonged to a clade sister to *Swima* with paired subulate branchiae arranged in rows and main branchiae located only on the achaetonous region. The holotype, WAM:VER:V9620, was sequenced for *16S*, *18S*, *28S*, *COI*, and *CYTB* and the

paratype, WAM:VER:V9663, was sequenced for *COI* only, while paratype WAM:VER:V9621 had no DNA sequenced and was used for morphological analysis only. *Paraswima ethanquicki* n. gen. n. sp. holotype and paratype, WAM:VER:V9663, had a maximum pairwise intraspecific distance of 0.01% (Table 1.6). *Paraswima ethanquicki* n. gen. n. sp. was recovered as the sister species of the undescribed Horned bomber, a bomber worm with paired subulate branchiae from Astoria Canyon (USA) at 1850 meters, with a high bootstrap support of 99% and posterior probability of 1.0 (Figure 1.7). The minimum pairwise interspecific distance between the undescribed Horned bomber and *Paraswima ethanquicki* n. gen. n. sp. was 16.58% (Table 1.6), well above the minimum expected interspecific distance for acrocirrids of 13%. ROV *SuBastian* footage showed a close interaction with the seafloor with a large gathering of worms in Hood canyon swimming just above the seafloor (Figure 1.11C). It was unclear if this large group is a mating event or a unique life history trait of *Paraswima ethanquicki* n. gen. n. sp.

DISCUSSION

The phylogenetic results of this study recovered the same swimming clade as Osborn & Rouse 2011. The position of the Juanita Worm was unstable when comparing the ML and Bayesian trees from this study with the Bayesian tree from Osborn & Rouse 2011. The Osborn & Rouse 2011 tree found the Juanita Worm sister to the other pelagic acrocirrids (1.0 posterior probability), the ML analysis of this study found the Juanita Worm sister to Teuthidodrilus but with low bootstrap support of 41% (Figure 1.7), and the Bayesian analysis including the morphological matrix found the Juanita Worm sister to a clade of *Chauvinelia*, *Helmetophorus*, *Paraswima* n. gen., and *Swima* with high support (0.74 posterior probability) (Figure 1.8). The tree also differed by the addition of *Actaedrilus yanbarensis, Macrochaeta pege,* and

Macrochaeta sp. from unpublished mitogenome data, note that data attributed to *Macrochaeta* sp. from Osborn & Rouse 2011 were changed to *Macrochaeta* cf. *westheidei* due to the sampling location and morphology aligning the specimen to *Macrochaeta westheidei*, an important distinction to avoid confusion with the unpublished mitogenome data under *Macrochaeta* sp. The analyses consistently recovered a clade, including the undescribed Horned and Tiburon bombers and two of the new species now placed in *Paraswima* n. gen. *Paraswima* n. gen. is like *Swima* sharing features such as swimming ability, elliptical segmental branchiae, and subulate branchiae but differ by the positioning of their subulate branchiae and location of the segmental branchiae. When taxa with no DNA data were included in the analysis, the tree topology was consistent with Osborn & Rouse 2011 except for the position of the clade consisting of *Helmetophorus* and *Chauvinelia*, which have character traits aligning them with members of Flabelligeridae such as the presence of a cephalic hood, *Swima* such as a medial, subulate branchiae, and *Paraswima* n. gen. such as short body papillae and a convoluted nuchal organ.

Osborn & Rouse 2011 found that *Chauvinelia* and *Helmetophorus* formed a clade with *Paraswima* with a posterior probability of 0.52, while the tree from this study finds that *Chauvinelia* and *Helmetophorus* formed a clade with *Swima* with similar support, 0.42. The Bayesian analysis reveals a clade that consists of *Paraswima* n. gen that has paired subulate branchiae and a clade that consists of *Swima*, *Chauvinelia*, and *Helmetophorus* that have at least one medial subulate branchiae (Figure 1.8). Morphology alone has provided unstable positions for *Chauvinelia* and *Helmetophorus*. Expeditions to the Arctic and Southern Oceans with the goal of collecting and extracting DNA from these taxa should be of top priority to resolve a stable position in the tree and draw more refined conclusions on the evolutionary history of these deep-sea acrocirrids.

This study represented the first record of swimming acrocirrids from the Indian Ocean off the Western coast of Australia. Additionally, the recovery of two new species into a clade with two undescribed swimming acrocirrids, the Tiburon Bomber and Horned Bomber, and the presence of *Chauvinelia* and *Helmetophorus* between this clade and *Swima,* provided sufficient evidence for the erection of a new genus, *Paraswima* n. gen. This new genus formally consists of *Paraswima sonjae* n. gen. n. sp. and *Paraswima ethanquicki* n. gen. n. sp. bringing the total number of described swimming acrocirrid genera to three. The addition of *Teuthidodrilus australis* n. sp. expanded the range of the previously monotypic *Teuthidodrilus* to include the deep-sea canyons of the Indian Ocean west of Australia, while the addition of *Swima osbornae* n. sp. expanded the range of *Swima* to include the deep-sea canyons of Northwest Australia. Given that *Swima bombiviridis* and *Swima fulgida* were discovered off California, over 14000 kilometers from Western Australia, were shown to be more closely related in the phylogeny to *Swima osbornae* n. sp. (Figure 1.7-1.8) than *Swima tawitawiensis* discovered off the Philippines, ~3000 kilometers from Western Australia, suggests that the connectivity of *Swima* likely includes other continental margins across the global ocean, which has profound implications for the biodiversity and evolutionary history of swimming annelids.

All three described swimming genera have large geographic ranges, and *Swima tawitawiensis* and *Teuthidodrilus samae* had high connectivity despite distances of over 3000 and 17000 kilometers, respectively. *Swima tawitawiensis* differed by two base pairs in *COI* between the Celebes Sea and Northwest Australia, and *Teuthidodrilus samae* differed by only five base pairs in *COI* between the Celebes Sea and the Galápagos Rift (Figure 1.3-1.4). This high level of connectivity suggests that deep-sea canyons across the globe should be a high priority for sampling. Describing new species and improving the ranges of existing swimming

annelids is an exciting avenue of continued research for understanding the high diversity of body plans and life history strategies in a family currently containing relatively few taxa. Additionally, this study provided evidence for habitat use and life history strategies for swimming acrocirrids.

Direct evidence of *Teuthidodrilus australis* n. sp. with palps full of sediment and *Paraswima* n. gen. associated within a couple of hundred meters of the seafloor underscored a benthopelagic lifestyle, while evidence of *Swima osbornae* n. sp. and *Swima tawitawiensis* neutrally buoyant or swimming in the water column more than 400 meters above the seafloor suggested a consistently pelagic lifestyle, which was additionally supported by past observations (Osborn et al. 2011b). These histories differ drastically from the life history strategies of their benthic acrocirrid relatives. These swimming worms were shown in a phylogenetic context to represent a third origin of pelagicism within Cirratuliformia, with *Flota* and *Poeobius*, two members of Flabelligeridae with drastic body plan changes from their benthic flabelligerid relatives, representing the other two independent origins (Osborn & Rouse 2008; Figure 1.7-1.8). Understanding how selective pressures such as deep-sea environments could have altered the genomes of these worms, particularly the mitogenome, may improve evolutionary explanations for body plan differences and habitat diversity that we see within Cirratuliformia, and that is the focus of Chapter 2.

Table 1.1: New specimens collected for this study with voucher, site, depth, and collection information. Holotype = *, Juvenile = ▲.

Species	Voucher	Site	Coordinates	Depth (m)	Date	Cruise & Dive	Collector/Identifier
Paraswima ethanquicki n. gen. n. sp.	WAM:VER:V9620*	Hood Canyon, Western Australia	34.743° S; 119.655° E	1550	1-2-20	FK200126 S0315	Hosie, A.M. & Hara, A.
	WAM:VER:V9621						
	WAM:VER:V9663						
Paraswima sonjae n. gen. n. sp.	WAM:VER:V9877*	Cloates Canyon, Western Australia	22.208° S; 112.599° E	3386	4-4-20	FK200308 S0350	Wilson, N.G. & Hosie, A.M.
	WAM:VER:V9878						
Swima osbornae n. sp.	WAM:VER:V9872*	Cloates Canyon, Western Australia	22.253° S; 112.892° E	2600	2-4-20	FK200308 S0349	Wilson, N.G. & Hosie, A.M.
	WAM:VER:V9873						
	WAM:VER:V9876						
Swima tawitawiensis	WAM:VER:V9829	Cape Range Canyon, Western Australia	21.844° S; 113.014° E	2496.5	3-15-20	FK200308 S0336	Rouse, G. & Wilson, N.G.
	WAM:VER:V9874	Cloates Canyon, Western Australia	22.253° S; 112.892° E	2480	2-4-20	FK200308 S0349	Wilson, N.G. & Hosie, A.M.
Teuthidodrilus australis n. sp.	WAM:VER:V9662	Perth Canyon, Western Australia	32.095° S; 114.864° E	1924.7	2-20-20	FK200126 S0328	Hosie, A.M. & Hara, A.
	WAM:VER:V9804*	Cape Range Canyon, Western Australia	21.942° S; 113.121° E	2175.7	3-14-20	FK200308 S0332	Rouse, G. & Wilson, N.G.
	WAM:VER:V9805						
	WAM:VER:V9831▲		21.830° S; 112.926° E	2525	3-16-20	FK200308 S0337	
Teuthidodrilus samae	MCZ:IZ:70186	Galápagos Rift, Ecuador	0.766° N; 85.899° W	2555	6-20-15	NA063 H1433	-
	MCZ:IZ:70357						

Table 1.2: Morphology matrix with characters described in Table 1.3.

Characters		**1**	**2**	**3**	**4**	**5**	**6**	**7**	**8**	**9**	**10**	**11**	**12**	**13**	**14**	**15**	**16**	**17**	**18**	**19**	**20**	**21**	**22**	**23**	**24**	**25**	**26**	**27**	**28**
Flabelligeridae	*Flabesymbios commensalis*	1	1	?	1	0	0	0	0	1	2	1	1	0	0	1	0	0	?	0	1	0	1	1	0	2	1	1	-
	Flota sp.	1	1	?	0	0	1	0	0	2	2	0	1	0	0	1	3	0	0	?	1	0	1	0	0	-	1	1	-
	Pherusa bengalensis	1	1	?	1	0	0	?	1	0	2	1	1	0	0	1	1	0	?	0	0	0	1	0	0	-	?	1	-
	Poeobius meseres	1	1	-	-	1	1	?	0	2	1	0	1	0	0	1	0	0	0	0	0	-	3	-	-	-	1	1	-
Acrocirridae	*Acrocirrus validus*	0	0	2	0	0	0	0	0	0	1	1	1	2	0	0	1	0	0	1	1	1	2	1	0	2	0	0	-
	Actaedrilus yanbarensis	0	0	3	0	1	0	-	0	0	3	0	0	-	0	0	3	0	1	1	0	1	2	1	0	2	?	?	-
	Chauvinelia arctica	0	1	5	0	0	0	1	0	2	1	0	1	2	1	0	3	?	?	?	1	?	2	1	0	0	1	1	1
	Flabelligella macrochaeta	1	0	1	0	1	0	1	1	0	1	0	?	?	0	0	3	0	1	1	0	0	1	1	0	2	0	?	-
	Flabelligena sp.	0	0	?	0	1	0	1	1	0	1	?	?	?	0	0	1	0	1	1	0	1	2	1	0	2	0	0	-
	Flabelliseta incrusta	0	0	?	0	1	0	1	1	2	1	?	?	?	0	0	3	0	?	?	0	1	2	1	0	0	?	?	-
	Helmetophorus rankini	0	1	?	0	0	0	1	0	0/1	1	0	1	2	1	0	3	1	?	?	1	1	2	0	0	-	?	?	1
	Horned Bomber	0	0	3	0	0	0	2	0	1	1	0	1	2	1	0	1	2	1	1	1	0	2	1	0	0	1	1	0
	Juanita Worm	0	0	3	0	0	0	2	0	0	1	0	3	2	0	0	1	0	?	0	1	0	2	1	0	1	1	1	-
	Macrochaeta cf. *westheidei*	0	0	2	0	0	0	1	1	0	1	1	1	?	0	0	1	0	1	1	0	1	2	1	0	2	0	0	-
	Macrochaeta clavicornis	0	0	2	0	0	0	1	1	0	1	1	1	?	0	0	1	0	1	1	0	1	2	1	0	2	0	0	-
	Macrochaeta pege	0	0	2	0	0	0	1	1	0	1	1	1	?	0	0	1	0	1	1	0	1	2	1	0	2	0	0	-
	Macrochaeta sp.	0	0	2	0	0	0	1	1	0	1	1	1	?	0	0	1	0	1	1	0	1	2	1	0	2	0	0	-
	Paraswima ethanquicki n. gen. n. sp.	0	0	3	0	0	0	2	0	1	1	0	1	2	1	0	1	1	1	1	1	0	2	1	0	0	1	1	0
	Paraswima sonjae n. gen. n. sp.	0	0	3	0	0	0	2	0	1	1	0	1	2	1	0	1	2	1	1	1	0	2	1	0	0	1	1	0
	Swima bombivirids	0	0	3	0	0	1	2	0	2	1	0	1	0	1	0	1	1	1	1	1	0	2	0	0	-	1	1	1
	Swima fulgida	0	0	3	0	0	1	2	0	2	1	0	1	0	1	0	1	1	1	1	1	0	2	0	0	-	1	1	1
	Swima osbornae n. sp.	0	0	?	0	0	1	2	0	2	1	0	1	0	1	0	3	1	1	1	1	0	2	0	0	-	1	1	1
	Swima tawitawiensis	0	0	4	0	0	1	2	0	2	1	0	1	1	1	0	1	1	1	1	1	0	2	1	1	0	1	1	1
	Teuthidodrilus australis n. sp.	0	0	2	0	0	0	0	0	1	1	0	2	2	0	0	1	0	1	0	1	1	2	0	1	-	1	1	-
	Teuthidodrilus samae	0	0	2	0	0	0	0	0	1	1	0	2	2	0	0	1	0	1	0	1	1	2	0	1	-	1	1	-
	Tiburon Bomber	0	0	3	0	0	0	2	0	1	1	0	1	2	1	0	1	2	1	1	1	0	2	1	0	0	1	1	0

Table 1.3: Character coding for morphology matrix in Table 1.2.

Character States	0	1	2	3	4	5
1. Retractable head (inside first chaetigers)	absent	present	-	-	-	-
2. Cephalic hood	absent	present	-	-	-	-
3. Achaetonous anterior segments	absent	1	2	3	4	6
4. Cephalic cage (chaetae of 1st chaetiger at least 1/3 longer than those of midbody)	absent	present	-	-	-	-
5. Externally obvious segment margins on majority of body	present	absent	-	-	-	-
6. Body papillae	short	long, clavate	-	-	-	-
7. Interramal papillae	short	clavate	lollipop	balloon	-	-
8. Sediment adhered to body	absent	present	-	-	-	-
9. Gelatinous Sheath	absent	thin, doesn't obsure features	thick, obscures features such as parapodal rami	-	-	-
10. Prostomium shape	terminal, lobe-like, with projecting anterior margin	dorsal, plate-like, posterior margin smooth, not projecting posteriorly over segments	dorsal, plate-like, posterior margin projecting posteriorly over segments	heart-shaped, dorsally covering peristomium	-	-
11. Eyes	absent	present	-	-	-	-
12. Nuchal organs	pit only	ciliate ridge only	at least part of ciliated ridge on a free-standing, oppositely branched structure	at least part of ridge on free-standing, oppositely branched, and spiral pillar structures	-	-
13. Nuchal organs (ridge shape)	straight (with less than 180 degree bend)	U-shaped (with single 180 degree bend)	convoluted (with multiple bends more than 180 degrees)	-	-	-
14. Head branchiae	absent	subulate, not easily lost	-	-	-	-
15. Main branchiae	on one or more segments, not on branchial membrane	on branchial membrane	absent	-	-	-
16. Main branchiae (number pairs)	more than 4 pairs	4 pairs	3 pairs	2 pairs	-	-
17. Main branchiae (shape)	long, tapered	small, elliptical	large, elliptical, at least one pair larger than half body width at widest	-	-	-
18. Nephridiopores as papillae	absent	present	-	-	-	-
19. Nephridiopores (location)	branchial membrane	segmental	peristomial	-	-	-
20. Parapodia distinct from body wall	absent	present	-	-	-	-
21. Anterior chaetigers (one or more)	biramous	uniramous	-	-	-	-
22. Chaetae	smooth	cross-barred, segmented	spinous	absent	-	-
23. Compound chaetae	absent	present	-	-	-	-
24. Broad, flattened chaetae	absent	present	-	-	-	-
25. Neurochaetae (second element)	straight	curved	hooked	-	-	-
26. Discrete gonads in few segments	absent	present	-	-	-	-
27. Gut	straight	looped	-	-	-	-
28. Medial head branchiae	absent	present	-	-	-	-

Table 1.4: Genes, primers, and protocols used in this study.

Gene	Primer Set	Authority	Reaction Protocol
COI	LCO1490/HCO2198	Folmer *et al.* 1994	94°C/180s - (94°C/30s - 47°C/45s - 72°C/60s) * 5 cycles (94°C/30s - 52°C/45s - 72°C/60s) * 30 cycles - 72°C/300s
	polyLCO/polyHCO	Carr *et al.* 2011	95°C/180s - (95°C/40s - 42°C/45s - 72°C/50s) * 40 cycles - 72°C/300s
CytB	CytB424F/CytB876R	Present study	94°C/120s - (94°C/30s - 45°C/60s - 68°C/60s) * 35 cycles - 68°C/420s
16S	16SarL/16SbrH	Palumbi *et al*. 1996	95°C/180s - (95°C/40s - 50°C/40s - 72°C/50s) * 35 cycles - 72°C/300s
18S	18S-1F/18S-5R	Giribet *et al.* 1996	95°C/180s - (95°C/30s - 50°C/30s - 72°C/90s) * 40 cycles - 72°C/480s
	18S-3F/18S-bi	Giribet *et al.* 1996/Whiting *et al.* 1997	95°C/180s - (95°C/30s - 52°C/30s - 72°C/90s) * 40 cycles - 72°C/480s
	18S-a2.0/18S-9R	Giribet *et al.* 1996/Whiting *et al.* 1997	95°C/180s - (95°C/30s - 50°C/30s - 72°C/90s) * 40 cycles - 72°C/480s
28S	Po28F1/Po28R4	Struck *et al.* 2006	95°C/180s - (95°C/30s - 55°C/40s - 72°C/75s) * 40 cycles - 72°C/300s

Table 1.5: Species and GenBank numbers for sequences in this study. New sequences are **bold.** Sequenced from holotypes = *.

Family	Species	*16S rRNA*	*18S rRNA*	*28S rRNA*	*COI*	*CYTB*	Voucher	Authority
Flabelligeridae	*Flabesymbios commensalis*	-	HQ326965	-	-	-	SIO:BIC:A1843	(Moore, 1909)
	Flabesymbios commensalis	**OR166196**	-	**OQ813500**	**OR166196**	**OR166196**	SIO:BIC:A14246	
	Flota sp.	-	EU694116	EU694122	-	-	SIO:BIC:A1131	Hartman, 1967
	Flota sp.	**OQ807203**	-	-	**OQ807203**	**OQ807203**	SIO:BIC:A14078	
	Pherusa bengalensis (unpublished)	MZ557347	-	-	MZ557347	MZ557347	-	(Fauvel, 1932)
	Poeobius meseres	-	EU694115	EU694123	-	-	SIO:BIC:A1130	Heath, 1930
	Poeobius meseres	**OQ807199**	-	-	**OQ807199**	**OQ807199**	SIO:BIC:A9529	
Acrocirridae	*Acrocirrus validus*	-	FJ944491	-	-	-	SIO:BIC:A1290	Marenzeller, 1879
	Acrocirrus validus	**OQ807197**	-	**OQ804812**	**OQ807197**	**OQ807197**	SIO:BIC:A4142	
	Actaedrilus yanbarensis	LC545955	LC545956	LC545957	LC543642	LC545958	NSMT-Pol P-809	Jimi, Fujimoto, Imura, 2020
	Flabelligella macrochaeta	**OR166197**	**OQ804406**	**OQ804813**	**OR166197**	**OR166197**	SIO:BIC:A9789	(Fauchald, 1972)
	Flabelligena sp.	**OQ807198**	EU694120	EU694121	**OQ807198**	**OQ807198**	SIO:BIC:A1126	Gillet, 2001
	Horned Bomber	FJ944512	FJ944500	FJ944521	FJ944534	FJ944547	SIO:BIC:A1287	undescribed from Osborn *et al*. 2009
	Juanita Worm	FJ944514	FJ944502	FJ944523	FJ944536	FJ944549	SIO:BIC:A1289	undescribed from Osborn *et al*. 2009
	Macrochaeta cf. *westheidei*	-	EU700414	-	-	-	SIO:BIC:A1127	Santos & Silva, 1993
	Macrochaeta cf. *westheidei*	**OQ807196**	-	**OQ804814**	**OQ807196**	**OQ807196**	SIO:BIC:A4873	
	Macrochaeta clavicornis	HQ326957	EU791461	-	EU791463	-	SIO:BIC:A1087	(M. Sars, 1835)
	Macrochaeta clavicornis	-	-	DQ779696	-	-	SMNH:75829	
	Macrochaeta pege	**OQ807200**	**OQ804407**	**OQ804815**	**OQ807200**	**OQ807200**	SIO:BIC:A15670	Banse, 1969
	Macrochaeta sp. (unpublished)	MT877119	-	-	MT877119	MT877119	MD01-Achotines-A1	Grube, 1850
	Paraswima ethanquicki n. gen n. sp.*	**OQ722173**	**OQ724826**	**OQ724822**	**OQ713618**	**OQ718582**	WAM:VER:V9620	Present study
	Paraswima sonjae n. gen. n. sp.*	**OQ722174**	**OQ724828**	**OQ724824**	**OQ713620**	**OQ718584**	WAM:VER:V9877	Present study
	Swima bombiviridis	-	GQ422143	GQ422144	-	-	SIO:BIC:A1282	Osborn, Haddock, Pleijel, Madin, & Rouse, 2009
	Swima bombiviridis	**OQ807202**	-	-	**OQ807202**	**OQ807202**	SIO:BIC:A14014	
	Swima fulgida	-	FJ944497	-	-	-	SIO:BIC:A1285	Osborn, Haddock, & Rouse, 2011
	Swima fulgida	-	-	FJ944519	-	-	SIO:BIC:A1286	
	Swima fulgida	**OQ807201**	-	-	**OQ807201**	**OQ807201**	SIO:BIC:A14013	
	Swima osbornae n. sp.*	**OQ722175**	**OQ724827**	**OQ724823**	**OQ713623**	**OQ718583**	WAM:VER:V9873	Present study
	Swima tawitawiensis	-	FJ944499	FJ944520	-	-	NMA:04327	Osborn, Haddock, & Rouse, 2011
	Swima tawitawiensis	**OQ807206**	-	-	**OQ807206**	**OQ807206**	WAM:VER:V9829	
	Teuthidodrilus australis n. sp.*	**OQ807205**	**OQ724829**	**OQ724825**	**OQ807205**	**OQ807205**	WAM:VER:V9804	Present study
	Teuthidodrilus samae	-	FJ944503	FJ944524	-	-	NMA:04342	Osborn, Madin, & Rouse, 2011
	Teuthidodrilus samae	**OQ807204**	-	-	**OQ807204**	**OQ807204**	MCZ:IZ:70357	
	Tiburon Bomber	FJ944513	FJ944501	FJ944522	FJ944535	FJ944548	SIO:BIC:A1288	undescribed from Osborn *et al*. 2009

Table 1.6: Uncorrected *COI* pairwise distances for swimming acrocirrids with *Flabelligena* sp. as the outgroup. Rounded to two decimal places with pairwise distances less than 13% in **bold**. Holotype = *.

	Acrocirridae	**1**	**2**	**3**	**4**	**5**	**6**	**7**	**8**	**9**	**10**	**11**	**12**	**13**	**14**	**15**	**16**	**17**	**18**	**19**	**20**	**21**	**22**	**23**
1	*Flabelligena* sp. EU694126	-																						
2	Horned Bomber FJ944534	22.24	-																					
3	Juanita Worm FJ944536	22.58	19.83	-																				
4	*Paraswima ethanquicki* n. sp. OQ713618*	20.03	17.04	21.27	-																			
5	*Paraswima ethanquicki* n. sp. OQ713619	20.17	16.58	21.43	**0.01**	-																		
6	*Paraswima sonjae* n. sp. OQ713620*	22.00	18.01	20.52	19.15	19.00	-																	
7	*Paraswima sonjae* n. sp. OQ713621	22.46	18.34	20.68	19.15	19.00	**0.00**	-																
8	*Swima bombiviridis* FJ944527*	22.32	20.11	17.81	20.64	20.49	18.93	19.26	-															
9	*Swima fulgida* FJ944531*	22.82	20.06	19.21	21.15	20.68	18.97	19.28	14.89	-														
10	*Swima osbornae* n. sp. OQ713623*	21.99	19.27	18.11	19.61	19.15	18.69	18.85	15.14	13.45	-													
11	*Swima osbornae* n. sp. OQ713622	21.99	19.27	18.11	19.61	19.15	18.69	18.85	15.14	13.45	**0.00**	-												
12	*Swima osbornae* n. sp. OQ713624	21.99	19.27	18.11	19.61	19.15	18.69	18.85	15.14	13.45	**0.00**	**0.00**	-											
13	Swima tawitawiensis FJ944533* Celebes Sea, Philippines	23.19	20.56	19.53	22.69	22.07	19.11	19.44	16.62	15.49	16.44	16.44	16.44	-										
14	*Swima tawitawiensis* OQ716776 Cape Range Canyon, Australia	22.32	20.55	19.41	22.13	21.52	19.26	19.42	16.44	15.30	16.06	16.06	16.06	**0.00**	-									
15	*Swima tawitawiensis* OQ716775 Cloates Canyon, Australia	22.89	20.48	19.71	22.19	21.58	19.3	19.45	16.35	15.47	15.96	15.96	15.96	**0.00**	**0.00**	-								
16	*Teuthidodrilus australis* n. sp. OQ784046	22.18	19.46	19.40	18.85	19.00	22.19	22.34	19.33	23.04	19.76	19.76	19.76	19.50	19.32	19.00	-							
17	*Teuthidodrilus australis* n. sp. OQ784049*	21.84	19.23	19.29	18.78	18.93	22.13	22.29	19.26	22.89	19.70	19.70	19.70	19.26	19.01	18.94	**0.00**	-						
18	*Teuthidodrilus australis* n. sp. OQ784048	21.58	19.16	19.02	18.72	18.87	22.09	22.25	19.22	22.72	19.67	19.67	19.67	19.21	18.63	18.90	**0.00**	**0.00**	-					
19	*Teuthidodrilus australis* n. sp. OQ784047	22.12	20.17	19.51	19.70	19.88	22.04	22.40	18.72	22.91	19.72	19.72	19.72	20.05	20.14	19.76	**0.00**	**0.00**	**0.00**	-				
20	Teuthidodrilus samae FJ944537* Celebes Sea, Philippines	21.29	19.56	18.42	19.44	19.12	20.24	20.70	19.59	21.52	19.92	19.92	19.92	20.06	19.57	19.90	15.30	15.07	14.85	15.57	-			
21	*Teuthidodrilus samae* OQ716777 Galápagos Rift, Ecuador	21.73	19.86	18.05	19.68	19.37	19.81	20.11	19.56	21.36	19.69	19.69	19.69	19.56	19.60	19.68	15.51	15.34	15.28	15.59	**0.01**	-		
22	*Teuthidodrilus samae* OQ716778 Galápagos Rift, Ecuador	21.83	20.48	18.05	20.23	19.91	20.08	20.39	19.65	21.50	19.93	19.93	19.93	19.70	19.62	19.45	15.84	15.83	15.84	15.62	**0.01**	**0.01**	-	
23	Tiburon Bomber FJ944535	21.02	20.68	19.77	19.08	19.26	15.83	16.00	21.79	21.71	19.31	19.31	19.31	21.94	21.48	21.85	21.24	21.19	21.14	21.84	20.16	19.93	20.23	-

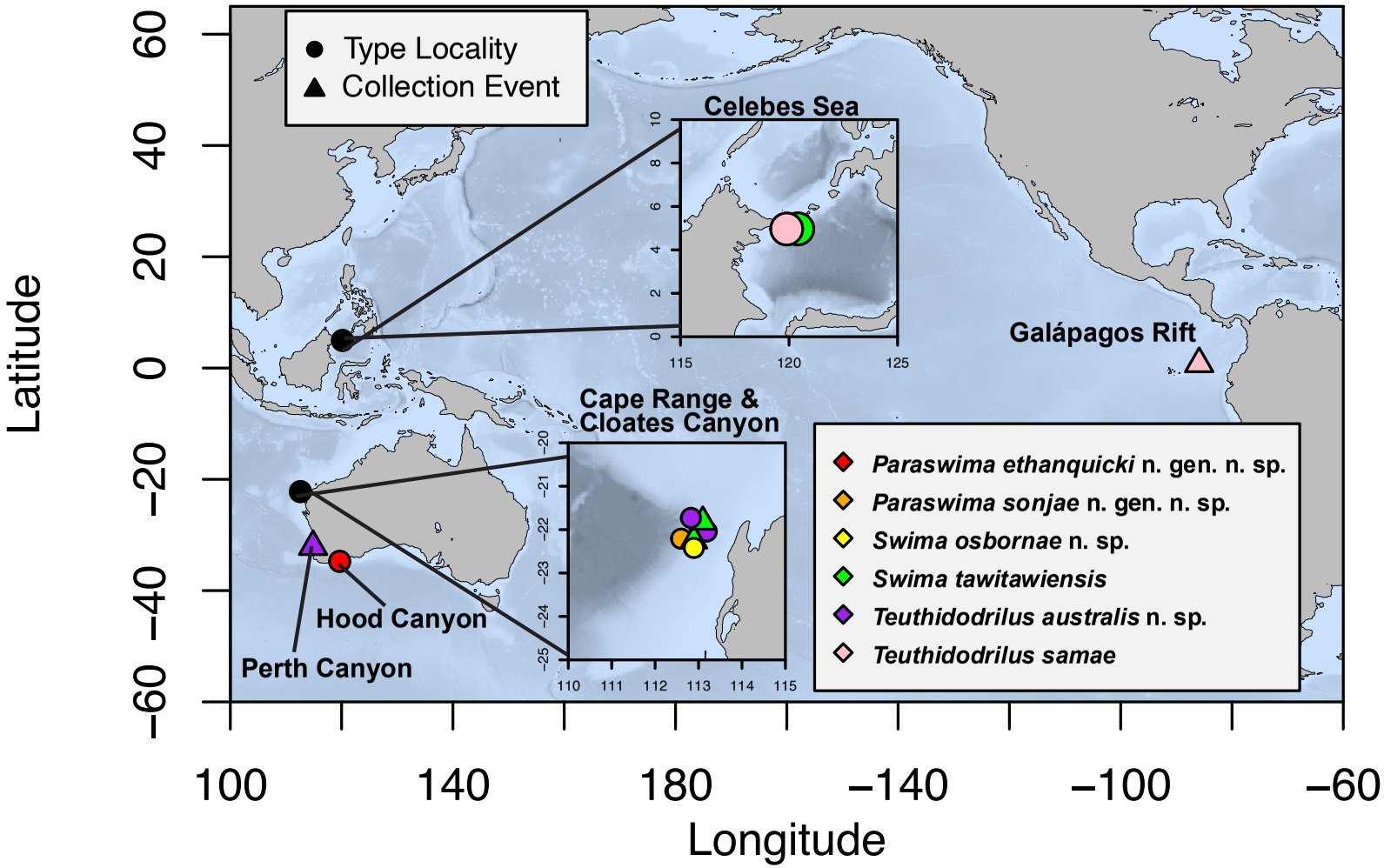

Figure 1.1: Map of new specimen collection localities listed in Table 1.1 generated using the R package marmap R package (Pante & Simon-Bouhet 2013) and modified with Adobe Illustrator (Adobe Inc. 2019).

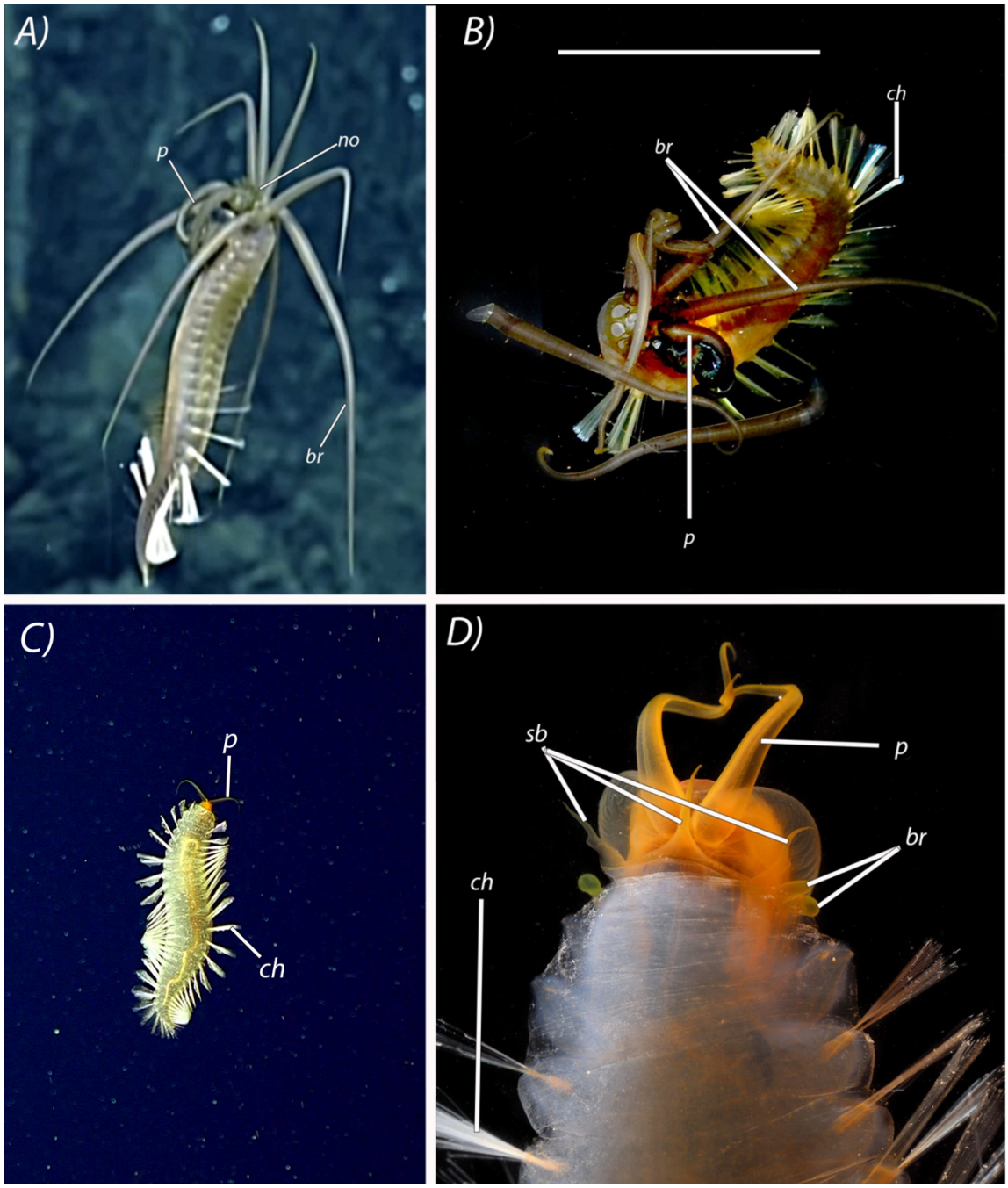

Figure 1.2: *Teuthidodrilus samae* (A-B) and *Swima tawitawiensis* (C-D). A) ROV *Little Hercules* footage of *Teuthidodrilus samae* from the Galápagos Rift at 2555 meters showing palps (p), elongate branchiae (br), and branched nuchal organ (no). Credit: Nautilus Live Ocean Exploration Trust. B) Ventral view of *Teuthidodrilus samae* paratype, MCZ:IZ:70186, scalebar = 40 mm C) ROV *SuBastian* footage of *Swima tawitawiensis* paratype, WAM:VER:V9874, from Cloates Canyon at 2480 meters. Credit: Schmidt Ocean Institute. D) Dorsal view of *Swima tawitawiensis* paratype, WAM:VER:V9829, head showing the single row of three subulate branchiae (sb) and elliptical, main branchiae (br). ch= chaetae.

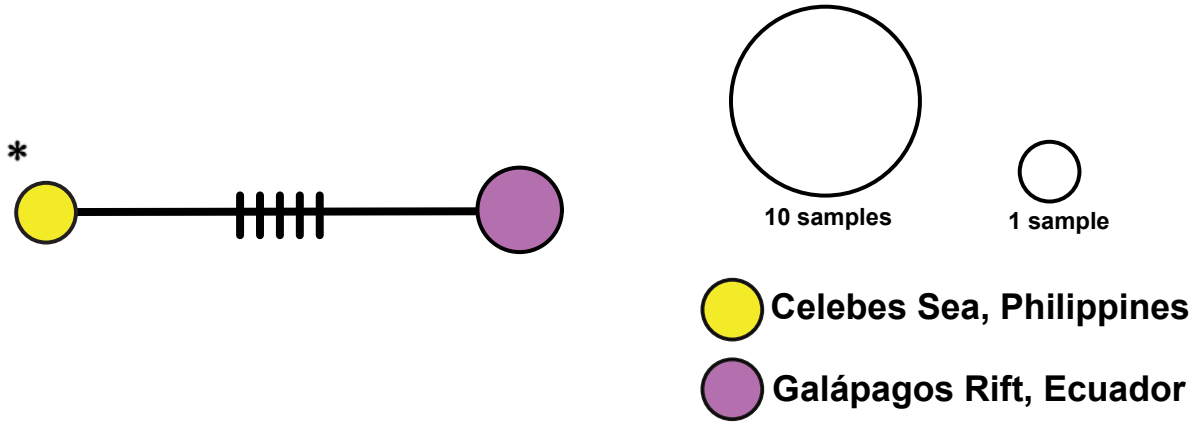

Figure 1.3: *COI* haplotype network for *Teuthidodrilus samae.* Circles are haplotypes and the dash is a single nucleotide substitution. Holotype= *.

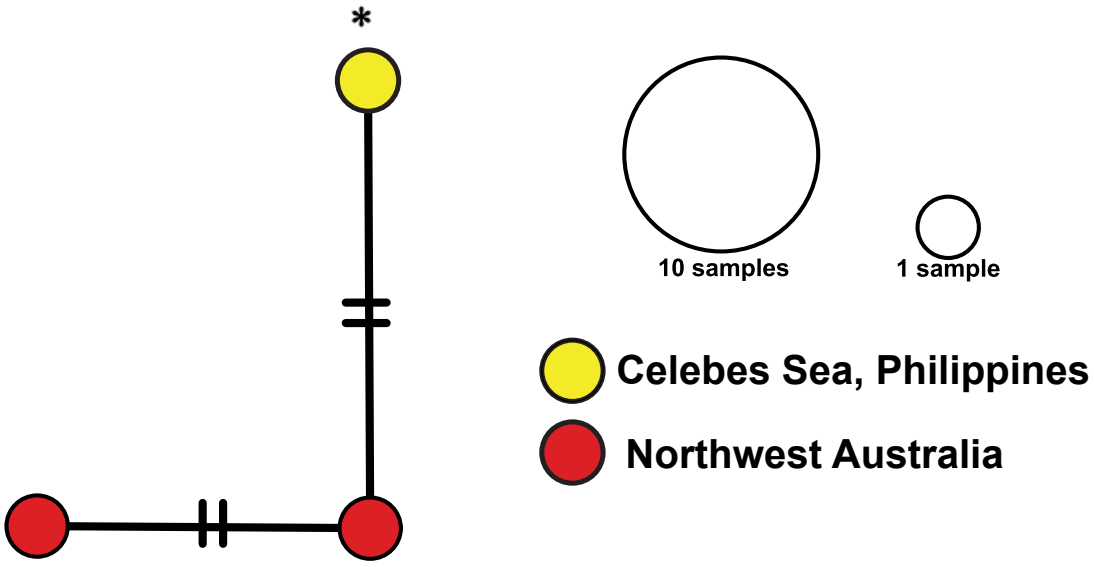

Figure 1.4: *COI* haplotype network for *Swima tawitawiensis.* Circles are haplotypes and the dash is a single nucleotide substitution. Holotype=*.

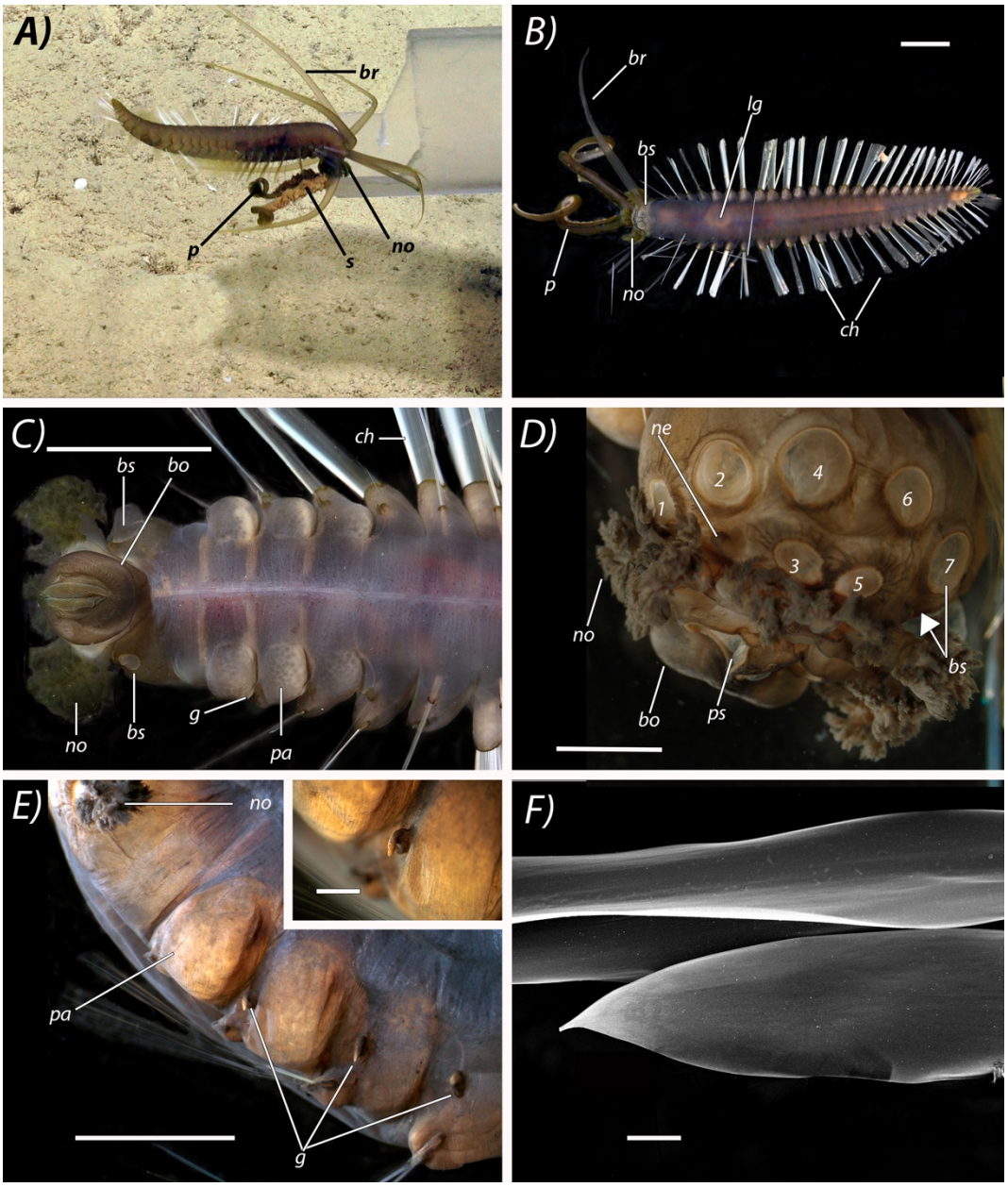

Figure 1.5: *Teuthidodrilus australis* n. sp. A) ROV *SuBastian* footage of *Teuthidodrilus australis* n. sp. just above the seafloor, 2175 meters, with palps (p) full of sediment (s). Credit: Schmidt Ocean Institute. B) Live dorsal view of *Teuthidodrilus australis* n. sp. holotype, WAM:VER:V9804, scalebar = 10 mm. C) Live ventral view of *Teuthidodrilus australis* n. sp. paratype, WAM:VER:V9805, scalebar = 10 mm. D) Dorsal view of *Teuthidodrilus australis* n. sp. paratype, WAM:VER:V9805, head showing branchial scars (bs) as numbers with a white arrow pointing to the hidden eighth scar, scalebar = 5 mm. E) Anterolateral view of *Teuthidodrilus australis* n. sp. paratype, WAM:VER:V9805, ventral parapodia, scalebar = 5 mm, and inset showing magnified gonopore (g), scalebar = 1 mm. F) SEM image of *Teuthidodrilus australis* n. sp. holotype, WAM:VER:V9804, notochaetae distal tip, scalebar = 100 microns. br=branchiae, no=nuchal organ, lg=looped gut, ch=chaetae, bo=buccal organ, pa=parapodium, ne=nephridiopore, ps=palp scar.

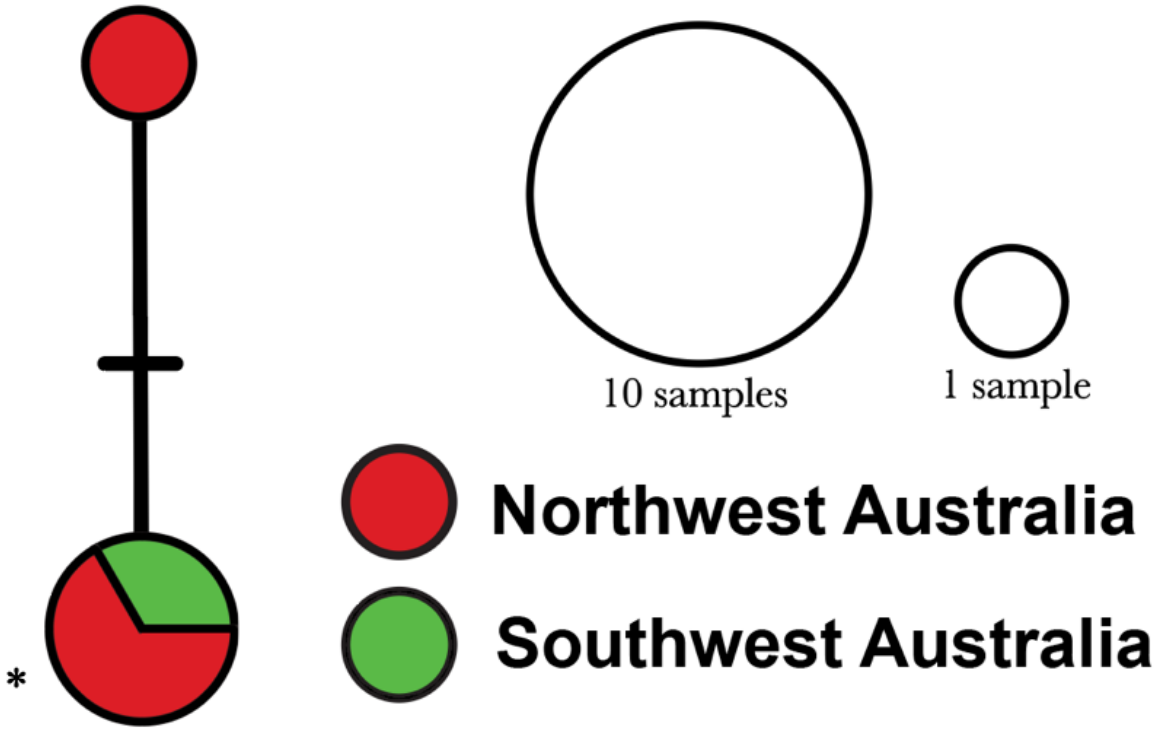

Figure 1.6: *COI* haplotype network for *Teuthidodrilus australis* n. sp. Circles are haplotypes, and the dash is a single nucleotide substitution. Holotype=*.

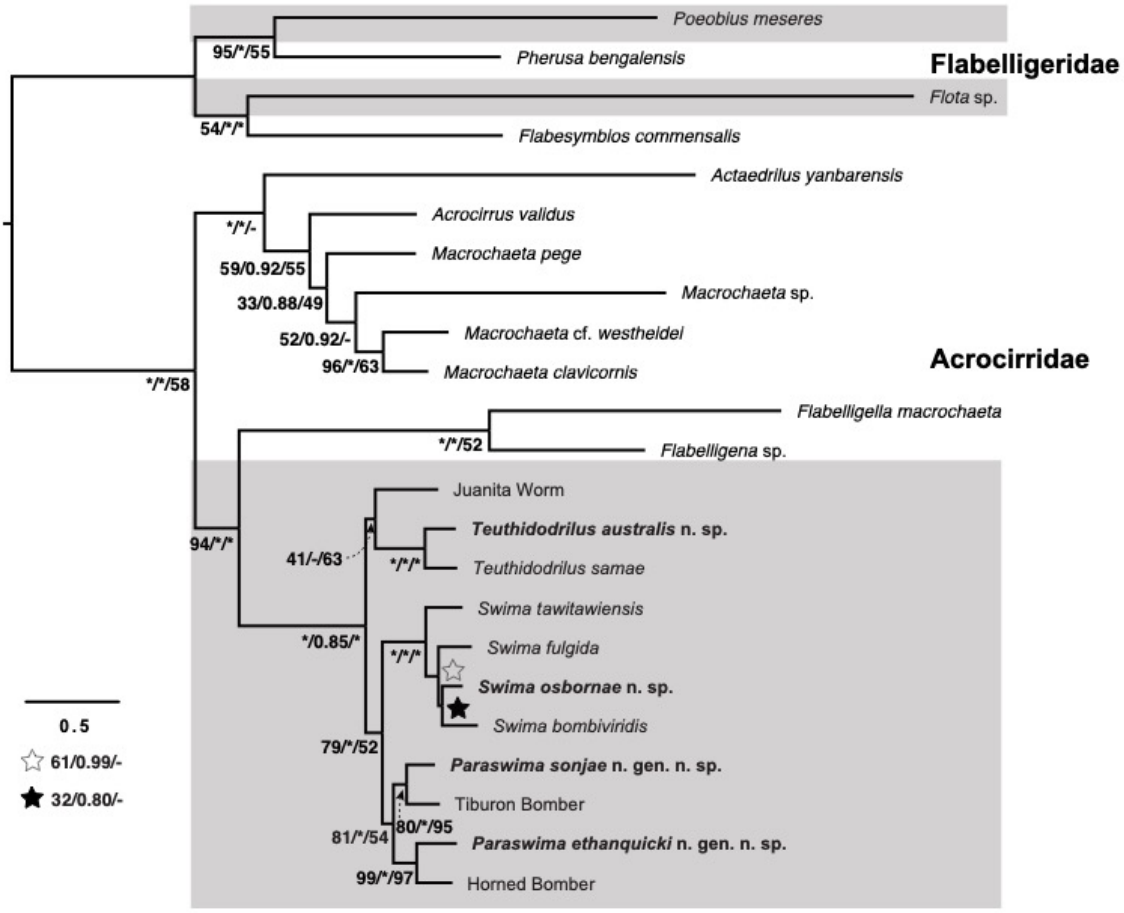

Figure 1.7: Maximum likelihood Acrocirridae phylogeny of five concatenated genes with data partitioned by gene with Flabelligeridae as the outgroup. The topology of the Bayesian tree was the same except that the Juanita Worm formed a clade with *Paraswima* n. gen. and *Swima* with high support, 0.85. The topology of the strict consensus tree from the parsimony analysis was the same except *Actaedrilus yanbarensis* was sister to rest of Acrocirridae with high bootstrap support of 100%, *Macrochaeta* sp. formed a clade with *Flabelligella macrochaeta* and *Flabelligena* sp. with low bootstrap support of 47%, and *Swima fulgida* and *Swima bombiviridis* formed a clade sister to *Swima osbornae* n. sp. with 54% bootstrap support. Support is indicated as bootstraps from the maximum likelihood analysis/posterior probabilities from the Bayesian analysis/bootstraps from the maximum parsimony analysis with asterisks representing 100% bootstrap support or 1.0 posterior probability. Taxa in gray boxes are pelagic.

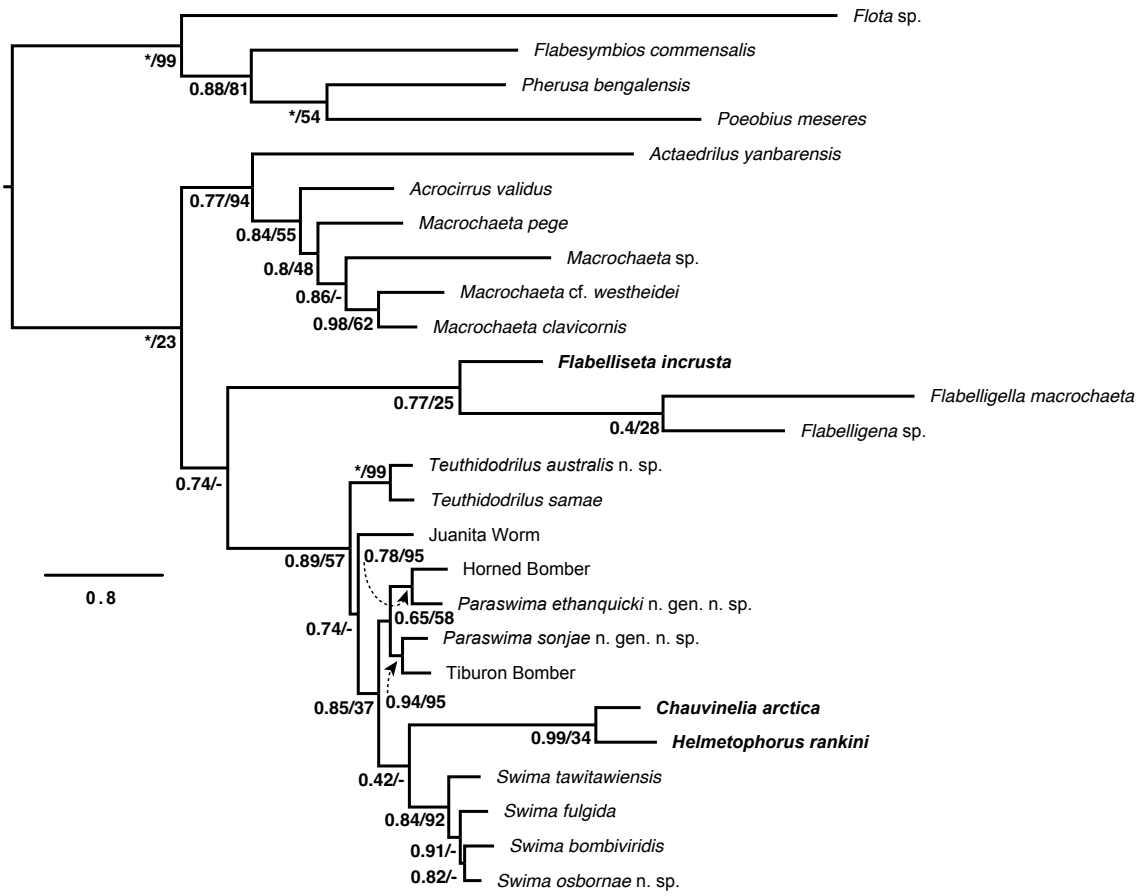

Figure 1.8: Bayesian Acrocirridae phylogeny of five concatenated genes and 28 morphological characters including species with no DNA data in **bold** with parameters the same as the analysis in Figure 1.7 with Flabelligeridae as the outgroup. The topology of the strict consensus tree from the parsimony analysis was the same except *Macrochaeta* sp. formed a clade with *Flabelligella macrochaeta, Flabelligena* sp., and *Flabelliseta incrusta* with low bootstrap support of 25%, Juanita Worm formed a clade with *Teuthidodrilus* with bootstrap support 64%, *Chauvinelia* and *Helmetophorus* were sister to all other swimming acrocirrids with 44% bootstrap support, and *Swima fulgida* and *Swima bombiviridis* formed a clade sister to *Swima osbornae* n. sp. with 50% bootstrap support. Support is indicated as posterior probabilities from the Bayesian analysis/bootstraps from the maximum parsimony analysis with asterisks representing 1.0 posterior probability and 100% bootstrap support.

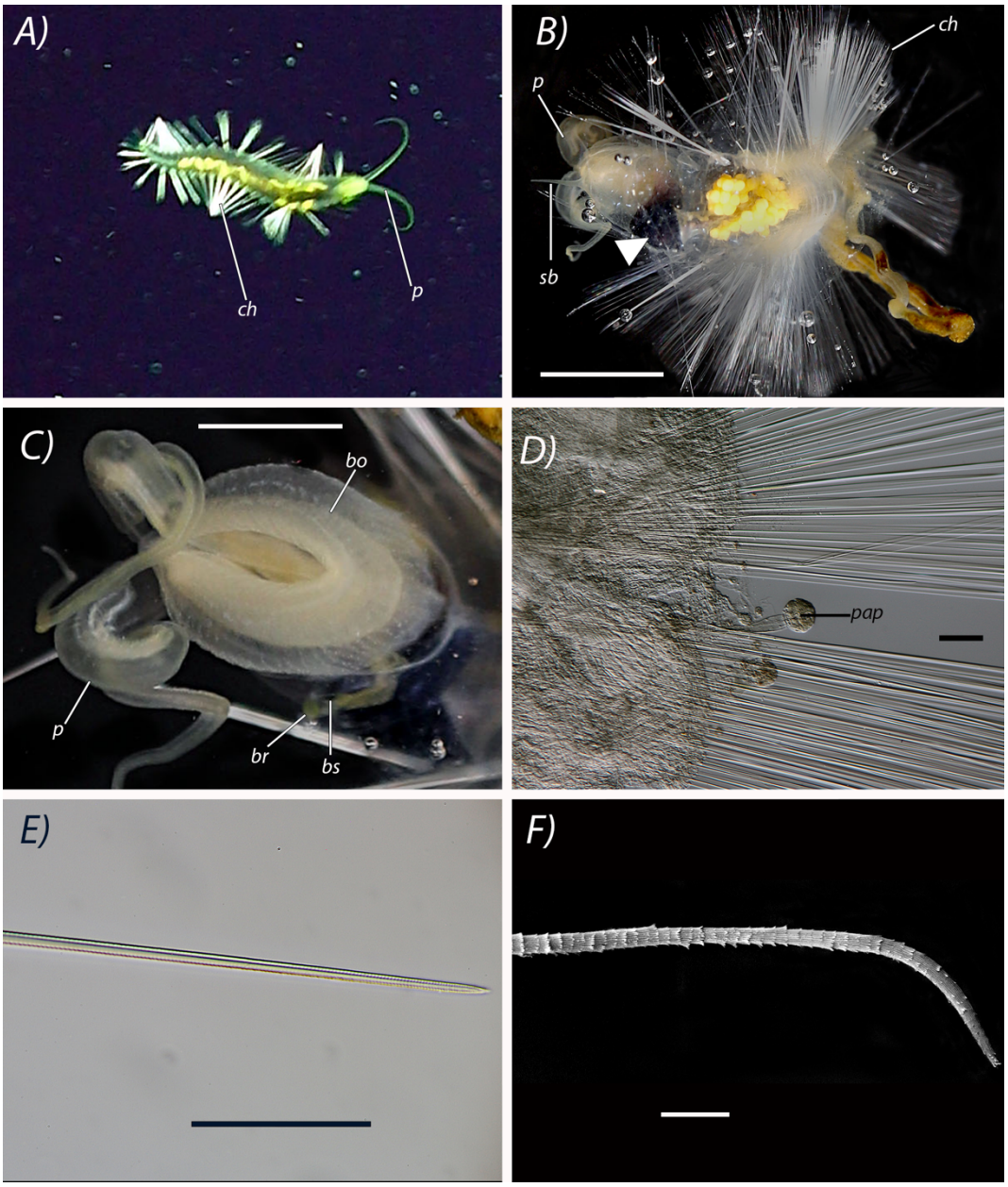

Figure 1.9: *Swima osbornae* n. sp. A) ROV *SuBastian* of *Swima osbornae* n. sp. from Cloates Canyon at 2600 meters. Credit: Schmidt Ocean Institute. B) Live dorsal view of *Swima osbornae* n. sp. holotype, WAM:VER:V9872 showing medial subulate branchiae (sb) and the dark anterior gut (white arrow), scalebar = 5 mm. C) Live ventral view of *Swima osbornae* n. sp. holotype, WAM:VER:V9872, head showing muscular buccal organ (bo), elliptical branchiae (br), and branchial scar (bs), scalebar = 2 mm. D) Compound image of *Swima osbornae* n. sp. holotype, WAM:VER:V9872, parapodia showing interramal lollipop papillae (pap), scalebar = 100 microns. E) Compound image of *Swima osbornae* n. sp. paratype, WAM:VER:V9876, chaetae distal tip, scalebar = 1 mm. F) SEM image of *Swima osbornae* n. sp. paratype, WAM:VER:V9873, notochaetae, scalebar = 10 microns. p= palp, ch= chaetae.

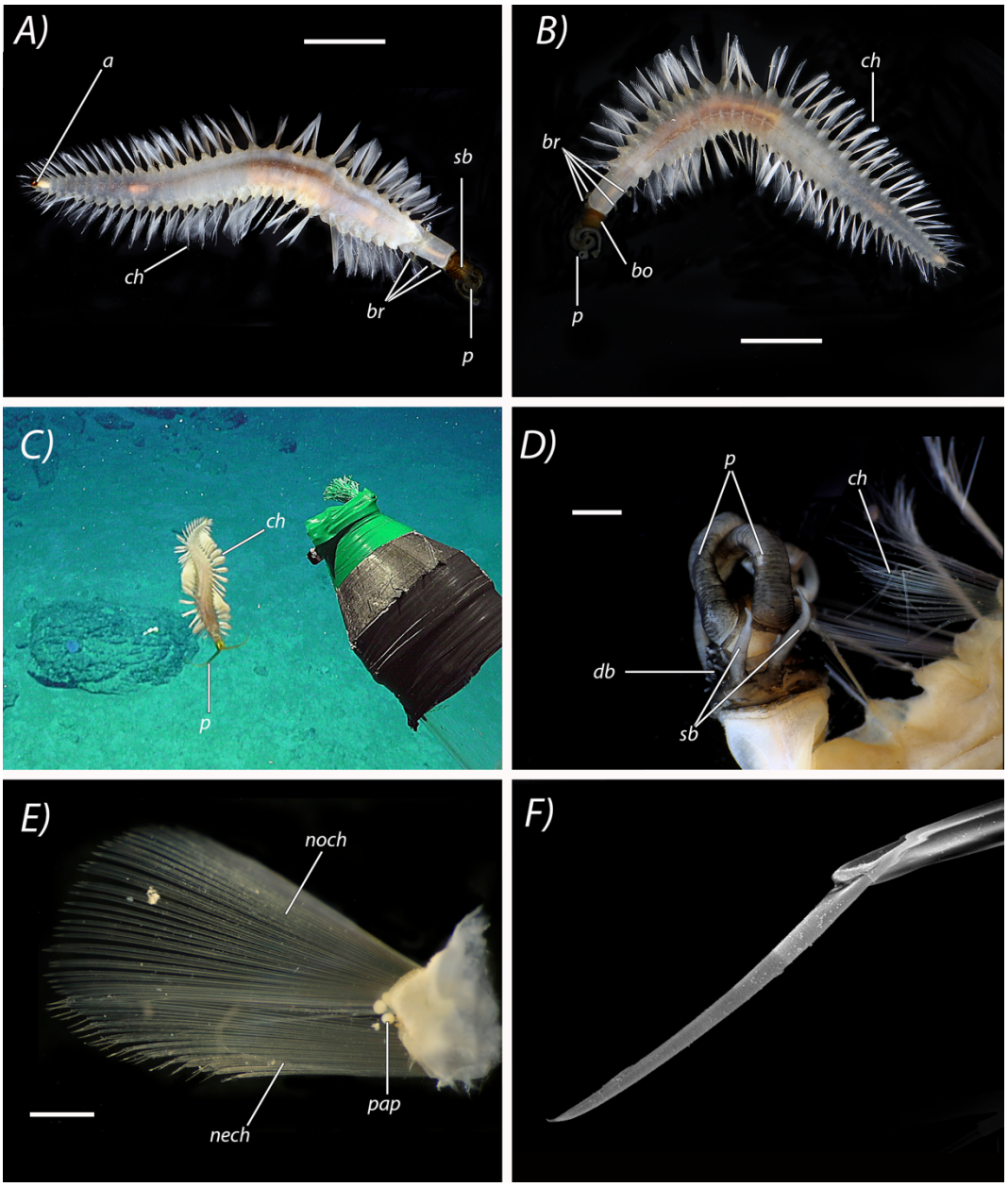

Figure 1.10: *Paraswima sonjae* n. gen. n. sp. A) Dorsal view of *Paraswima sonjae* n. gen. n. sp. holotype, WAM:VER:V9877, showing elliptical branchiae (br) and red midgut and anus (a), scalebar = 10 mm. B) Ventral view of *Paraswima sonjae* n. gen. n. sp. holotype, WAM:VER:V9877, showing elliptical branchiae (br) and red midgut and buccal organ (bo), scalebar = 10 mm. C) ROV *SuBastian* footage of *Paraswima sonjae* n. gen. n. sp. in Cloates Canyon at 3386 meters. Credit: Schmidt Ocean Institute. D) Dorsal view of *Paraswima sonjae* n. gen. n. sp. holotype, WAM:VER:V9877, head showing pair of subulate branchiae (sb) posterior to palps (p), scale bar = 1 mm. E) Chaetiger six of *Paraswima sonjae* n. gen. n. sp. holotype, WAM:VER:V9877, showing lollipop interramal papillae (pap), scale bar = 1 mm. F) SEM image of *Paraswima sonjae* n. gen. n. sp. holotype, WAM:VER:V9877, showing distal tip of neurochaetae. ch=chaetae, db=digitiform branchiae, noch=notochaetae, neurochaetae.

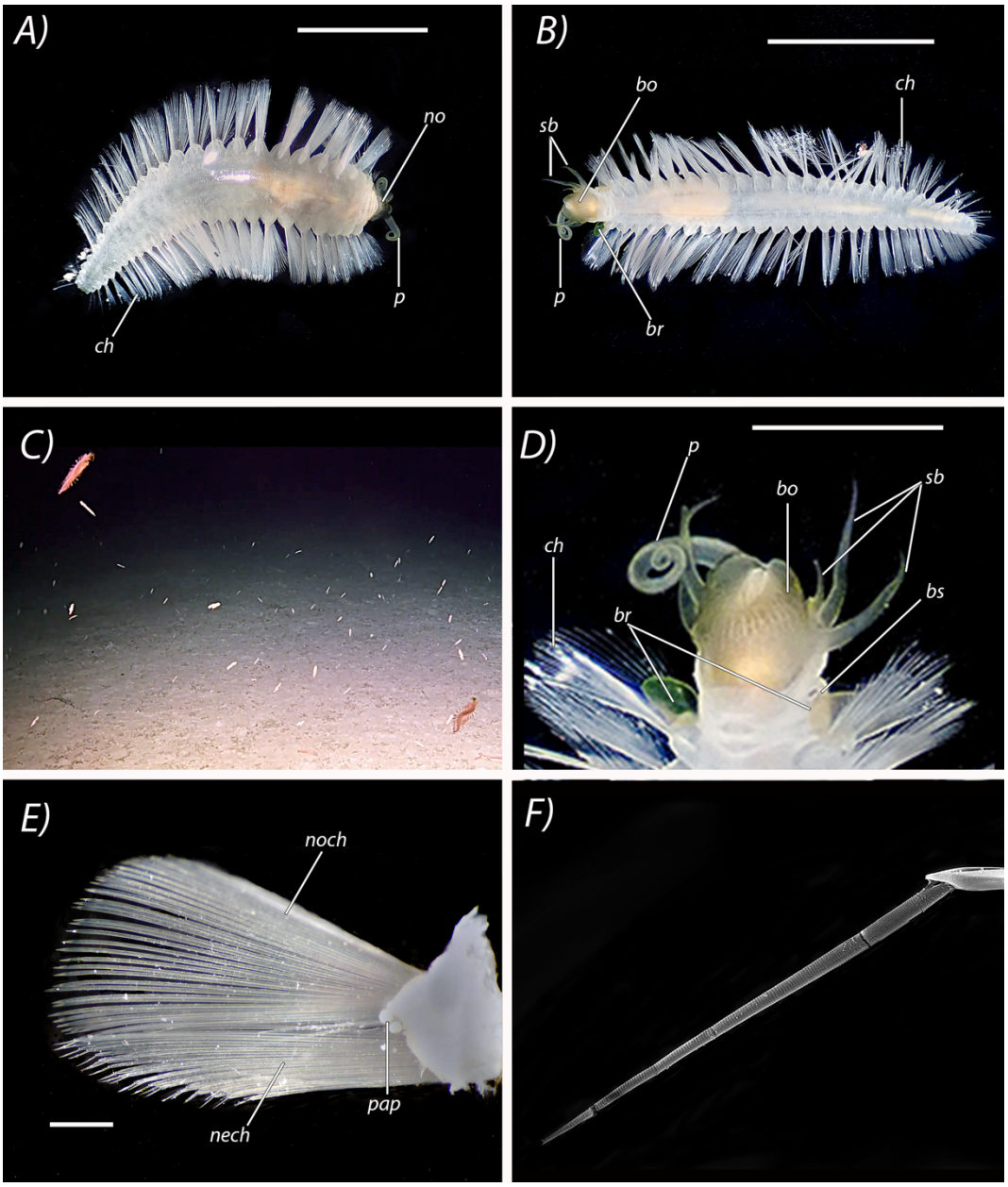

Figure 1.11: *Paraswima ethanquicki* n. gen. n. sp. A) Dorsal view of *Paraswima ethanquicki* n. gen. n. sp. paratype, WAM:VER:V9621, scalebar = 10 mm. B) Ventral view of *Paraswima ethanquicki* n. gen. n. sp. holotype, WAM:VER:V9620, scalebar = 10 mm. C) ROV *SuBastian* footage of *Paraswima ethanquicki* n. gen. n. sp. in Hood Canyon at 1550 meters. Credit: Schmidt Ocean Institute. D) Enlarged image of Figure 1.11B showing rows of subulate branchiae (sb), elliptical branchiae (br), and branchial scars (bs), scalebar = 3 mm. E) Chaetiger six of *Paraswima ethanquicki* n. gen. n. sp. holotype, WAM:VER:V9620, showing lollipop-shaped interramal papillae (pap), scale bar = 1 mm. F) SEM image of *Paraswima ethanquicki* n. gen. n. sp. neurochaetae distal tip from holotype, WAM:VER:V9620. ch=chaetae, no=nuchal organ, p=palp, bo=buccal organ, noch=notochaetae, nech=neurochaetae.

Acknowledgments

Chapter 1 is currently being prepared for submission for publication of the material. Proctor, Paul P.; Wilson, Nerida G.; Hara, Ana; Hosie, Andrew; Rouse, Greg W. The thesis author was the primary investigator and author of this material.

CHAPTER 2: Mitogenomic Insights of Cirratuliformia

INTRODUCTION

Prior to the development of Sanger sequencing, morphological data was the primary evidence used to generate phylogenies for evaluating evolutionary relationships (Wiens 2004). However, morphology alone provides poorly resolved phylogenies with homoplasy, making the ability to track the origin of traits such as habitat use challenging. For example, histological and morphological analyses created unstable positions for *Flota* and *Poeobius* in the annelid family tree (Salazar-Vallejo & Zhadan 2007). When Rouse and Pleijel 2003 addressed the paraphyly of Flabelligeridae, it laid the groundwork for the transfer of pelagic annelids *Flota* and *Poeobius* into Flabelligeridae (Osborn & Rouse 2008; Burnette et al. 2005). This focus provided the opportunity to use DNA evidence to answer the question: do *Flota* and *Poeobius* share a common pelagic ancestor or has pelagicism originated more than once within Flabelligeridae? A Bayesian analysis of Flabelligeridae did not recover *Flota* and *Poeobius* as sister taxa suggesting two independent origins of pelagicism within Flabelligeridae (Osborn & Rouse 2008). The discovery of a pelagic clade of annelids in Acrocirridae revealed a third origin of pelagicism within Cirratuliformia (Osborn et al. 2009; Osborn et al. 2011b), which was confirmed in Chapter 1 of this study even with the addition of new data and species.

Pelagicism is rare in annelids, with most residing within Phyllodocida (Halanych et al. 2007). Lopadorrhynchidae, Iospilidae, Typhloscolecidae, and Tomopteridae are exclusively pelagic families, while other families have pelagic members: Phyllodocidae (Alciopini), Chaetopteridae (*Chaetopterus pugaporcinus*), Polynoidae (*Drieschia*, *Podarmus*, *Drieschiopsis*, *Gesiella*, and *Pelagomacellicephala*), and Acrocirridae (*Teuthidodrilus, Swima*, and *Paraswima* n. gen.) (Gonzalez et al. 2021). Prior to the transfer of *Flota* and *Poeobius* as well as the

discovery of pelagic acrocirrids *Swima* and *Teuthidodrilus,* all representatives of Cirratuliformia were benthic (Rouse & Pleijel 2001).

The body plans of benthic and pelagic cirratuliforms are drastically different, with pelagic cirratuliforms having modifications such as transparent bodies, specialized feeding modes, defensive strategies like the bioluminescent 'bombs' of *Swima*, modified chaetae, or, in the case of *Poeobius*, the complete loss of morphological traits common in most annelids such as chaetae, parapodia, and obvious segmentation (Gonzalez et al. 2021; Osborn & Rouse 2008). Given that these pelagic members are nestled within a primarily benthic group suggests different evolutionary constraints on these organisms. Researchers have been interested in the evolutionary shift from benthic to pelagic habitats and whether that shift drives macroevolution in metazoan lineages, even as DNA was actively becoming a standard in phylogenetics (Fuiman 1997; Hollingsworth Jr et al. 2013; Lindgren et al. 2012). One way to study this is using information from mitochondrial genomes or mitogenomes.

Mitogenomics is a rapidly advancing field in phylogenetics due to the ability to study evolutionary history deeply with high resolution because of an increase in total DNA evidence and the fact that mitogenomes are highly conserved across Metazoa (Bernt et al. 2013b). There are other traits that make mitogenomes desirable for resolving evolutionary relationships as well such as genes evolving at different rates within the mitogenomes, uniparental inheritance to trace lineages, and low recombination rates (Gissi et al. 2008). This improves the resolution of phylogenetic hypotheses, but also provides a complete genome to study mechanisms underlying the evolution of the mitogenome. Mitogenome features such as genome size, gene content, gene order, and the location and size of non-coding regions can be used to compare and unravel changes in lineages over time (Gissi et al. 2008). Another advantage to using mitogenomes is

that advancements in high-throughput sequencing technologies and next-generation sequencing platforms have made getting large amounts of sequencing data in a short time both accessible and cost-effective.

Next-generation sequencing and bioinformatic software have provided the tools to assemble and compare complete mitogenomes affordably and quickly. This improves the study of phylogenetic relationships and provides an avenue to further explore the mechanisms behind genomic evolution that can help understand evolutionary transitions among closely related taxa. Chapter 2 of this thesis provides the first mitogenome phylogeny of Cirratuliformia and further supports the phylogenetic results of Chapter 1. Additionally, assembling whole mitogenomes for pelagic and closely related benthic members of Cirratuliformia will aid in understanding ecological transitions from benthic to pelagic habitats by analyzing what effects the varying evolutionary pressures have on the composition of the mitogenomes within Cirratuliformia.

MATERIALS AND METHODS

Taxa Included

Representative taxa were chosen carefully due to monetary and time constraints. Within Acrocirridae, the goal was to select a member of each benthic and pelagic genus with DNA extractions available, with an emphasis to choose the type species when possible. Additionally, to make up for the lack of flabelligerid sampling, two benthic taxa closely related to *Flota* and *Poeobius* were chosen for in-family comparison. Three cirratulids with complete mitogenomes available on GenBank were chosen as the outgroup to root the tree and properly analyze the three independent origins of pelagicism within Cirratuliformia. All taxa chosen had their whole mitochondrial genome annotated and submitted to GenBank or were already published

sequences (Table 2.1). Unverified or unpublished GenBank sequences were included in the analysis after careful verification using NCBI Blast (Altschul et al. 1990) and Geneious Prime v.11.0.14 (Kearse et al. 2012). Voucher specimens are housed in the Scripps Institution of Oceanography Benthic Invertebrate Collection (SIO:BIC) at the University of California San Diego, San Diego, CA, USA, National Marine Biodiversity Institute of Korea (MABIK), Seocheon County, South Korea, Western Australia Museum Worms Collection (WAM:VER), Welshpool DC, Western Australia, Australia, National Museum of the Philippines (NMA), Manila, Philippines, and Museum of Comparative Zoology, Department of Invertebrate Zoology (MCZ:IZ) at Harvard University, Cambridge, MA, USA.

Genomic Sequencing

Genomic DNA (gDNA) was extracted from tissue subsamples using the Zymo Research DNA-Tissue Miniprep or Microprep kits (Irvine, California, USA), depending on tissue size, using the manufacturer's protocol. Extracted gDNA was visualized on a 1.5% agarose gel and quantified using a Qubit dsDNA HS Assay Kit (ThermoFisher, Pittsburgh, PA, USA) then shipped to Novogene (en.novogene.com) for library preparation and whole genome sequencing. This was completed using the Illumina NovaSeq6000 platform to generate 150 base pair (bp) paired-end aligned reads. Reads were cleaned and trimmed with Trimmomatic v.0.39 (Bolger et al. 2014). Table 2.2 shows the number and total length of paired-end 150 bp raw reads per sample along with the number of reads after trimming.

Genome Assembly, Annotation, and Composition

Mitogenomes were assembled using MitoFinder v.1.4 (Allio et al. 2020) using the UC San Diego Research Cluster (research-it.ucsd.edu) using the Invertebrate Mitochondrial Code (NCBI; transl_table = 5) to translate the 13 protein-coding genes. The reference file used for MitoFinder contained the complete records for all RefSeq annelid mitogenomes publicly available on NCBI GenBank. The integrated MitoFinder pipeline with MEGAHIT v.1.2.9 (Li et al. 2016) and Arwen v.1.2.3 (Laslett & Canbäck 2008) parameters were used to annotate the assembled mitochondrial genomes. The MITOS Web Server (Bernt et al. 2013a) was used to check annotations for completeness and accuracy, and Geneious Prime v.11.0.14 (Kearse et al. 2012) was used to manually modify annotated assemblies where necessary, extract nucleotide sequences of genes, and translate protein coding genes into amino acids using the Invertebrate Mitochondrial Code (NCBI; transl_table = 5). The paired-end reads were also used to obtain mapped *18S* and *28S* sequences as referenced in Chapter 1. AT and GC nucleotide skew patterns were calculated independently for all newly assembled mitogenomes according to the following formulas: AT-skew = (A − T) / (A + T) and GC-skew = (G − C) / (G + C) (Perna & Kocher 1995).

Comparison of Mitochondrial Gene Order

The software CREx63 (Bernt et al. 2007) was used to conduct pairwise comparisons of the mitogenomes orders within Cirratuliformia taxa. CREx inferred the most plausible scenarios for gene rearrangements based on common intervals.

Mitogenome Phylogeny

All taxa in Table 2.1 were included in the analysis including unverified or unpublished GenBank sequences. Cirratulidae was used as the outgroup to root the tree using three published cirratulid mitogenomes. The dataset used the 13 protein coding genes (PCGs) of the mitogenome either as nucleotides or amino acid translations, mitochondrial *12S rRNA* (*12S*) and *16S*, and nuclear *18S* and *28S*. Individual genes were aligned in Mesquite v.3.7 (Maddison & Maddison 2023) using MAFFT (Katoh & Standley 2013) with default settings for the rRNA genes and Muscle (Edgar 2004) with default settings for the other genes. The 17 gene partitions were concatenated using SequenceMatrix (Vaidya et al. 2011), and a maximum likelihood analysis was run once with PCGs as amino acids and once with PCGs as nucleotides using RAxML-NG (Kozlov et al. 2019) and RAxML GUI v.2.0 (Edler et al. 2020). Optimal models were chosen for each partition using the RAxML GUI interface and are shown in Table 2.3. Node support was assessed through bootstrapping with 1000 pseudoreplicates. The mitogenome maximum likelihood tree was visualized using FigTree (Rambaut 2009) and enhanced with Adobe Illustrator (Adobe Inc. 2019).

RESULTS

The maximum likelihood analysis using the 17 gene dataset recovered both families, Flabelligeridae and Acrocirridae, as monophyletic (Figure 2.1). The nucleotide only analysis differs from the PCGs as amino acid translations analysis by *Flota* sp. and *Flabesymbios commensalis* forming a clade with 58% support sister to the clade of *Poeobius meseres* and *Pherusa bengalensis*. Within Acrocirridae there are three clades, two benthic and one pelagic. One benthic clade consists of *Macrochaeta* and *Acrocirrus* while the other consists of

Flabelligena sp. and *Flabelligella macrochaeta*. All nodes have over 50% bootstrap support with all being 100% supported in either the amino acid or nucleotide analysis except the node supporting the clade of *Poeobius meseres* and *Pherusa bengalensis* and the node supporting the benthic clade *Flabelligena* and *Flabelligella* as sister to the pelagic acrocirrid clade.

Complete, circularized mitogenomes from a single contig were found with the following coverages: 20X (*Acrocirrus validus*), 73X (*Flabelligella* macrochaeta), 77X (*Flabelligena* sp.), 64X (*Flabesymbios* commensalis), 11X (*Flota* sp.), 75X (*Poeobius meseres*), 66X (*Macrochaeta* cf. *westheidei*), 20X (*Macrochaeta pege*), 191X (*Swima bombiviridis*), 123X (*Swima fulgida*), 142X (*Swima tawitawiensis*), 35X (*Teuthidodrilus australis* n. sp.), and 86X (*Teuthidodrilus samae*). Mitogenome sizes are included in Table 2.4 as well as in the center of their complete assembled mitochondrial genomes (Figure 2.2-2.14).

The putative control region (CR) within Cirratuliformia is found between *tRNA L1* / *tRNA L2* (*Cirriformia* cf. *tentaculata* and *Timarete posteria*), *tRNA N* / *16S* (*Raricirrus* sp.), *tRNA I* / *tRNA N* (*Flabesymbios commensalis, Flota* sp., and *Pherusa bengalensis*), *tRNA C* / *tRNA I* (*Poeobius meseres*), *tRNA I* / *tRNA K* (*Acrocirrus validus, Swima bombiviridis, Swima fulgida, Swima tawitawiensis, Teuthidodrilus australis* n. sp., and *Teuthidodrilus samae*), *ND4* / *tRNA-C* (*Flabelligella macrochaeta*), *tRNA E* / *tRNA S1* (*Flabelligena* sp.), *tRNA K* / *ND3* (*Macrochaeta* cf. *westheidei* and *Macrochaeta* sp.), and *tRNA I* / *tRNA S1* (*Macrochaeta pege*). Excluding tRNAs, which are highly variable, the CR is found between *16S* / *ND1* (*Cirriformia* cf. *tentaculata* and *Timarete posteria*), *COI* / *16S* (*Raricirrus* sp.), *ND1* / *COX2* (*Flabesymbios commensalis, Flota* sp., and *Pherusa bengalensis*), *ND4* / *12S* (*Poeobius meseres*), *ND1* / *ND3* (*Acrocirrus validus*, *Macrochaeta* cf. *westheidei*, *Macrochaeta* sp., *Swima bombiviridis, Swima fulgida, Swima tawitawiensis, Teuthidodrilus australis* n. sp., and *Teuthidodrilus samae*), *ND4* /

12S (*Flabelligella macrochaeta*) and *ND3* / *ND2* (*Flabelligena* sp. and *Macrochaeta pege*). The length of the CR for each species is as follows: *Cirriformia* cf. *tentaculata* 524 bp, *Raricirrus* sp. 443 bp, *Timarete posteria* 532 bp, *Flabesymbios commensalis* 604 bp, *Flota* sp. 1943 bp, *Pherusa bengalensis* 952 bp, *Poeobius meseres* 2472 bp, *Acrocirrus validus* 897 bp, *Flabelligella macrochaeta* 808 bp, *Flabelligena* sp. 950 bp, *Macrochaeta* cf. *westheidei* 1231 bp, *Macrochaeta pege* 1013 bp, *Macrochaeta* sp. 1366 bp, *Swima bombiviridis* 1540 bp, *Swima fulgida* 1267 bp, *Swima tawitawiensis* 1692 bp, *Teuthidodrilus same* 1364 bp, *Teuthidodrilus australis* n. sp. 654 bp.

Other notable non-coding regions (>50 bp) include: *Raricirrus* sp. between *COX2 / ATP8* (66 bp) and *tRNA-S1 / ND2* (70 bp), *Timarete posteria* between *tRNA-V / 16S* (55 bp), *Flabesymbios commensalis* between *CYTB / tRNA-H* (101 bp), *tRNA-E / tRNA-C* (63 bp), *tRNA-C / 12S* (60 bp), *tRNA-L2 / tRNA-G* (525 bp), *ND6 / tRNA-W* (123 bp), *tRNA-R / tRNA-S* (100 bp), *ND2 / ND5* (84 bp), *ND4 / tRNA-M* (70 bp), and *tRNA-S2 / ND1* (62 bp). *Flota* sp. between *tRNA-Q / ND6* (52 bp), *tRNA-K / ND5* (61 bp), *tRNA-V / 16S* (173 bp), and *16S / tRNA-L* (55 bp), *Poeobius meseres* between *tRNA-I / tRNA-M* (164 bp) and *ND1 / tRNA-N* (220 bp), *Acrocirrus validus* between *16S / tRNA-L* (58 bp) and *tRNA-V / 16S* (159 bp), *Flabelligella macrochaeta* between *tRNA-V / 16S* (150 bp) and *ND1 / tRNA-I* (609 bp), *Flabelligena* sp. between *tRNA-G / COX3* (94 bp), *tRNA-C / tRNA-M* (213 bp), *tRNA-I / tRNA-T* (81 bp), *tRNA-P / ND3* (70 bp), and *ND3 / tRNA-E* (91 bp), *Macrochaeta pege* between *tRNA-V / 16S* (87 bp) and *ND1 / tRNA-K* (59 bp), and *Macrochaeta* sp. between *ND2 / COI* (93 bp), *tRNA-V / 16S* (158 bp), *16S / tRNA-L* (55 bp), and *tRNA-I / tRNA-K* (112 bp).

All 13 mitochondrial PCGs, 22-23 tRNAs, and both ribosomal genes were recovered in all complete mitogenomes with all genes encoded on the same strand with unique gene orders

presented in Figure 2.15. All taxa have duplications of *tRNA-L* and *tRNA-S* and duplications of *tRNA-M* are present in the following species: *Cirriformia* cf. *tentaculata*, *Raricirrus* sp., *Timarete posteria*, and *Flota* sp. (Figure 2.15A-B, D). Gene order is highly variable within Cirratuliformia with nine different arrangements including tRNAs, *Pherusa bengalensis* (Figure 2.15E) has the same order as *Flota* sp. (Figure 2.15D) but lacks a duplicated *tRNA-M* and *Macrochaeta* cf. *westheidei* and *Macrochaeta* sp. (Figure 2.15J) have the same gene order as the swimming acrocirrids and *Acrocirrus validus* as they only differ by the position of the CR so considered here an identical gene order. When excluding *tRNAs*, there are five different arrangements. When excluding the variable position of the non-coding CR, *Poeobius meseres* (Figure 2.15P) has the same gene order as *Flota* sp. and *Pherusa bengalensis* (Figure 2.15O), and all the acrocirrids (Figure 2.15Q-S) share the same gene order. Inferred genomic rearrangements including *tRNAs* are presented in Table 2.5 as a pairwise distance matrix and inferred genomic rearrangements excluding *tRNAs* are mapped onto the mitogenome phylogeny in Figure 2.16 with the putative ground pattern for Cirratulidae suggested by Struck et al. 2023.

There are gene overlaps between adjacent PCGs between *ND4L* and *ND4* (7 bp) in all mitogenomes and *ND6* and *CYTB* (8 bp) in all mitogenomes except *Cirriformia* cf. *tentaculata*, *Timarete posteria*, *Flabesymbios commensalis, Macrochaeta* cf. *westheidei*, *Macrochaeta pege*, and *Macrochaeta* sp. There are also additional overlaps between PCGs, tRNAs, and both PCGs and tRNAs included in Table 2.6. Noteworthy overlaps include between *ND2* and *COI* (23 bp) for *Pherusa bengalensis*, between *COX3* and *tRNA-Q* (5 bp) for *Acrocirrus validus, Macrochaetae* cf. *westheidei*, *Macrochaeta pege*, and *Macrochaeta* sp., between *COI* and *tRNA-K* (16 bp) for *Flabesymbios commensalis*, and between *12S* and *tRNA-V* (5-8 bp) for *Cirriformia* cf. *tentaculata*, *Flota* sp. and *Macrochaeta* sp.,

All mitogenomes are AT rich (>52%) with flabelligerids and acrocirrids being noticeably more AT rich than cirratulids (Table 2.4). T is slightly more frequent than A in all except *Macrochaeta* sp. where T is almost double A and *Pherusa bengalensis* and *Raricirrus* sp. which have more A than T. C is less frequent than A or T except in *Raricirrus* sp. where it is most frequent. G is least frequent in all mitogenomes except *Macrochaeta* sp. where G is more frequent than C but less than A or T (Table 2.4). AT-skew is negative for all mitogenomes except *Pherusa bengalensis* and *Raricirrus* sp. and GC-skew is negative for all mitogenomes except *Macrochaeta* sp. The GC-skew is more pronounced than the AT-skew in all mitogenomes except *Flabesymbios commensalis* that has a slightly lower GC-skew, *Flabelligena* sp. where the AT-skew is slightly higher, and *Macrochaeta* sp. where GC-skew is weaker than a more pronounced AT-skew (Table 2.4).

All PCGs for all newly assembled mitogenomes, *Cirriformia* cf. *tentaculata*, and *Pherusa bengalensis* have start codon ATG. *Timarete posteria* has one TTG start codon, while *Raricirrus* sp. has 4 ATA start codons and *Macrochaeta* sp. has 5 ATA and 1 ATT start codons. It should be noted that both *Raricirrus* sp. and *Macrochaeta* sp. are unverified by NCBI GenBank and the PCGs could have an ATG start. The most common stop codon was TAA occurring 13 times in *Flabesymbios commensalis*, 12 times in *Poeobius meseres*, 11 times in *Timarete posteria*, 10 times in *Pherusa bengalensis*, 9 times in *Cirriformia* cf. *tentaculata*, *Flota* sp., *Flabelligella macrochaeta*, and *Macrochaeta pege*, 8 times in *Raricirrus* sp., *Swima bombiviridis, Swima fulgida, Teuthidodrilus australis* n. sp., and *Teuthidodrilus samae*, 7 times in *Acrocirrus validus* and *Swima tawitawiensis*, 6 times in *Macrochaeta* cf. *westheidei* and *Flabelligena* sp., and 5 times in *Macrochaeta* sp. TAG was the stop codon 3 times in *Cirriformia* cf. *tentaculata*, *Raricirrus* sp., *Pherusa bengalensis*, and *Macrochaeta* cf. *westheidei*, 2 times in *Flota* sp.,

Acrocirrus validus, *Macrochaeta* sp., *Flabelligena* sp., and *Swima tawitawiensis*, and once in *Timarete posteria*, *Macrochaeta pege*, *Swima bombiviridis*, *Swima fulgida*, *Teuthidodrilus australis* n. sp., and *Teuthidodrilus samae*. Truncated stop codons (T, TA) occurred 6 times in *Macrochaeta* sp., 5 times in *Flabelligena* sp., 4 times in *Acrocirrus validus, Flabelligella macrochaeta*, *Macrochaeta* cf. *westheidei*, all *Swima* sp., and both *Teuthidodrilus* sp., 3 times in *Macrochaeta pege*, 2 times in *Raricirrus* sp. and *Flota* sp., and 1 time in *Cirriformia* cf. *tentaculata*, *Timarete posteria*, and *Poeobius meseres.*

Codon usage bias is favored toward NNA as the most common followed by NNT, then NNC, and NNG being the least frequent (Table 2.7). This pattern differs for all three cirratulids with NNC being the most used for *Cirriformia* cf. *tentaculata* and *Raricirrus* sp. and NNC being more frequent than NNT for *Timarete posteria*. *Flabesymbios commensalis* differs with NNC as the most frequent, *Flabelligena* sp. differs with NNT the most frequent, *Macrochaeta* sp. differs with NNT the most frequent and NNC the least frequent, and *Teuthidodrilus australis* n. sp. differs with NNC being more frequent than NNT (Table 2.7). Relative synonymous codon usage (RSCU) analysis reveals that those with A and T occur more often than G and C with some exceptions: *Cirriformia* cf. *tentaculata* (Arginine, Asparagine, Aspartic acid, Cysteine, Histidine, and Tyrosine), *Raricirrus* sp. (Alanine, Asparagine, Aspartic acid, Cysteine, Histidine, Isoleucine, Phenylalanine, Tyrosine), *Timarete posteria* (Asparagine, Aspartic acid, Cysteine, Histidine, and Tyrosine), *Flota* sp. (Aspartic acid), *Pherusa bengalensis* (Histidine), *Acrocirrus validus* (Cysteine), *Flabelligella macrochaeta* (Aspartic acid), *Macrochaeta* sp. (Glutamic acid, Glycine, and Tryptophan), *Teuthidodrilus australis* n. sp. (Alanine, Cysteine, Glycine, Histidine, and Tyrosine), and *Teuthidodrilus samae* (Alanine, Aspartic acid, Cysteine, Glycine, and Histidine) (Figure 2.17-2.20). Three of the four most common codons (ATT, TTA, and TTT)

encode for three of the four most common amino acids (Isoleucine, Leucine, and Phenylalanine) with amino acid frequencies shown in Figure 2.21-2.24.

DISCUSSION

The maximum likelihood analysis on the mitogenome dataset revealed four observations. First, the combined clade of Acrocirridae and Flabelligeridae were both recovered as monophyletic families that are sister to Cirratulidae consistent with the tree presented by Rouse 2001. Second, the swimming clade of acrocirrids was recovered along with two benthic acrocirrid clades, one consisting of *Acrocirrus* and *Macrochaeta* and the other *Flabelligella* and *Flabelligena.* Third, this tree confirms with DNA evidence the delineation of *Flabelligella* as a separate genus sister to *Flabelligena.* Lastly, this tree provides further evidence supporting three independent origins of pelagicism as parsimony principles suggest that *Flota* sp. and *Poeobius meseres* came to be pelagic independently of one another, the same conclusion as Osborn & Rouse 2008, and the maximum likelihood analysis using only nucleotides recovered two independent origins. The mitogenome phylogeny is highly supported with all nodes above 62% bootstrap support, and the phylogeny provides further support to the findings of Chapter 1 and clarity to the relationship between *Flabelligella* and *Flabelligena*.

All cirratuliform mitogenomes for this study are between 15350 and 17500 bp, which is mostly consistent with the usual mitogenome size of annelids which is around 16000 bp (Weigert & Bleidorn 2016). Notable larger mitogenome sizes include: *Swima tawitawiensis* (16402 bp), *Flabesymbios commensalis* (16629 bp), *Flota* sp. (16793 bp), and *Poeobius meseres* (17500 bp). The control region is highly variable in annelids (Cejb et al. 2022), and this study provides further support to this as the CR is found in 9 different locations including *tRNAs* and 6 different locations excluding *tRNAs*. The length of the CR also varies between 443-2472 bp. While the

benthic taxa tend to have shorter CR length, 443-1366 bp, than the pelagic taxa, 654-2472 bp, the lengths overlap with some benthic acrocirrids like *Macrochaeta* having a long, 1013-1366 bp, CR and the pelagic acrocirrid *Teuthidodrilus australis* n. sp. having a shorter CR, 654 bp. *Flabesymbios commensalis*, *Flota* sp., *Poeobius meseres*, *Flabelligella macrochaeta*, *Flabelligena* sp., *Macrochaeta* sp., *Swima bombiviridis, Swima tawitawiensis*, and *Teuthidodrilus samae* all have a CR longer than 1600 bp. All taxa except *Cirriformia* cf. *tentaculata*, *Pherusa bengalensis*, *Macrochaeta* cf. *westheidei*, and the pelagic acrocirrids have at least one other non-coding region besides the CR that is at least 50 bp.

The gene order of Acrocirridae from this study were consistent with the ancestral pattern of Sedentaria Lamarck, 1818 suggested by Weigert et al. 2016 (Figure 2.15), while Cirratulidae and Flabelligeridae both showed two different arrangements between three taxa. Pelagic and deep-sea taxa showed identical gene orders to benthic relatives in Cirratuliformia. This finding is consistent with work on other invertebrates like vesicomyids, alvinocaridids, and actiniids that have found that gene order is often the same in deep sea taxa as compared to shallower relatives suggesting that gene order may not always be affected by mitochondrial evolution (Yang et al. 2019, Yu et al. 2015, Zhang et al. 2017). All cirratuliform mitogenomes have slightly more T than A except *Raricirrus* sp. and *Pherusa bengalensis*, while the mitogenomes also have approximately a quarter more C than G except *Macrochaeta* sp. Gene content differs slightly between cirratuliform taxa, but there are as many differences between all taxa as there are between benthic and pelagic relatives of the same family suggesting that the evolution of gene content of the mitogenome has undergone relatively few changes and a better understanding of genome nucleotide skews can explain or predict gene rearrangements (Sahyoun et al. 2014).

The assembly of 13 mitogenomes and the 5 mitogenomes available on GenBank provide the first complete mitogenome data for Cirratuliformia. While looking at gene content and gene order has not revealed a clear explanation for how the different evolutionary pressures of deep-sea and shallow taxa have shaped their individual mitogenomes, there are future directions that could help answer these questions. More care should be taken into looking at the variation and conserved regions in *tRNAs* within the mitogenomes of benthic and pelagic cirratuliforms. The *tRNAs* are essential for protein synthesis and its co-evolution with molecular components and the genetic code make it a prime candidate of study to better understand evolutionary relationships (Farias et al. 2014; Lei and Burton 2020). Additionally, a natural selection analysis would provide evidence for the different selection pressures between shallow and deep-sea taxa. Mitogenomes typically have a higher mutation rate than nuclear genomes and generally are affected by strong purifying selection that does not favor new variants, but organisms in extreme conditions such as the deep-sea environment have shown more adaptive evolution through a relaxation of the purifying selection as has been reported in deep-sea fish and annelids (Castellana et al. 2011; Shen et al. 2019; Zhang et al. 2018). Finally, this work could be advanced through the addition of more assembled genomes from Cirratuliformia.

Chapter 2 of this study provides the first cirratuliform phylogeny constructed using whole mitochondrial genome data. The tree presented in Figure 2.1 shows high support where the trees generated in Chapter 1 had low to moderate support, such as the nodes supporting *Macrochaeta* and *Swima* (Figure 1.7-1.8). In Chapter 1, the swimming clade of acrocirrids is mostly resolved except the ambiguous positioning of the Juanita Worm. This worm is an important link in the evolutionary story as it is nearly benthic with less pelagic characteristics than *Teuthidodrilus* making it a prime candidate for mitogenome assembly to gain a better understanding of the

benthic to pelagic habitat transition within Acrocirridae (Osborn & Rouse 2011). It would also prove valuable to skim the genome of the three other new species from Chapter 1 with an emphasis on *Paraswima*, so that the mitogenome can be compared to the closely related *Swima*. The assembly of 13 cirratuliform mitogenomes added to the 5 mitogenomes previously published and not only improved the resolution of the Cirratuliformia phylogeny, but also provides data for future work to explore the evolutionary history of benthic worms and their pelagic relatives.

Table 2.1: Specimens chosen for whole mitogenome analyses. **Bold** sequence represents new whole mitochondrion. Holotype = *. ( ) in the voucher column represent a sequence identifier since no voucher information was provided by the authors.

Family	Species	Whole mitochondrion	18S rRNA	28S rRNA	Voucher	Location	Coordinates	Depth (m)
Cirratulidae	*Cirriformia* cf. *tentaculata* (Choi *et al.* 2017)	MG267394	-	-	MABIK:NA00146076-NA00146078	South Korea: Sea of Japan	-	-
	Raricirrus sp. (Sevigny *et al.* 2021)	MT877126	-	-	(MDD02-FG02-Achotines-C1)	Panama	9.540° N; 79.675° W	0.2
	Timarete posteria (Kim *et al.* 2019)	MK105766	-	-	MABIK:NA00146235	South Korea: Sea of Japan	-	-
Flabelligeridae	*Flabesymbios commensalis*	**OR166196**	-	**OQ813500**	SIO:BIC:A14246	USA: La Jolla, CA	32.830° N; 117.290° W	-
	Flabesymbios commensalis	-	HQ326965	-	SIO:BIC:A1843	USA: Malibu, CA	34.026° N; 118.780° W	-
	Flota sp.	**OQ807203**	-	-	SIO:BIC:A14078	Mexico: Red Hill, Jaich Maa Vent Field	23.942° N; 108.855° W	2319
	Flota sp.	-	EU694116	EU694122	SIO:BIC:A1131	USA: Monterey, CA	36.335° N; 122.917° W	3452
	Pherusa bengalensis (unpublished)	MZ557347	-	-	-	China: Bohai Sea of China	-	-
	Poeobius meseres	**OQ807199**	-	-	SIO:BIC:A9529	Chile: Southeast of Stockman Guyot	25.406° S; 81.742° W	1065
	Poeobius meseres	-	EU694115	EU694123	SIO:BIC:A1130	USA: Monterey, CA	35.766° N; 122.834° W	1801
Acrocirridae	*Acrocirrus validus*	**OQ807197**	-	**OQ804812**	SIO:BIC:A4142	Japan: Suruga Bay	34.843° N; 138.763° E	4-10
	Acrocirrus validus	-	FJ944491	-	SIO:BIC:A1290	Japan: Hayama, Sagami Bay	35.269° N; 139.567° E	-
	Flabelligella macrochaeta	**OR166197**	**OQ804406**	**OQ804813**	SIO:BIC:A9789	Costa Rica: Seamount 3	8.542° N; 85.153° W	1248
	Flabelligena sp.	**OQ807198**	EU694120	EU694121	SIO:BIC:A1126	Chile: Saguaro Field, Pacific Antarctic Ridge	31.863° S; 112.042° W	2334
	Macrochaeta cf. *westheidei*	**OQ807196**	-	**OQ804814**	SIO:BIC:A4873	Belize: Carrie Bow Cay	16.803° N; 88.078° W	15
	Macrochaeta cf. *westheidei*	-	EU700414	-	SIO:BIC:A1127	Belize	16.803° N; 88.078° W	17
	Macrochaeta pege	**OQ807200**	**OQ804407**	**OQ804815**	SIO:BIC:A15670	USA: Off Reid Rock, Washington	48.549° N, 122.992° W	100
	Macrochaeta sp. (Sevigny *et al.* 2021)	MT877119	-	-	(MD01-Achotines-A1)	Panama	7.41° N; 80.18° W	31.4
	Swima bombiviridis	**OQ807202**	-	-	SIO:BIC:A14014	Mexico: Dianne's Vent, Auka Vent Field	23.956° N, 108.864° W	2945.2
	Swima bombiviridis	-	GQ422143	GQ422144	SIO:BIC:A1282	USA: Monterey, CA	36.317°′N; 122.911°W	3054
	Swima fulgida	**OQ807201**	-	-	SIO:BIC:A14013	Mexico: Dianne's Vent, Auka Vent Field	23.956° N, 108.864° W	2945.2
	Swima fulgida	-	FJ944497	-	SIO:BIC:A1285	USA: Monterey, CA	35.767°N; 122.833°W	3267
	Swima fulgida	-	-	FJ944519	SIO:BIC:A1286	USA: Monterey, CA	36.342° N; 122.917° W	3478
	Swima tawitawiensis	**OQ807206**	-	-	WAM:VER:V9829	Australia: Cape Range Canyon, Western Australia	21.844° S; 113.014° E	2496.5
	Swima tawitawiensis	-	FJ944499	FJ944520	NMA:04327	Philippines: Celebes Sea	4.967°′N; 120.233°E	2836
	Teuthidodrilus australis n. sp.	**OQ807205**	**OQ724829**	**OQ724825**	WAM:VER:V9804*	Australia: Cape Range Canyon, Western Australia	21.942° S; 113.121° E	2175.7
	Teuthidodrilus samae	**OQ807204**	-	-	MCZ:IZ:70357	Ecuador: Galápagos Rift	0.766° N; 85.899° W	2555
	Teuthidodrilus samae	-	FJ944503	FJ944524	NMA:04342	Philippines: Celebes Sea	4.962°N; 120.162°E	2830

Table 2.2: Total number, total length, individual length of genome skimming raw reads from Novogene, and the number of reads retained after using Trimmomatic.

Family	Species	Total Number of Raw Reads (Paired-End)	Total Length of Raw Reads (Paired-End)	Individual Length of Raw Reads	Number of Reads Post-Trimmomatic (Paired-End)
Flabelligeridae	*Flabesymbios commensalis*	6,923,380	1,038,507,000	150	6,794,630 (98.14%)
	Flota sp.	6,828,177	1,024,226,550	150	6,670,131 (97.69%)
	Poeobius meseres	6,983,200	1,047,480,000	150	6,858,060 (98.21%)
Acrocirridae	*Acrocirrus validus*	7,168,425	1,075,263,750	150	7,009,409 (97.78%)
	Flabelligella macrochaeta	8,658,040	1,298,706,000	150	8,480,893 (97.95%)
	Flabelligena sp.	7,487,919	1,123,187,850	150	7,295,602 (97.43%)
	Macrochaeta cf. *westheidei*	9,787,539	1,468,130,850	150	9,617,555 (98.26%)
	Macrochaeta pege	7,944,475	1,191,671,250	150	7,695,764 (96.87%)
	Swima bombiviridis	8,059,451	1,208,917,650	150	7,851,022 (97.41%)
	Swima fulgida	8,670,616	1,300,592,400	150	8,466,184 (97.64%)
	Swima tawitawiensis	11,764,067	1,764,610,050	150	11,459,145 (97.41%)
	Teuthidodrilus australis n. sp.	8,191,469	1,228,720,350	150	7,935,472 (96.87%)
	Teuthidodrilus samae	8,532,438	1,279,865,700	150	8,308,342 (97.37%)

Table 2.3: Data type, nucleotide (NT) or amino acid (AA), and RAxML model test results for individual genes in the 30 gene concatenated dataset for mitogenome maximum likelihood analysis.

Gene	Data Type	Substitution Model	Stationary Frequencies	Proportion of Invariant Sites	Rate Heterogeneity
12S rRNA	NT	GTR	+F (empirical)	+I (ML estimate)	+GAMMA (mean)
16S rRNA	NT	TIM2	+F (empirical)	+I (ML estimate)	+GAMMA (mean)
18S rRNA	NT	TN93	+F (empirical)	+I (ML estimate)	+GAMMA (mean)
28S rRNA	NT	TIM3	-	-	+GAMMA (mean)
ATP6	AA	MTZOA	+F (empirical)	-	+GAMMA (mean)
ATP6	NT	GTR	+F (empirical)	+I (ML estimate)	+GAMMA (mean)
ATP8	AA	MTREV	-	-	+GAMMA (mean)
ATP8	NT	TPM3uf	+F (empirical)	-	+GAMMA (mean)
COI	AA	MTZOA	-	+I (ML estimate)	+GAMMA (mean)
COI	NT	GTR	+F (empirical)	+I (ML estimate)	+GAMMA (mean)
COX2	AA	MTREV	+F (empirical)	-	+GAMMA (mean)
COX2	NT	TIM3	+F (empirical)	-	+GAMMA (mean)
COX3	AA	MTZOA	-	+I (ML estimate)	+GAMMA (mean)
COX3	NT	TVM	+F (empirical)	+I (ML estimate)	+GAMMA (mean)
CYTB	AA	MTZOA	-	+I (ML estimate)	+GAMMA (mean)
CYTB	NT	TIM2	+F (empirical)	+I (ML estimate)	+GAMMA (mean)
ND1	AA	MTZOA	+F (empirical)	+I (ML estimate)	+GAMMA (mean)
ND1	NT	TIM2	+F (empirical)	+I (ML estimate)	+GAMMA (mean)
ND2	AA	MTMAM	+F (empirical)	+I (ML estimate)	+GAMMA (mean)
ND2	NT	GTR	-	+I (ML estimate)	+GAMMA (mean)
ND3	AA	MTMAM	-	+I (ML estimate)	+GAMMA (mean)
ND3	NT	TIM2	+F (empirical)	+I (ML estimate)	+GAMMA (mean)
ND4	AA	MTZOA	+F (empirical)	-	+GAMMA (mean)
ND4	NT	TVM	+F (empirical)	+I (ML estimate)	+GAMMA (mean)
ND4L	AA	MTREV	-	-	+GAMMA (mean)
ND4L	NT	K81uf	+F (empirical)	+I (ML estimate)	+GAMMA (mean)
ND5	AA	MTART	+F (empirical)	+I (ML estimate)	+GAMMA (mean)
ND5	NT	TVM	+F (empirical)	+I (ML estimate)	+GAMMA (mean)
ND6	AA	MTREV	+F (empirical)	+I (ML estimate)	+GAMMA (mean)
ND6	NT	GTR	+F (empirical)	+I (ML estimate)	+GAMMA (mean)

Table 2.4: Mitochondrial genome length, nucleotide frequencies, and nucleotide skews.

Family	Species	Length (bp)	A (%)	T (%)	G (%)	C (%)	AT (%)	GC (%)	AT Skew	GC Skew
Cirratulidae	*Cirriformia* cf. *tentaculata*	15495	29.45	30.04	13.60	26.91	59.49	40.51	-0.009763506	-0.3283416
	Raricirrus sp.	15696	26.99	25.66	14.91	32.44	52.65	47.35	0.025411423	-0.3702906
	Timarete posteria	15497	30.39	31.60	12.82	25.19	61.99	38.01	-0.019464973	-0.3256367
Flabelligeridae	*Flabesymbios commensalis*	16629	35.34	39.52	10.21	14.93	74.86	25.14	-0.05582778	-0.1880383
	Flota sp.	16793	34.54	36.37	10.50	18.59	70.91	29.09	-0.02569701	-0.2781986
	Pherusa bengalensis	15639	33.90	31.88	12.33	21.89	65.78	34.22	0.030715397	-0.279387
	Poeobius meseres	17500	34.41	37.75	10.94	16.90	72.16	27.84	-0.046246436	-0.2142857
Acrocirridae	*Acrocirrus validus*	15544	32.02	35.54	11.93	20.50	67.56	32.44	-0.052180537	-0.2641809
	Flabelligella macrochaeta	16077	30.50	36.07	11.53	21.90	66.57	33.43	-0.08372267	-0.3101395
	Flabelligena sp.	16268	28.90	38.52	12.40	20.18	67.42	32.58	-0.142596645	-0.2388679
	Macrochaeta cf. *westheidei*	15917	33.34	38.54	10.06	18.06	71.89	28.11	-0.072364971	-0.2844693
	Macrochaeta pege	15743	35.32	37.37	10.70	16.61	72.69	27.31	-0.028137015	-0.216562
	Macrochaeta sp.	16106	26.31	42.00	18.04	13.65	68.31	31.69	-0.229776404	0.1387147
	Swima bombiviridis	16267	33.33	36.83	11.22	18.62	70.16	29.84	-0.049855428	-0.2480429
	Swima fulgida	15986	32.60	36.40	11.54	19.47	69.00	31.00	-0.055122393	-0.2558515
	Swima tawitawiensis	16402	32.93	36.62	11.39	19.05	69.55	30.45	-0.053120617	-0.2515018
	Teuthidodrilus australis n. sp.	15350	30.31	32.61	12.83	24.25	62.92	37.08	-0.036653551	-0.3078004
	Teuthidodrilus samae	16071	30.07	33.23	12.99	23.70	63.31	36.69	-0.049931197	-0.2918433

Table 2.5: Results of pairwise comparisons of mitochondrial gene orders of Cirratuliformia using common intervals with the putative ground pattern of *Cirriformia* cf. *tentaculata* and *Timarete posteria*. Scores of CREx analysis of each comparison indicate the degree of similarity where 1326 and 1400 are the highest score and represent the highest score for species without *tRNA-M2* and with *tRNA-M2,* respectively.

Species	**CT**	**RA**	**FA**	**FP**	**PM**	**AM**	**FM**	**FS**	**MP**
Cirriformia cf. *tentaculata, Timarete posteria* **(CT)**	1400	94	20	80	72	96	94	42	104
Raricirrus sp. **(RA)**	94	1400	24	74	74	116	112	44	124
Flabesymbios commensalis **(FA)**	20	24	1326	84	70	60	70	62	58
Flota sp., *Pherusa bengalensis* **(FP)**	80	74	84	1400	760	536	472	332	492
Poeobius meseres **(PM)**	72	74	70	760	1326	330	318	258	302
Acrocirrus validus, Macrochaeta cf. *westheidei, Marochaeta* sp., *Swima bombiviridis, Swima fulgida, Swima tawitawiensis, Teuthidodrilus australis* , *Teuthidodrilus samae* **(AM)**	96	116	60	536	330	1326	1190	490	1188
Flabelligella macrochaeta **(FM)**	94	112	70	472	318	1190	1326	534	1060
Flabelligena sp. **(FS)**	42	44	62	332	258	490	534	1326	460
Macrochaeta pege **(MP)**	104	124	58	492	302	1188	1060	460	1326

Table 2.6: Number of base pair overlaps between genes in the 5 prime to 3 prime direction.

Family	Species	*12S rRNA / tRNA V*	*ATP6 / tRNA H*	*ATP6 / tRNA R*	*ATP8 / tRNA Y*	*COI / tRNA K*	*COX2 / tRNA D*	*COX3 / tRNA Q*	*CYTB / tRNA W*	*ND1 / tRNA I*	*ND2 / COI*	*ND3 / tRNA S1*	*ND4 / tRNA C*	*ND4 / tRNA D*	*ND5 / tRNA F*	*ND6 / tRNA R*	*tRNA A / tRNA S2*	*tRNA F / tRNA E*	*tRNA M / 12S rRNA*	*tRNA P / tRNA T*	*tRNA S1 / ND2*	*tRNA Y / tRNA G*
Cirratulidae	*Cirriformia* cf. *tentaculata*	5	1	-	-	-	-	-	-	-	-	-	-	3	-	2	-	-	1	-	-	-
	Raricirrus sp.	-	-	2	-	-	-	-	-	-	-	-	-	-	-	-	-	-	-	-	-	-
	Timarete posteria	-	-	-	-	-	-	-	-	-	-	-	-	2	-	-	-	-	1	-	-	-
Flabelligeridae	*Flabesymbios commensalis*	-	-	3	2	16	-	-	-	1	-	-	-	-	-	-	-	-	-	-	-	-
	Flota sp.	8	-	-	2	-	2	-	-	-	-	1	2	-	-	-	-	-	-	-	-	-
	Pherusa bengalensis	-	-	-	-	-	-	-	2	1	23	2	2	-	1	-	-	-	-	-	-	-
	Poeobius meseres	-	-	-	-	-	-	-	2	-	-	-	-	-	-	-	-	-	-	1	1	-
Acrocirridae	*Acrocirrus validus*	-	-	1	2	-	2	5	1	-	1	2	-	-	-	-	-	-	-	-	-	1
	Flabelligella macrochaeta	-	-	1	1	-	-	-	2	-	-	5	-	-	-	-	-	-	-	-	-	-
	Flabelligena sp.	-	-	3	2	-	-	-	2	-	-	-	-	-	-	-	-	-	-	-	-	-
	Macrochaeta cf. *westheidei*	-	-	2	2	-	2	5	1	-	-	2	2	-	3	-	1	-	-	-	-	1
	Macrochaeta pege	-	-	2	1	-	2	5	2	-	-	-	2	-	-	-	1	1	-	-	-	-
	Macrochaeta sp.	8	-	-	1	-	2	5	1	-	-	2	-	-	-	-	1	-	2	-	-	-
	Swima bombiviridis	-	-	2	-	-	-	-	2	2	-	-	-	-	-	-	-	-	-	-	-	1
	Swima fulgida	-	-	2	-	-	-	-	2	-	-	-	-	-	-	-	-	-	-	-	-	-
	Swima tawitawiensis	-	-	2	2	-	2	-	2	-	-	-	-	-	-	-	-	-	-	-	-	-
	Teuthidodrilus australis n. sp.	-	-	-	2	-	2	-	2	2	-	-	-	-	-	-	-	-	-	-	-	1
	Teuthidodrilus samae	-	-	-	1	-	2	-	2	2	-	-	-	-	3	-	-	-	-	-	-	-

Table 2.7: Codon frequencies calculated from the mitogenome content of each species.

Family	Species	NNA (%)	NNT (%)	NNC (%)	NNG (%)
Cirratulidae	*Cirriformia* cf. *tentaculata*	32.3149528	26.403378	33.3333333	7.94833582
	Raricirrus sp.	35.4409769	15.8208955	40.6784261	8.05970149
	Timarete posteria	38.6120043	26.9292605	28.6173633	5.84137192
Flabelligeridae	*Flabesymbios commensalis*	32.3149528	26.403378	33.3333333	7.94833582
	Flota sp.	43.721307	36.9430192	15.879017	3.45665676
	Pherusa bengalensis	46.1352006	27.7673041	22.6770805	3.42041476
	Poeobius meseres	44.0755735	38.4075574	14.5748988	2.94197031
Acrocirridae	*Acrocirrus validus*	41.6688329	34.5983884	19.5736938	4.159085
	Flabelligella macrochaeta	37.5472717	33.2522961	24.1220962	5.07833603
	Flabelligena sp.	33.9280887	43.3090024	17.2749392	5.48796972
	Macrochaeta cf. *westheidei*	44.0091507	40.6062339	13.7546468	1.62996854
	Macrochaeta pege	47.3925966	39.1786004	11.1591462	2.26965685
	Macrochaeta sp.	25.433526	49.5183044	5.31241398	19.7357556
	Swima bombiviridis	43.3819557	37.817396	14.8838466	3.91680173
	Swima fulgida	42.3824959	36.358725	17.3960022	3.86277688
	Swima tawitawiensis	42.0199838	36.7809884	17.0942479	4.10477991
	Teuthidodrilus australis n. sp.	37.1590602	27.7072644	28.1123413	7.02133405
	Teuthidodrilus samae	36.0691145	29.5896328	27.4838013	6.8574514

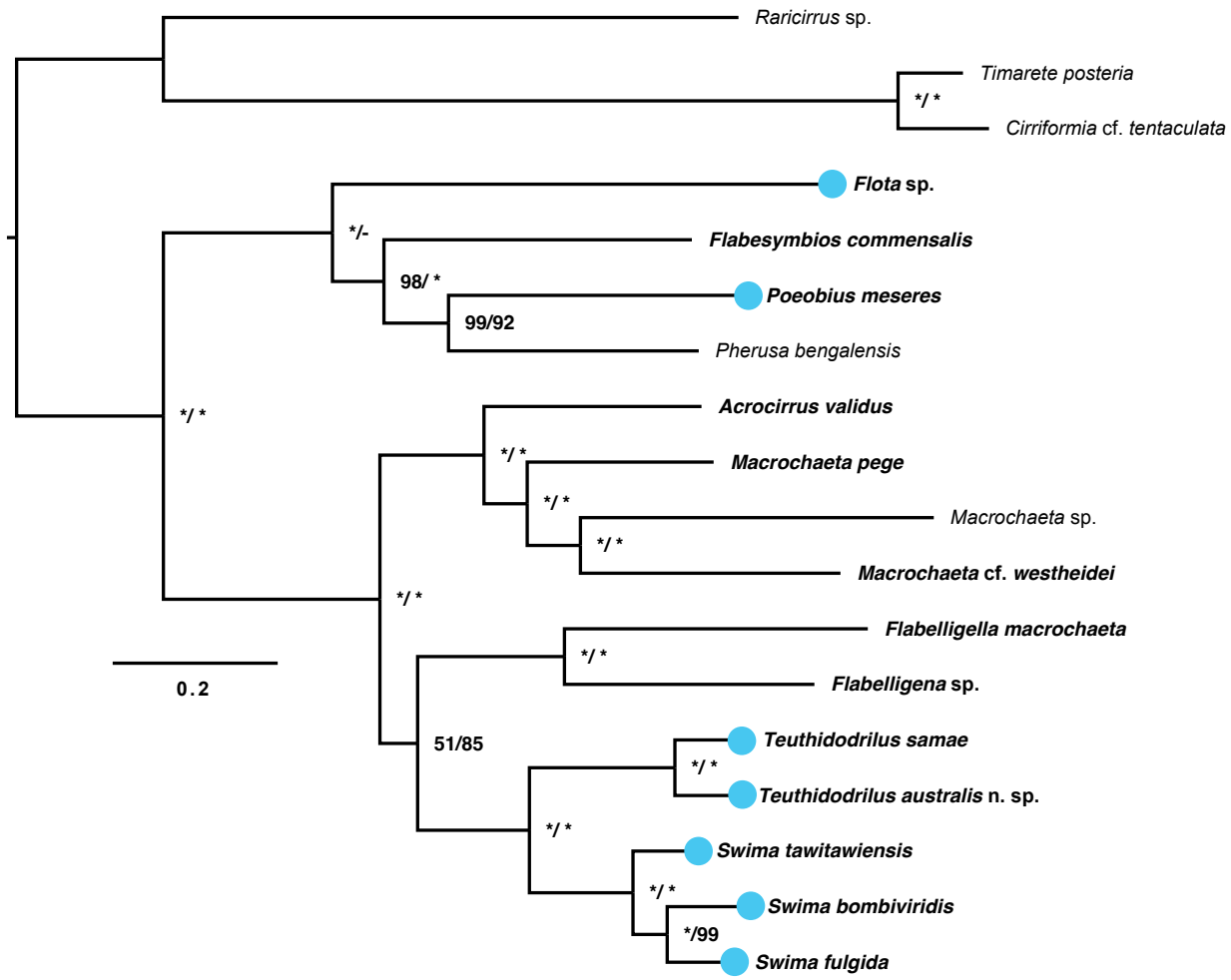

Figure 2.1: Maximum likelihood Cirratuliformia mitogenome phylogeny of 17 concatenated genes with PCGs as amino acid translations or nucleotides with data partitioned by gene with Cirratulidae as the outgroup. Nucleotide tree differs from the amino acid tree by *Flota* sp. and *Flabesymbios commensalis* forming a clade with 58% support sister to the clade of *Poeobius meseres* and *Pherusa bengalensis*. Blue circles represent pelagic taxa. Support is indicated as bootstraps from the amino acid maximum likelihood analysis/bootstraps from the nucleotide maximum likelihood analysis with asterisks representing 100% bootstrap support.

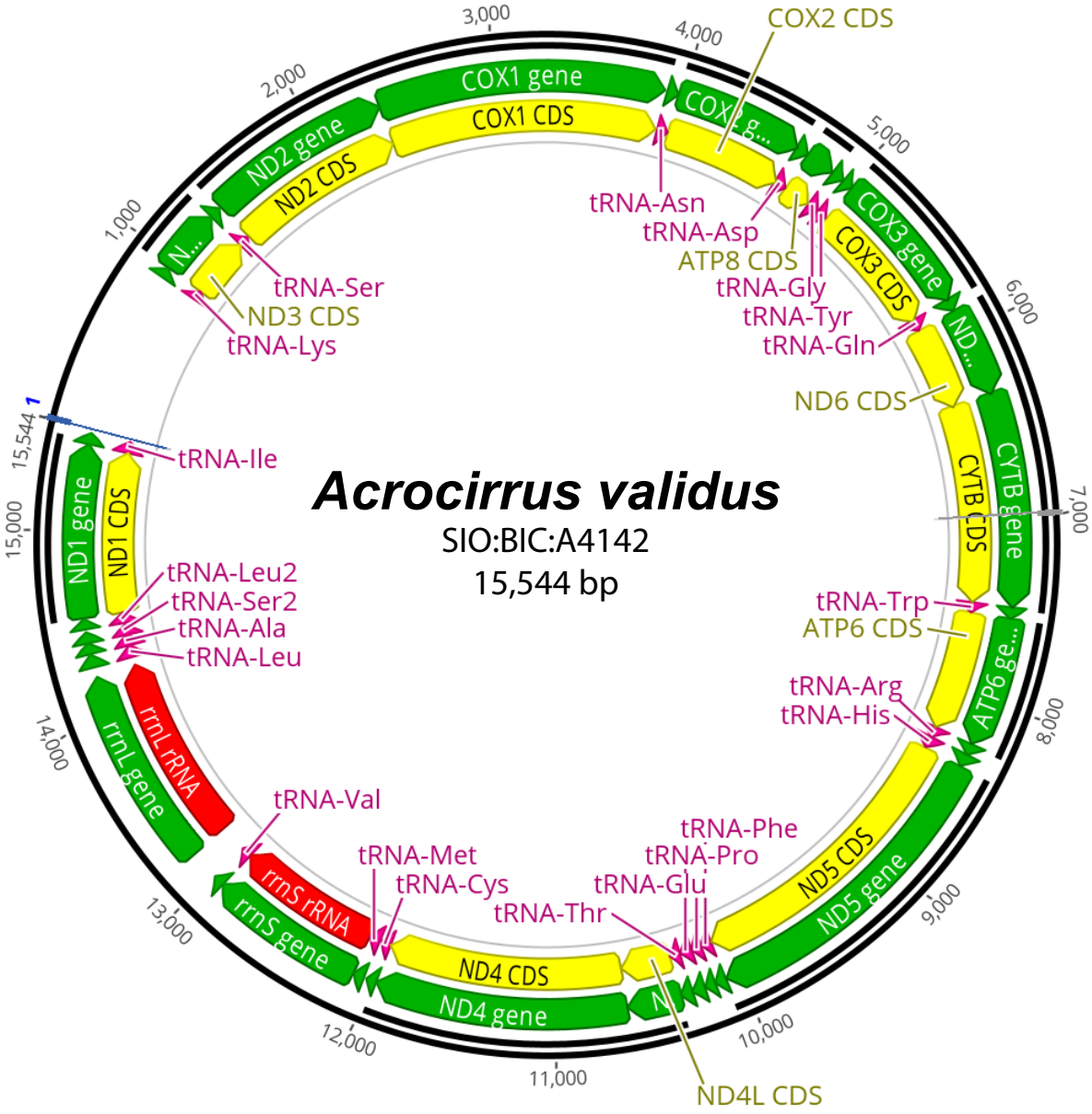

Figure 2.2: Circularized mitochondrial genome of *Acrocirrus validus*. Black outer circle is the nucleotide sequence with numbers representing individual nucleotides. Green arrows are genes, yellow arrows are protein-coding genes, red arrows are non-protein-coding genes, and pink arrows are tRNAs. The direction of the arrows is the direction of transcription.

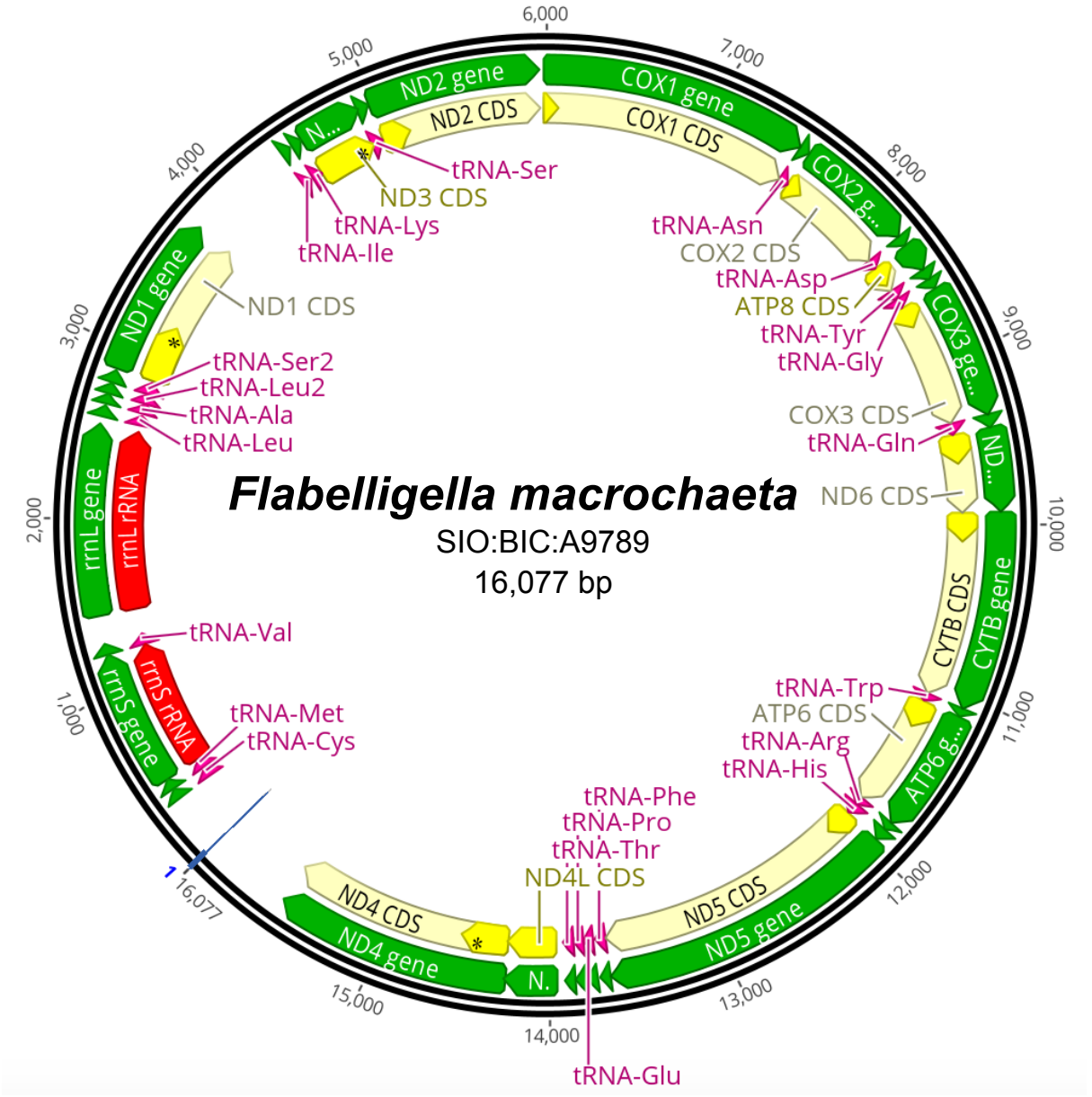

Figure 2.3: Circularized mitochondrial genome of *Flabelligella macrochaeta*. Black outer circle is the nucleotide sequence with numbers representing individual nucleotides. Green arrows are genes, yellow arrows are protein-coding genes, red arrows are non-protein-coding genes, and pink arrows are tRNAs. The direction of the arrows is the direction of transcription.

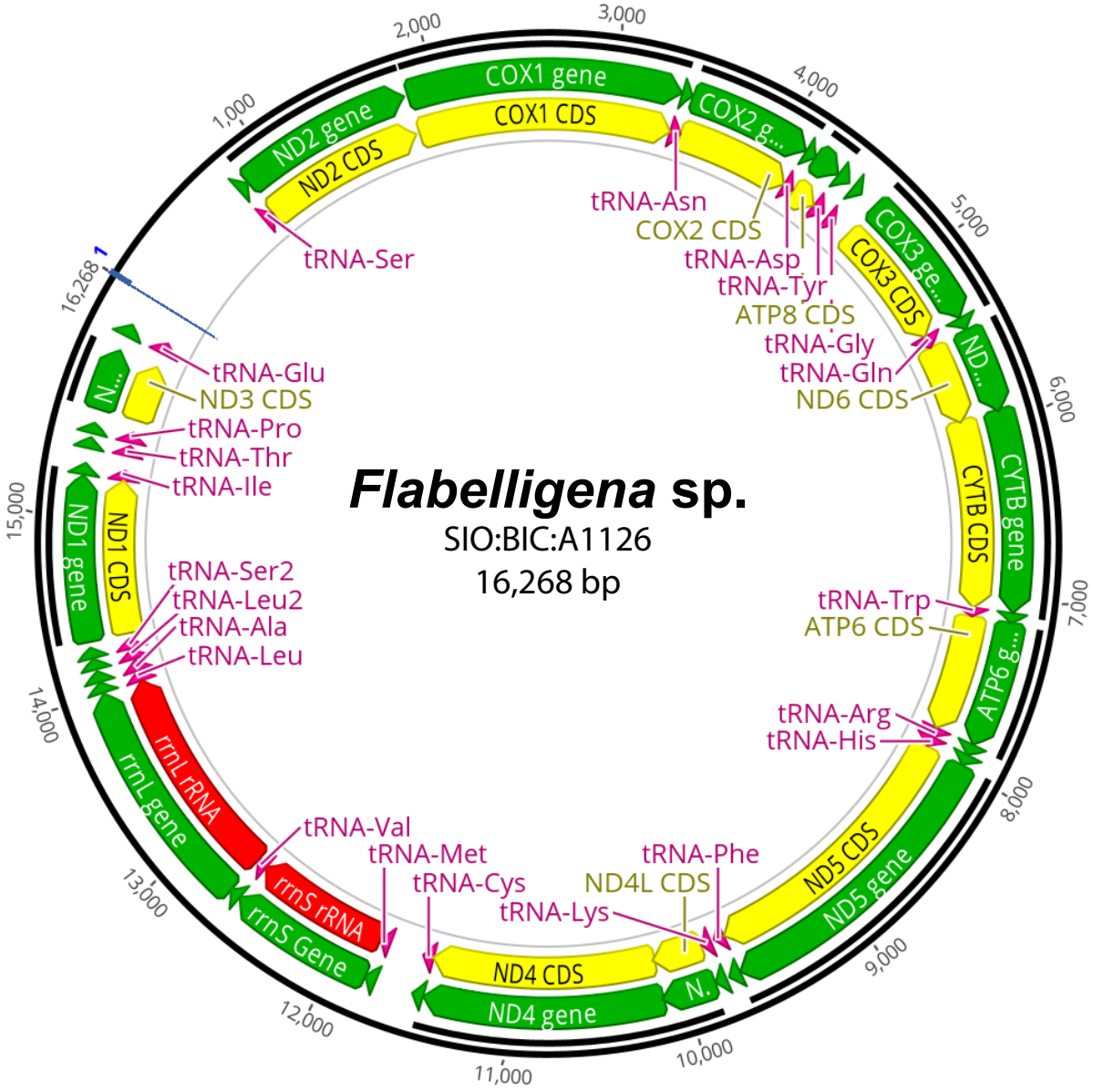

Figure 2.4: Circularized mitochondrial genome of *Flabelligena* sp. Black outer circle is the nucleotide sequence with numbers representing individual nucleotides. Green arrows are genes, yellow arrows are protein-coding genes, red arrows are non-protein-coding genes, and pink arrows are tRNAs. The direction of the arrows is the direction of transcription.

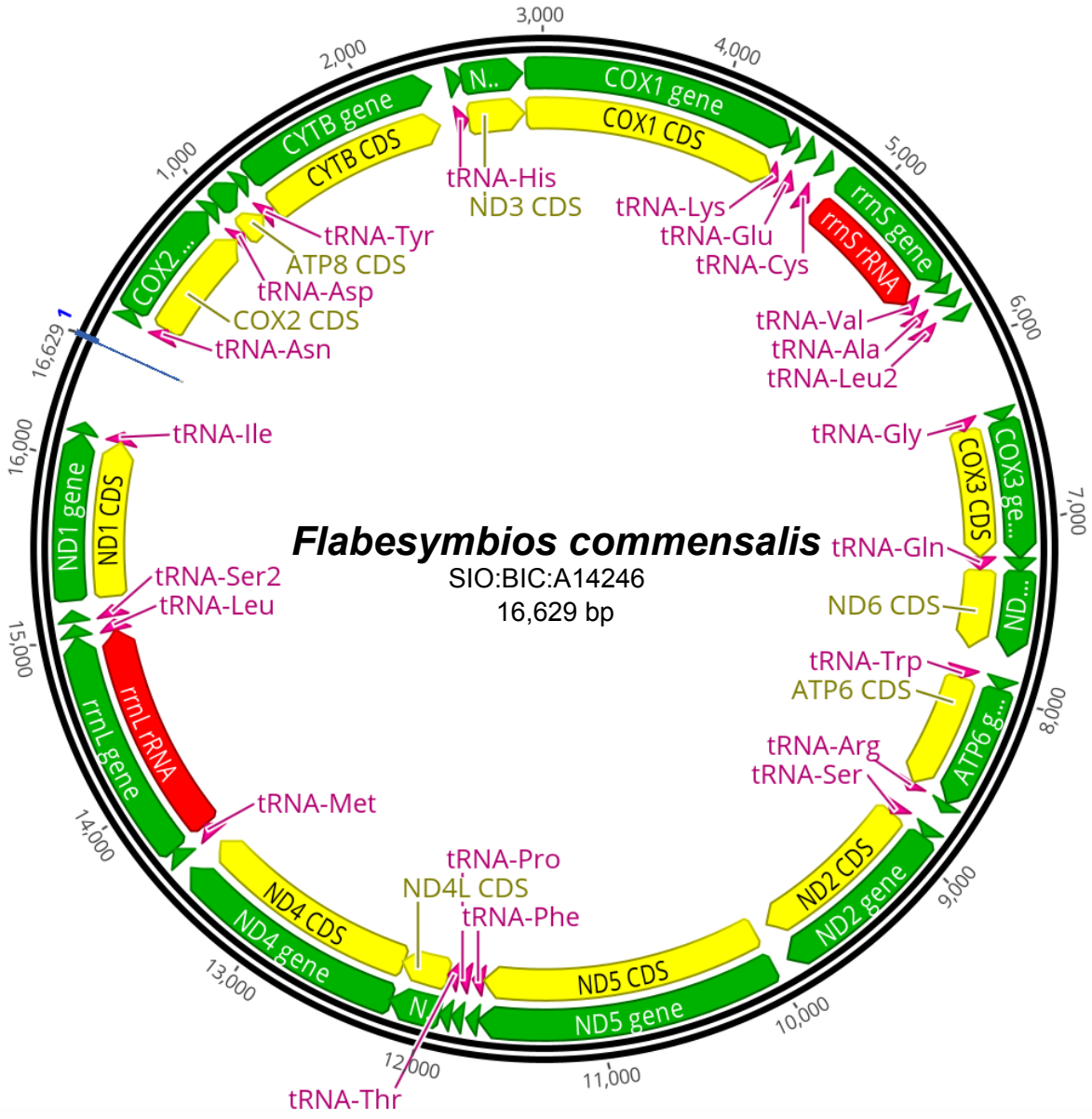

Figure 2.5: Circularized mitochondrial genome of *Flabesymbios commensalis*. Black outer circle is the nucleotide sequence with numbers representing individual nucleotides. Green arrows are genes, yellow arrows are protein-coding genes, red arrows are non-protein-coding genes, and pink arrows are tRNAs. The direction of the arrows is the direction of transcription.

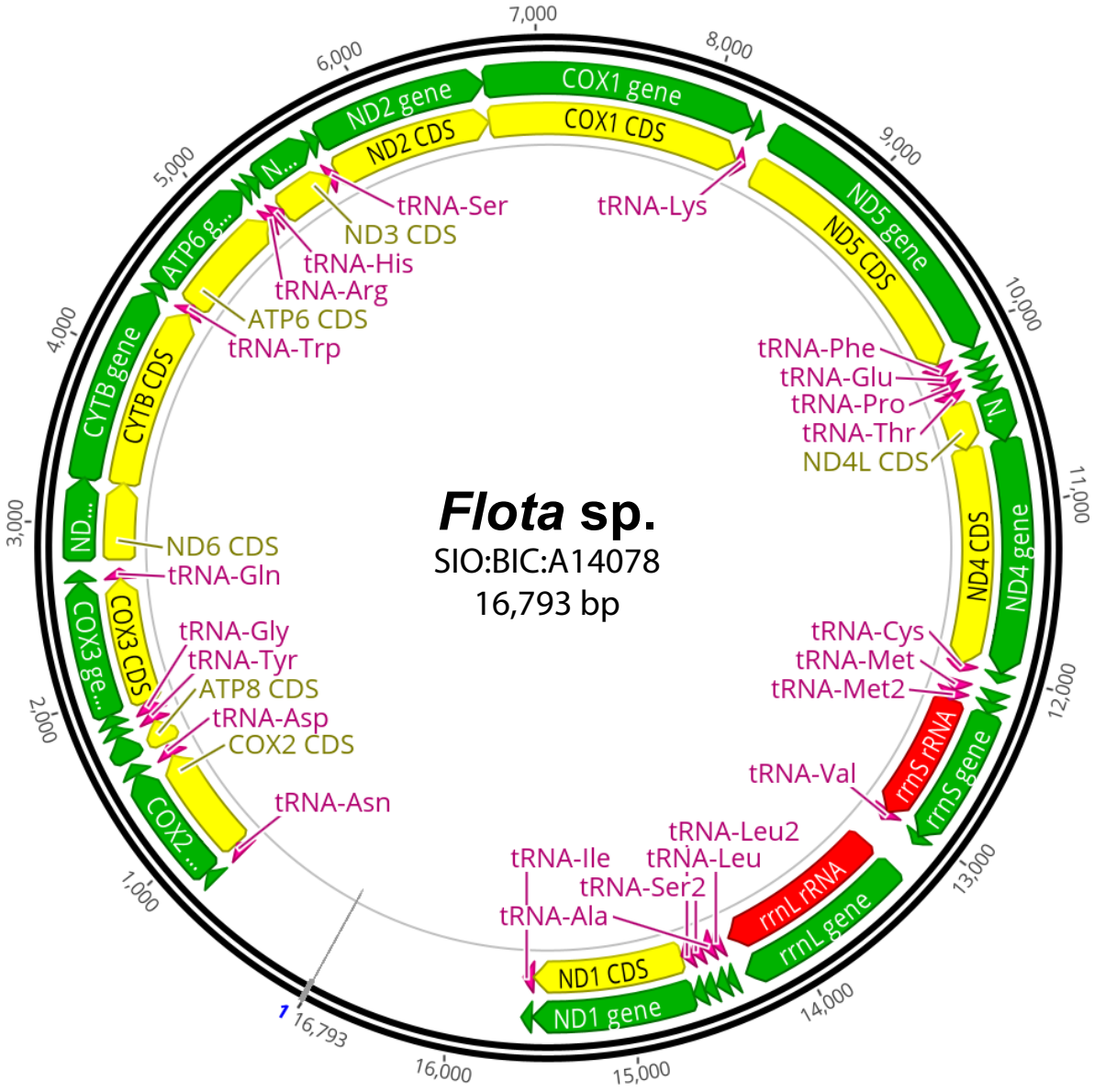

Figure 2.6: Circularized mitochondrial genome of *Flota* sp. Black outer circle is the nucleotide sequence with numbers representing individual nucleotides. Green arrows are genes, yellow arrows are protein-coding genes, red arrows are non-protein-coding genes, and pink arrows are tRNAs. The direction of the arrows is the direction of transcription.

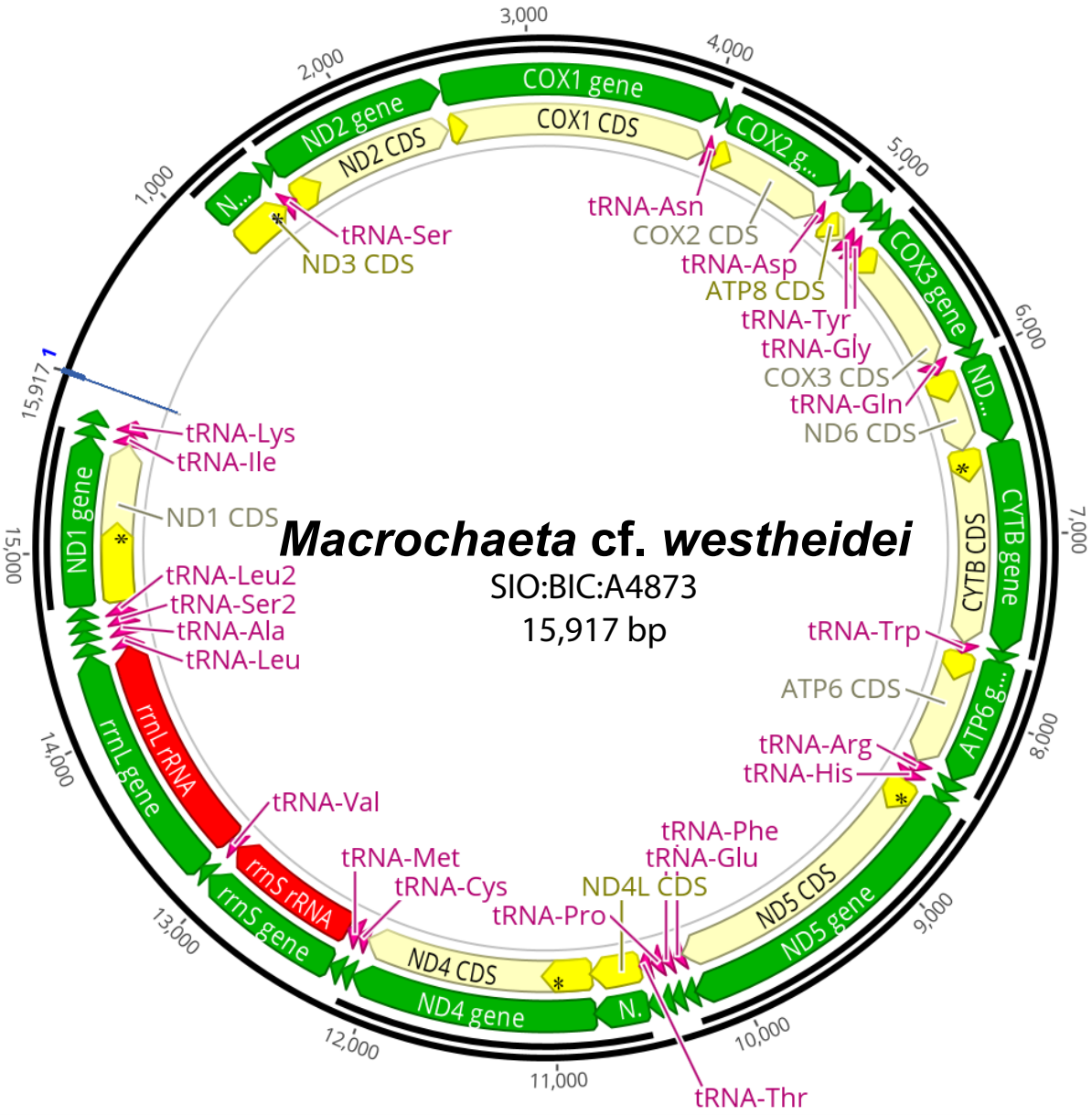

Figure 2.7: Circularized mitochondrial genome of *Macrochaeta* cf. *westheidei*. Black outer circle is the nucleotide sequence with numbers representing individual nucleotides. Green arrows are genes, yellow arrows are protein-coding genes, red arrows are non-protein-coding genes, and pink arrows are tRNAs. The direction of the arrows is the direction of transcription.

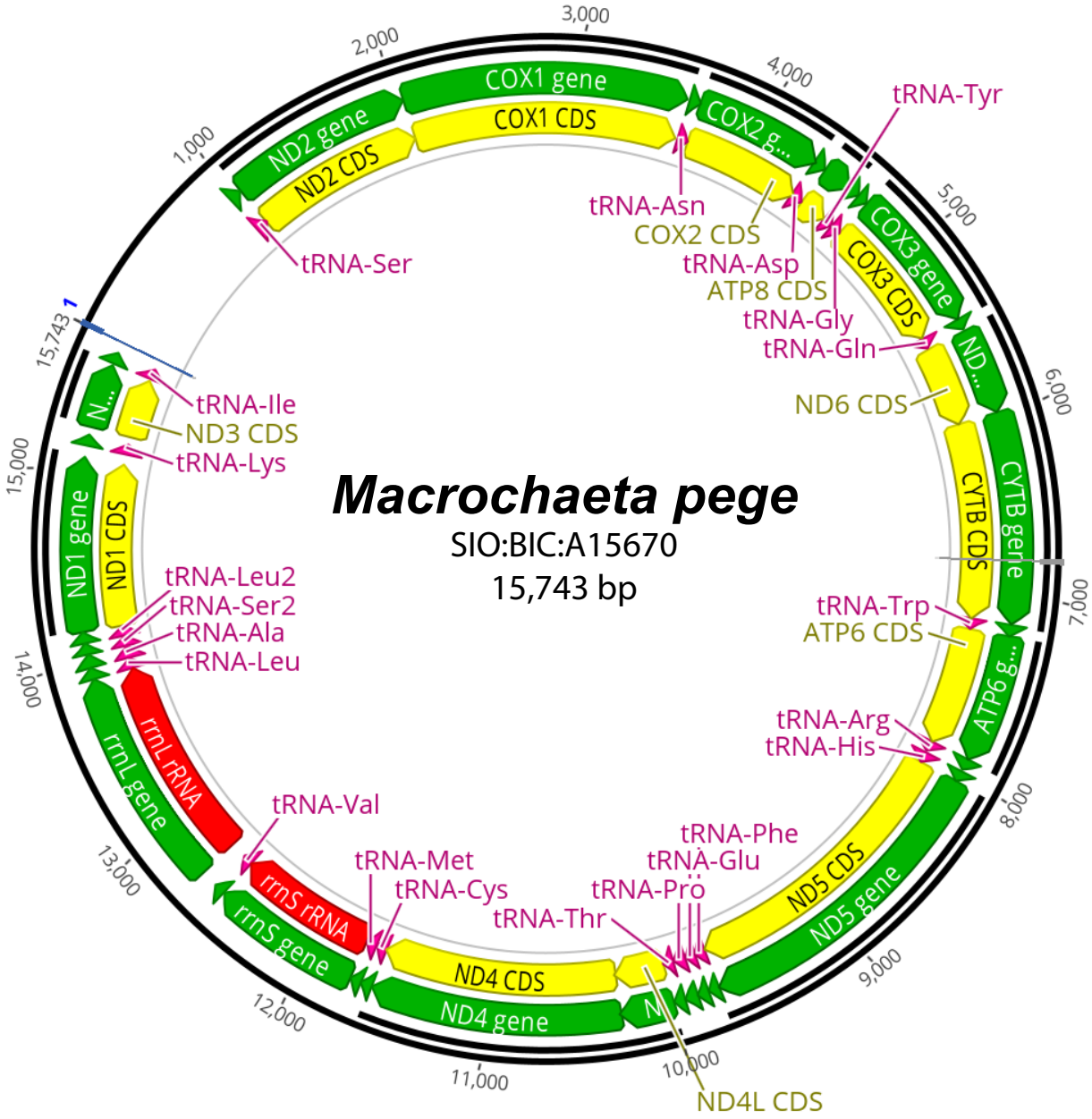

Figure 2.8: Circularized mitochondrial genome of *Macrochaeta pege*. Black outer circle is the nucleotide sequence with numbers representing individual nucleotides. Green arrows are genes, yellow arrows are protein-coding genes, red arrows are non-protein-coding genes, and pink arrows are tRNAs. The direction of the arrows is the direction of transcription.

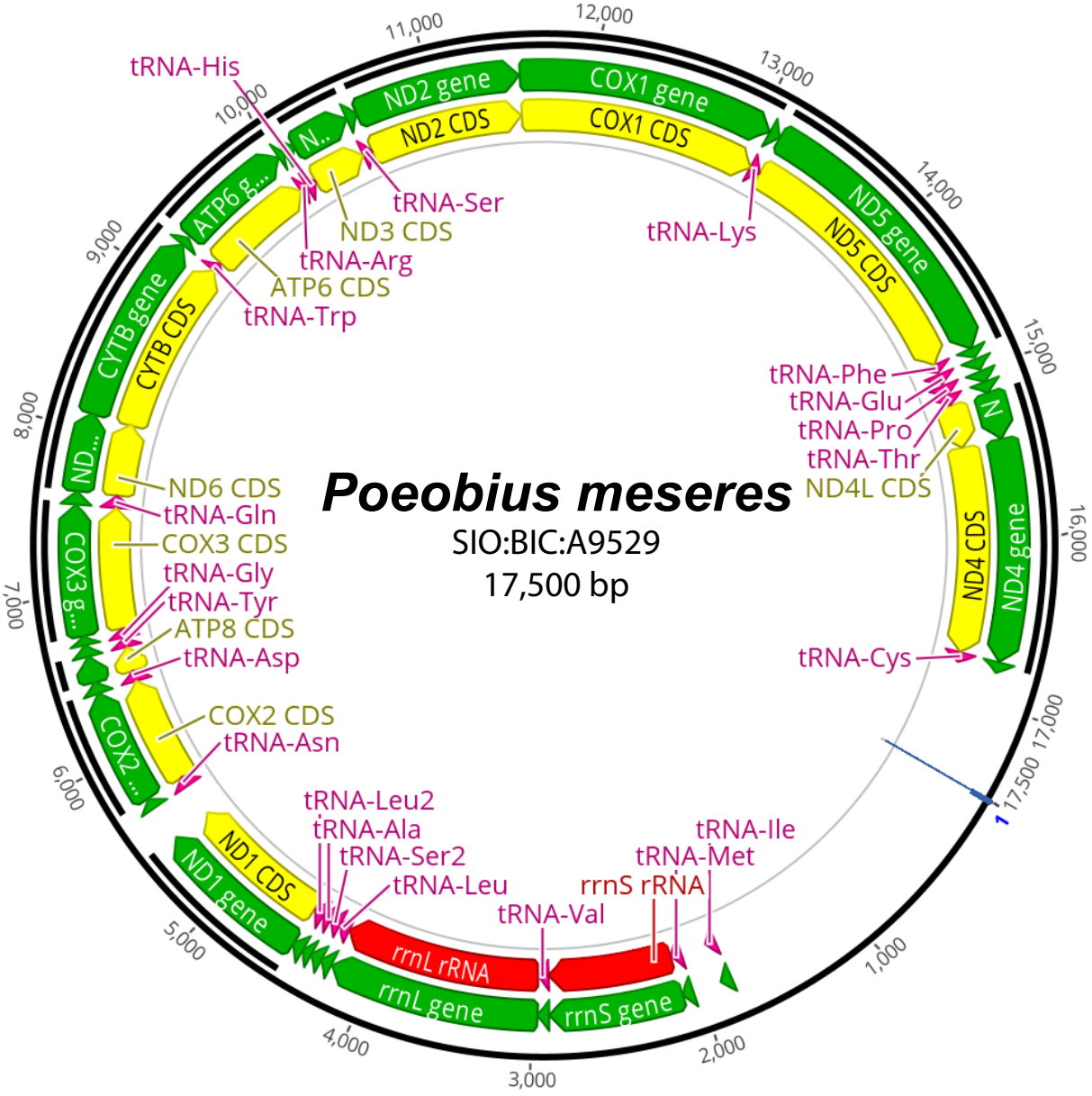

Figure 2.9: Circularized mitochondrial genome of *Poeobius meseres*. Black outer circle is the nucleotide sequence with numbers representing individual nucleotides. Green arrows are genes, yellow arrows are protein-coding genes, red arrows are non-protein-coding genes, and pink arrows are tRNAs. The direction of the arrows is the direction of transcription.

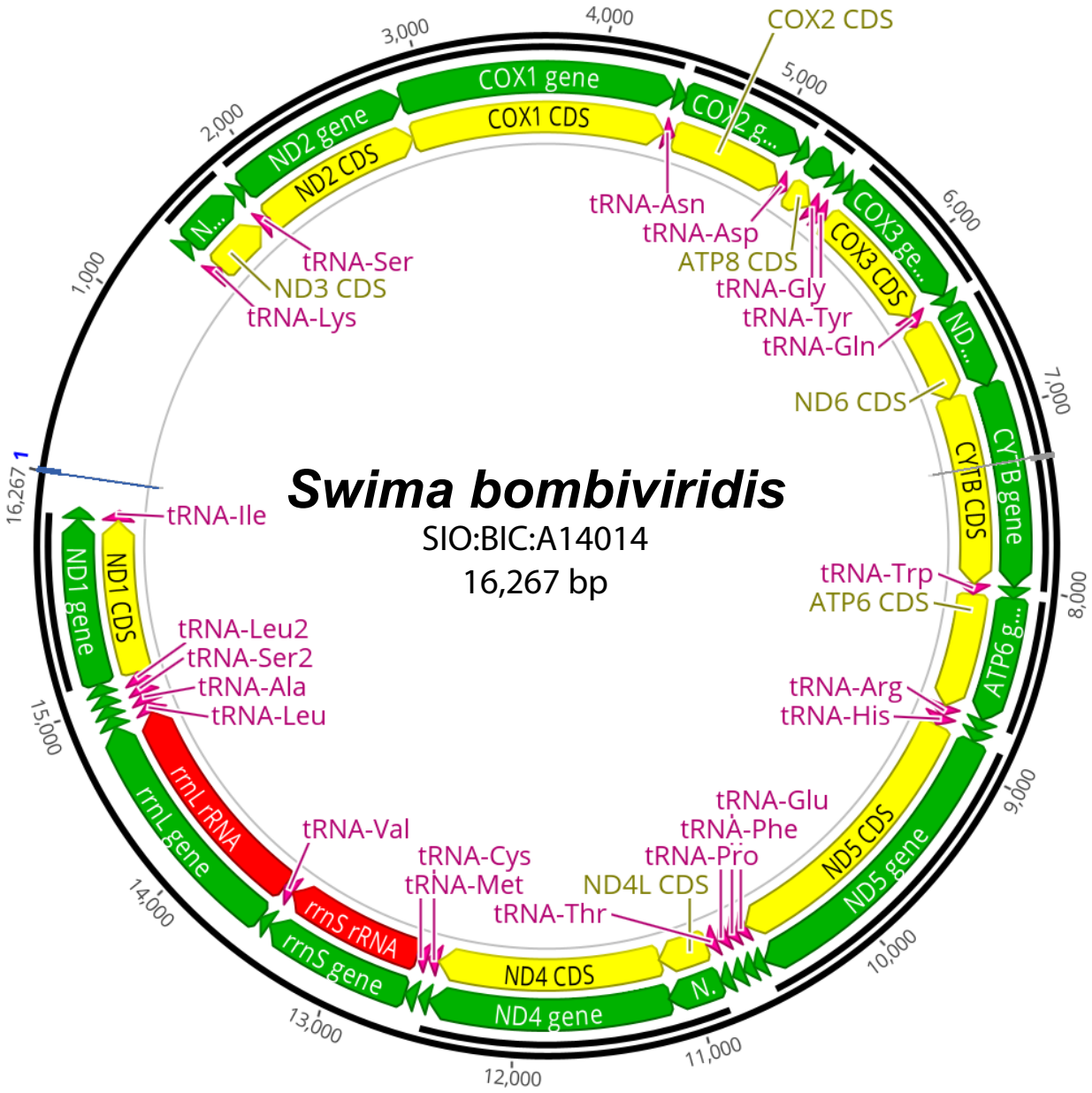

Figure 2.10: Circularized mitochondrial genome of *Swima bombiviridis*. Black outer circle is the nucleotide sequence with numbers representing individual nucleotides. Green arrows are genes, yellow arrows are protein-coding genes, red arrows are non-protein-coding genes, and pink arrows are tRNAs. The direction of the arrows is the direction of transcription.

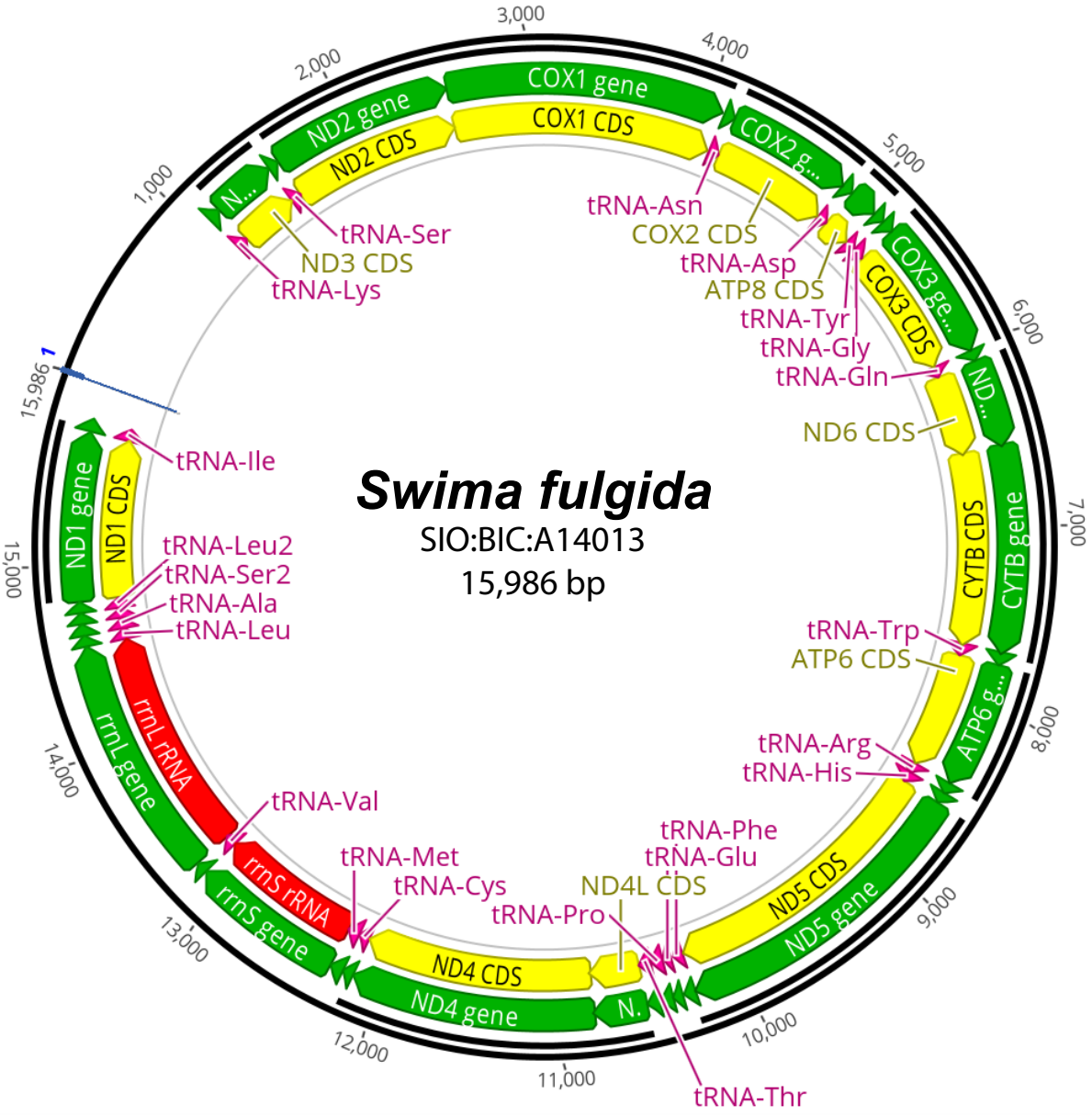

Figure 2.11: Circularized mitochondrial genome of *Swima fulgida*. Black outer circle is the nucleotide sequence with numbers representing individual nucleotides. Green arrows are genes, yellow arrows are protein-coding genes, red arrows are non-protein-coding genes, and pink arrows are tRNAs. The direction of the arrows is the direction of transcription.

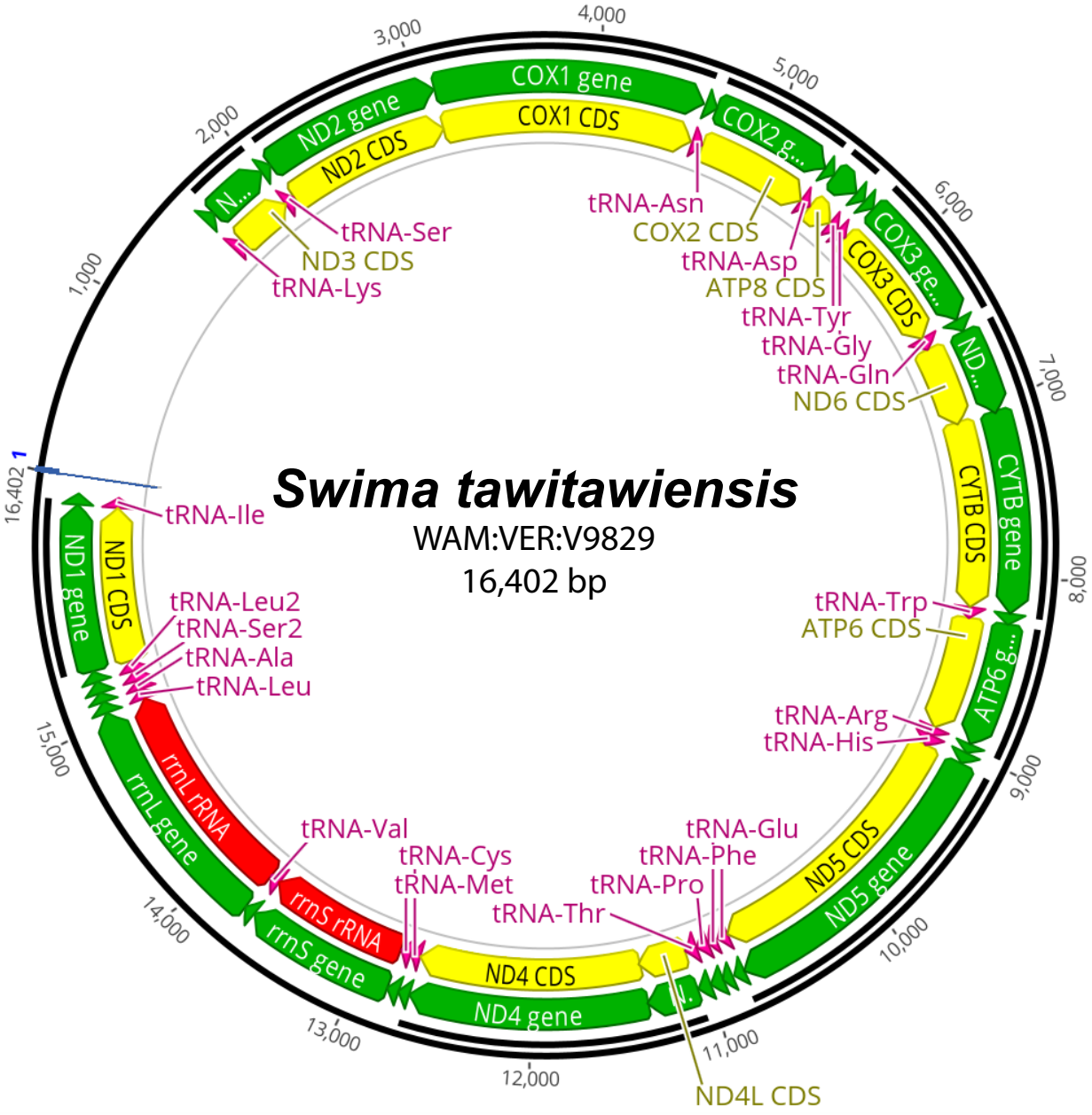

Figure 2.12: Circularized mitochondrial genome of *Swima tawitawiensis.* Black outer circle is the nucleotide sequence with numbers representing individual nucleotides. Green arrows are genes, yellow arrows are protein-coding genes, red arrows are non-protein-coding genes, and pink arrows are tRNAs. The direction of the arrows is the direction of transcription.

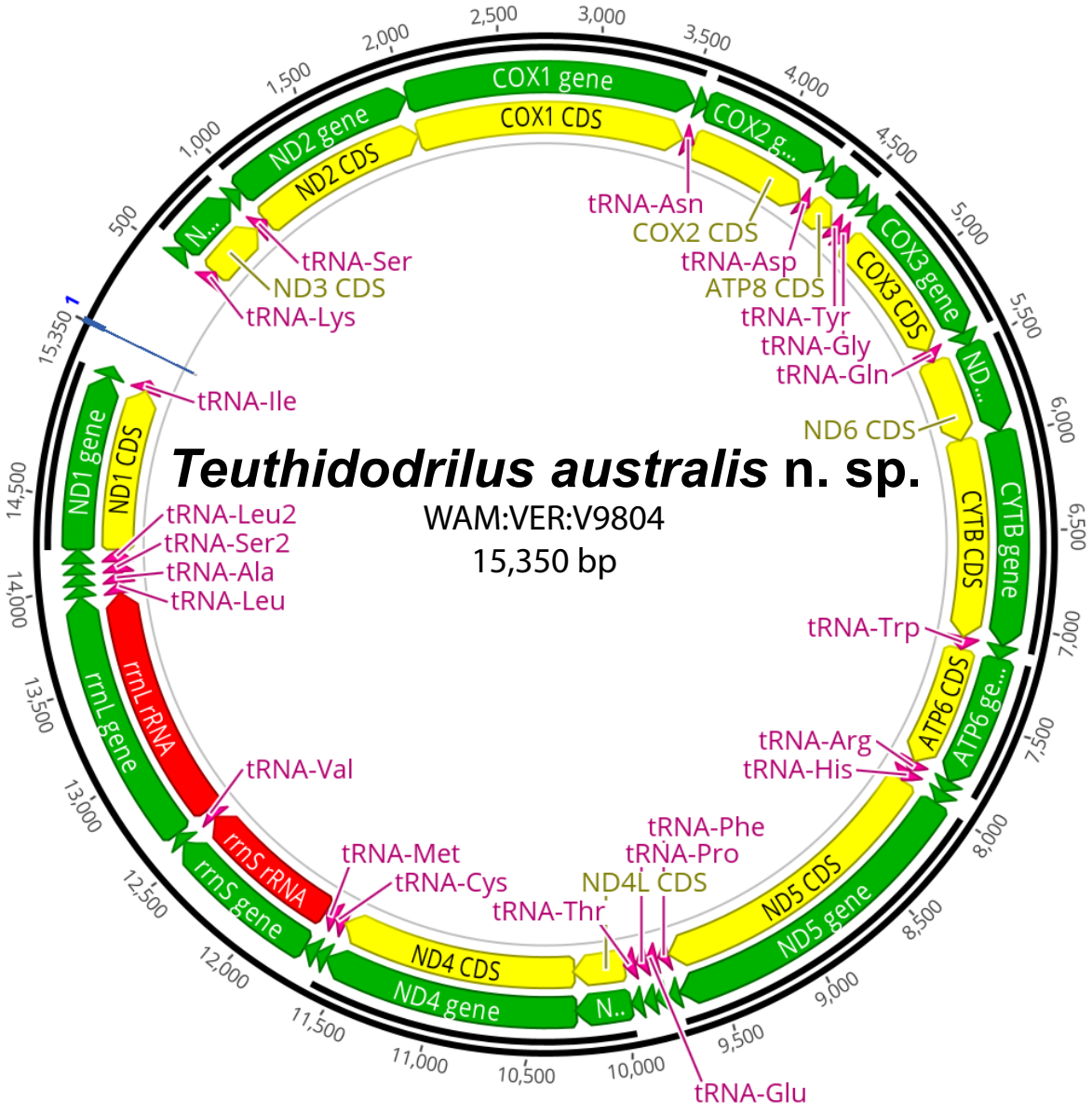

Figure 2.13: Circularized mitochondrial genome of *Teuthidodrilus australis* n. sp. Black outer circle is the nucleotide sequence with numbers representing individual nucleotides. Green arrows are genes, yellow arrows are protein-coding genes, red arrows are non-protein-coding genes, and pink arrows are tRNAs. The direction of the arrows is the direction of transcription.

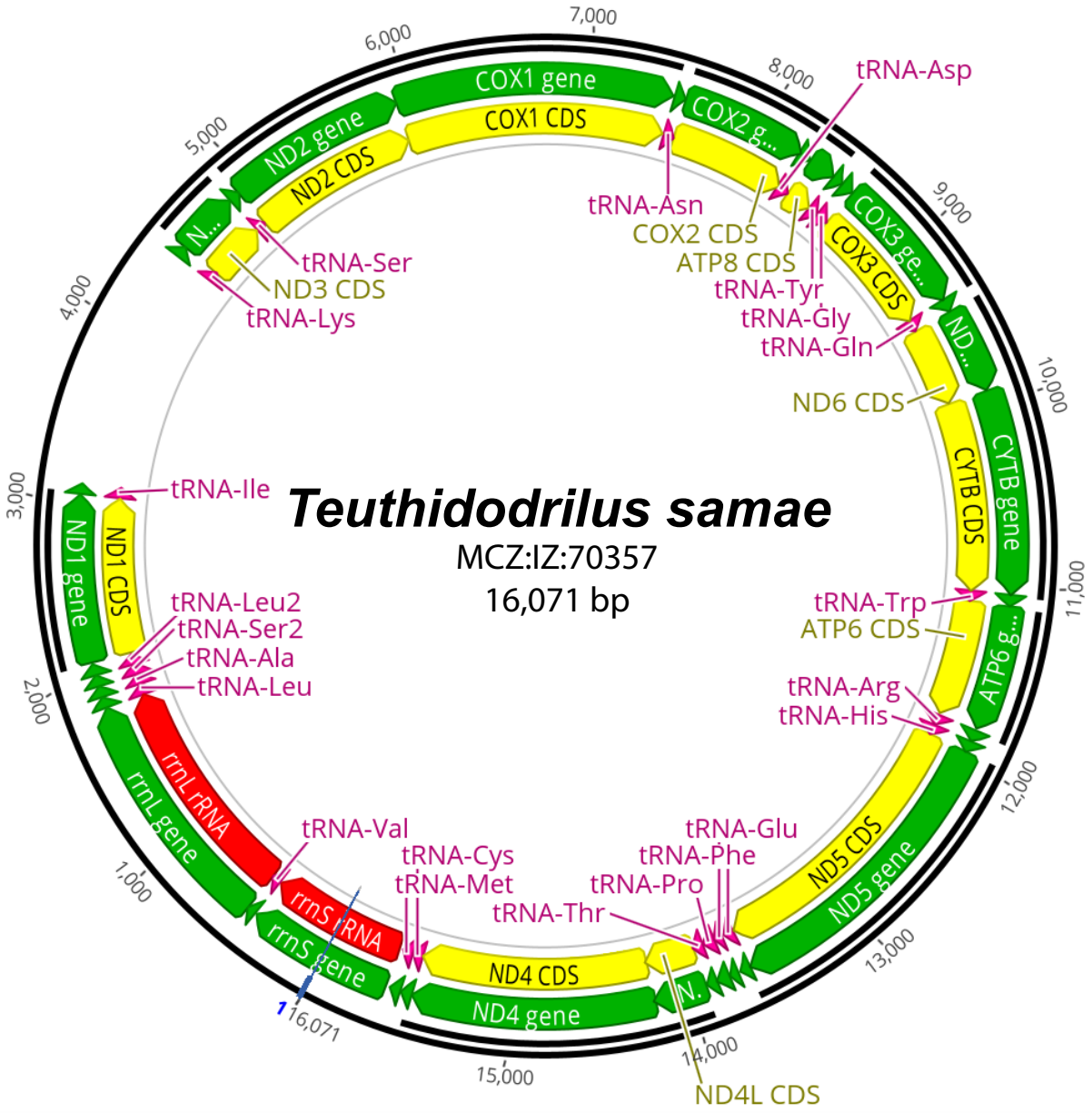

Figure 2.14: Circularized mitochondrial genome of *Teuthidodrilus samae.* Black outer circle is the nucleotide sequence with numbers representing individual nucleotides. Green arrows are genes, yellow arrows are protein-coding genes, red arrows are non-protein-coding genes, and pink arrows are tRNAs. The direction of the arrows is the direction of transcription.

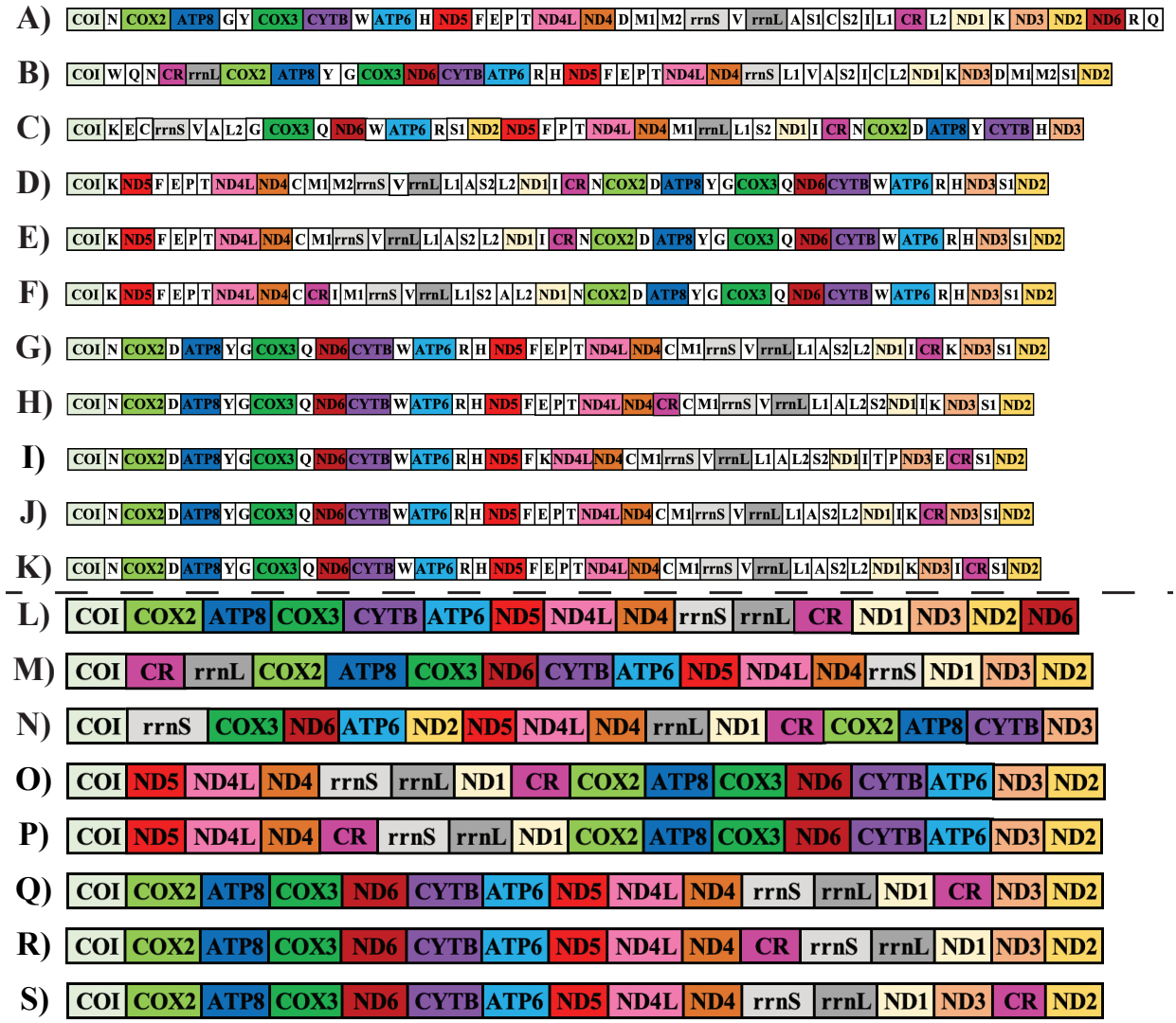

Figure 2.15: Unique Cirratuliformia gene orders for complete mitogenomes with *tRNAs* (A-K) and without *tRNAs* (L-S). A) *Cirriformia* cf. *tentaculata* & *Timarete posteria* B) *Raricirrus* sp. C) *Flabesymbios commensalis* D) *Flota* sp. E) *Pherusa bengalensis* F) *Poeobius meseres* G) *Acrocirrus validus*, *Swima bombiviridis*, *Swima fulgida*, *Swima tawitawiensis*, *Teuthidodrilus australis*, & *Teuthidodrilus samae* H) *Flabelligella macrochaeta* I) *Flabelligena* sp. J) *Macrochaeta* cf. *westheidei* & *Macrochaeta* sp. K) *Macrochaeta pege* L) *Cirriformia* cf. *tentaculata* & *Timarete posteria* M) *Raricirrus* sp. N) *Flabesymbios commensalis* O) *Flota* sp. & *Pherusa bengalensis* P) *Poeobius meseres* Q) *Acrocirrus validus*, *Macrochaeta* cf. *westheidei*, *Macrochaeta* sp., *Swima bombiviridis*, *Swima fulgida*, *Swima tawitawiensis*, *Teuthidodrilus australis*, & *Teuthidodrilus samae* R) *Flabelligella macrochaeta* S) *Flabelligena* sp. & *Macrochaeta pege*.

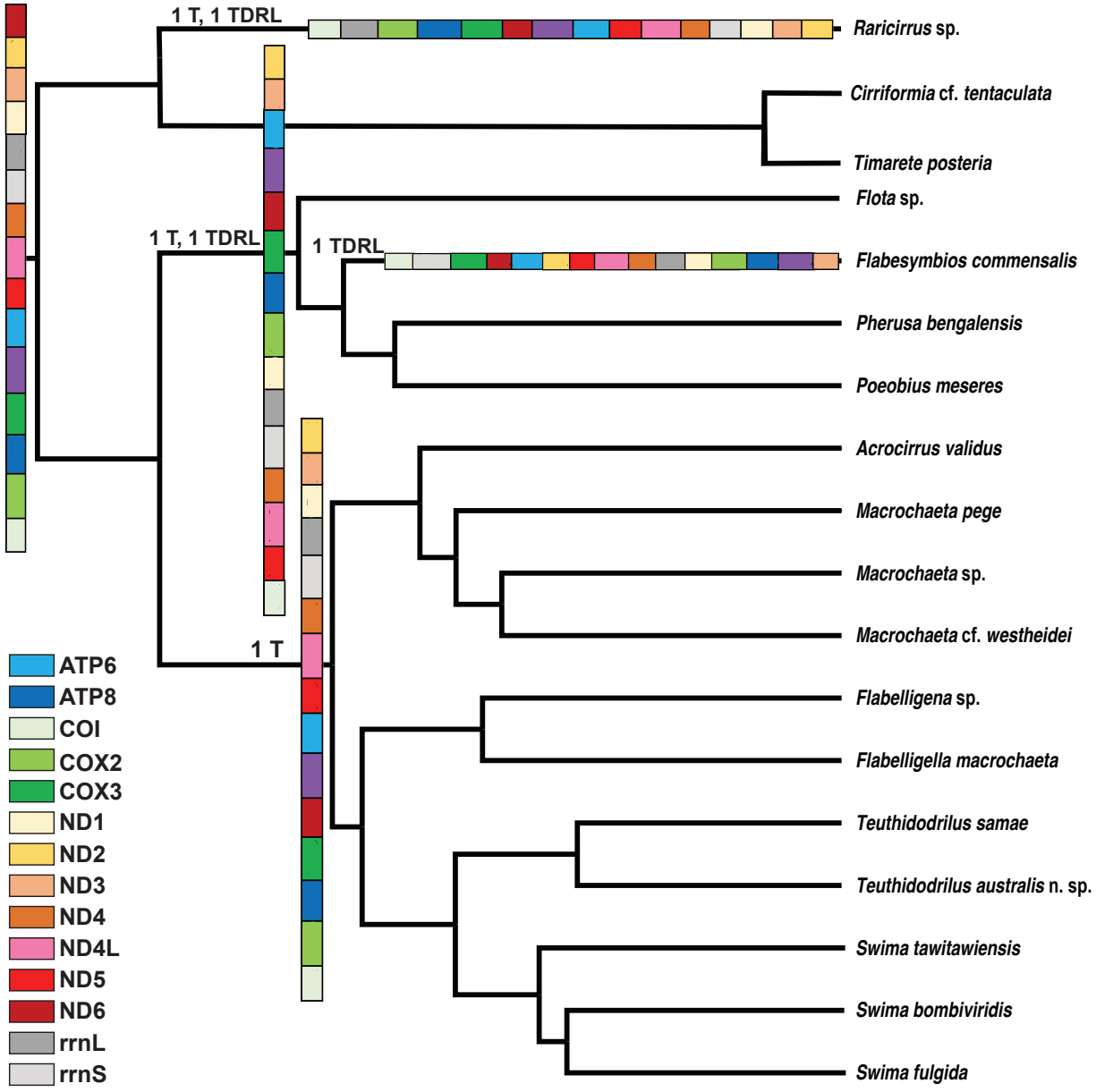

Figure 2.16: Inferred genomic rearrangements excluding *tRNAs* mapped onto the mitogenome phylogeny. Putative ancestral state from (Struck et al. 2023) with genes color-coded. T = transposition, TDRL = tandem-duplication random loss.

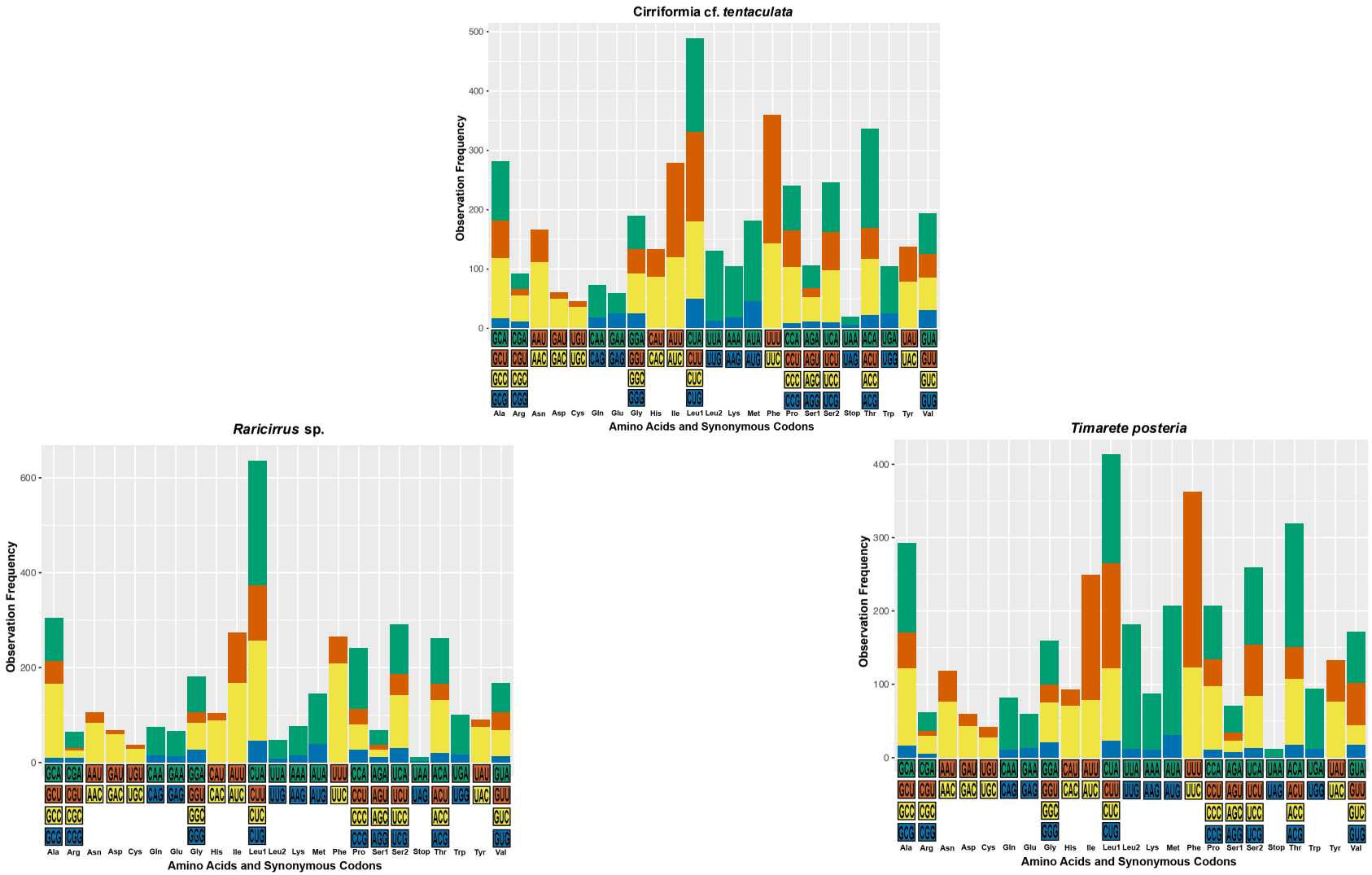

Figure 2.17. Relative synonymous codon usage of *Cirriformia* cf. *tentaculata*, *Raricirrus* sp., and *Timarete posteria*.

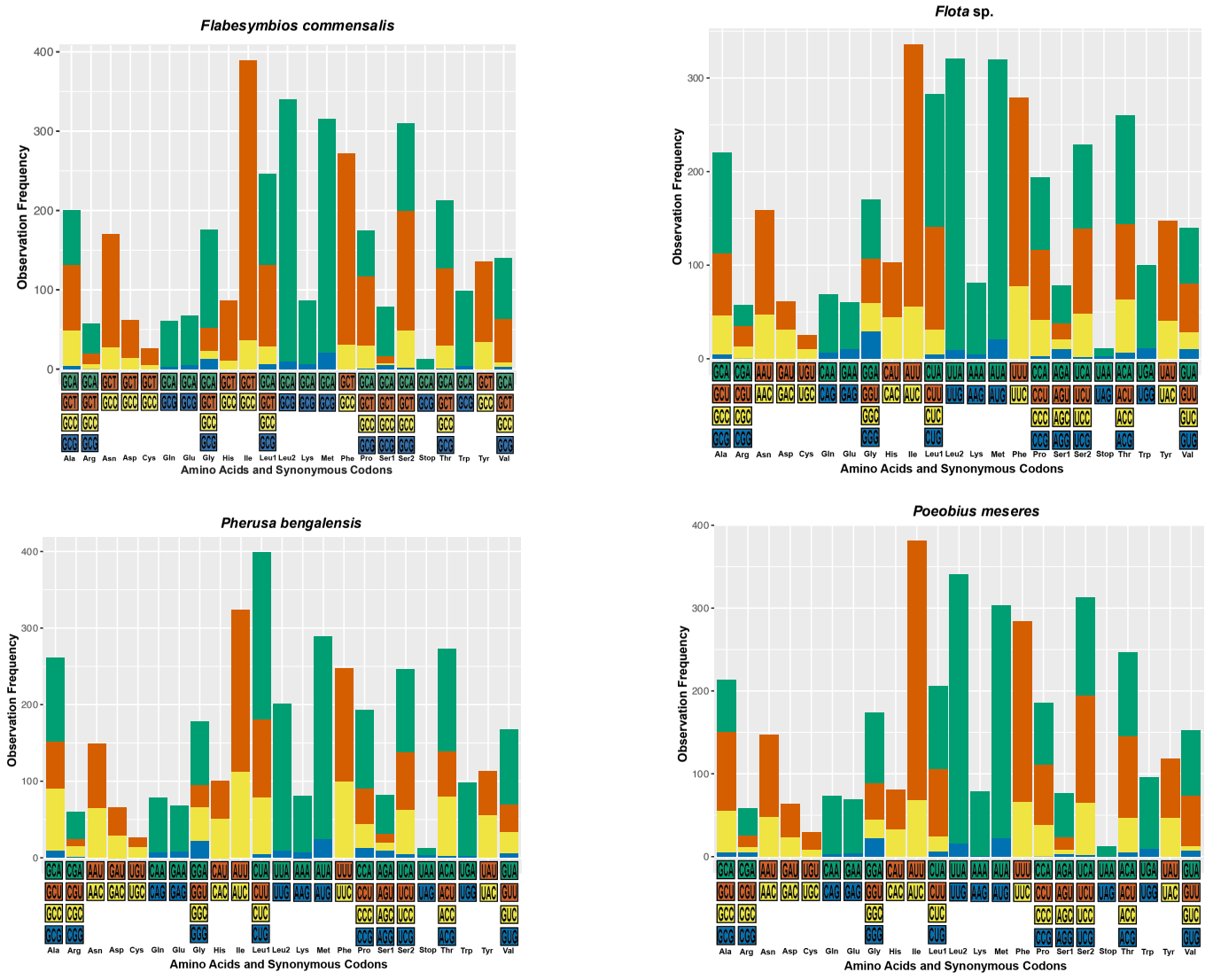

Figure 2.18. Relative synonymous codon usage of *Flabesymbios commensalis, Flota* sp., *Pherusa bengalensis*, and *Poeobius meseres*.

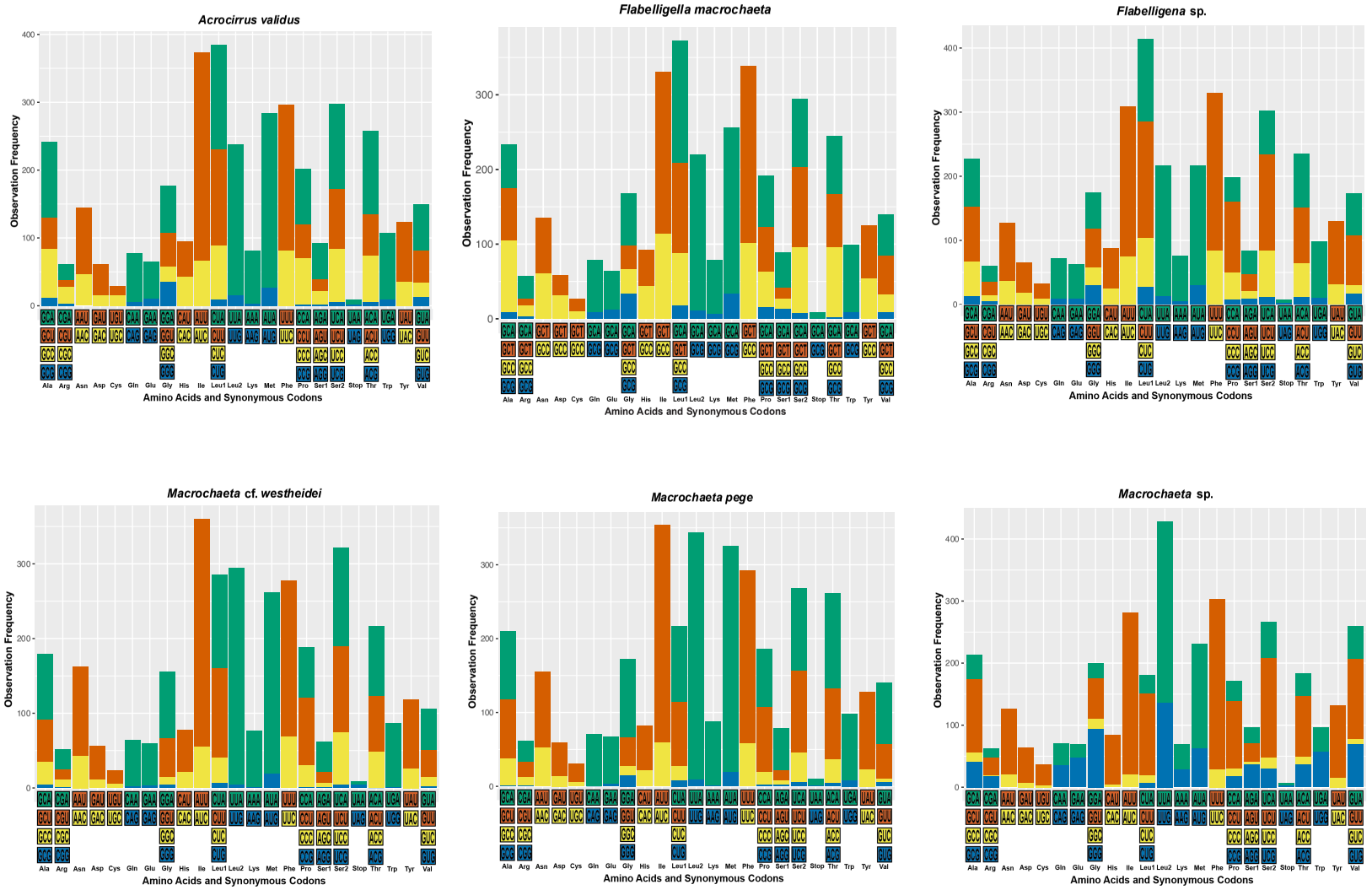

Figure 2.19. Relative synonymous codon usage of *Acrocirrus validus*, *Flabelligella macrochaeta, Flabelligena* sp., *Macrochaeta* cf. *westheidei*, *Macrochaeta pege*, and *Macrochaeta* sp.

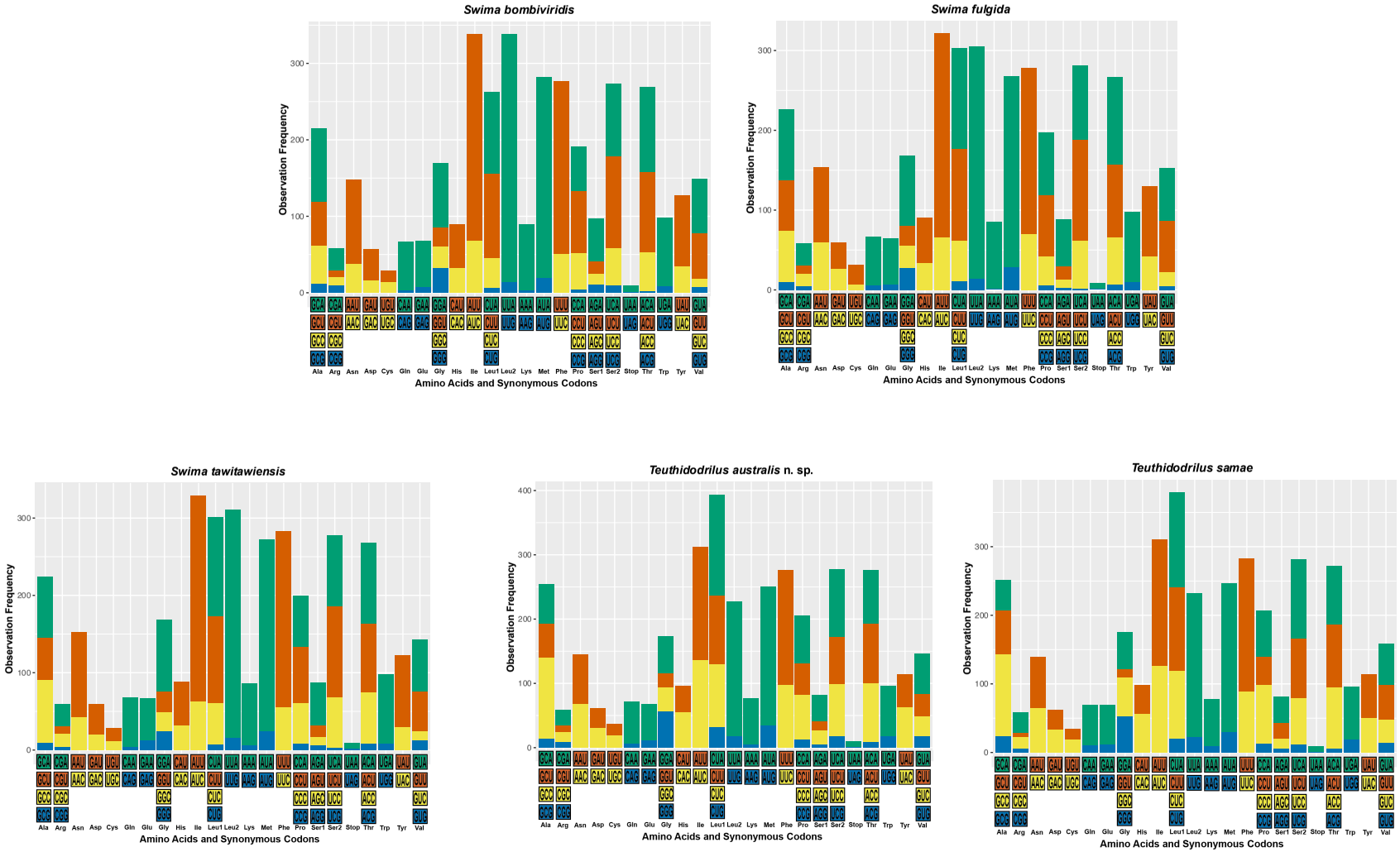

Figure 2.20. Relative synonymous codon usage of *Swima bombiviridis*, *Swima fulgida*, *Swima tawitawiensis*, *Teuthidodrilus australis* n. sp., and *Teuthidodrilus samae.*

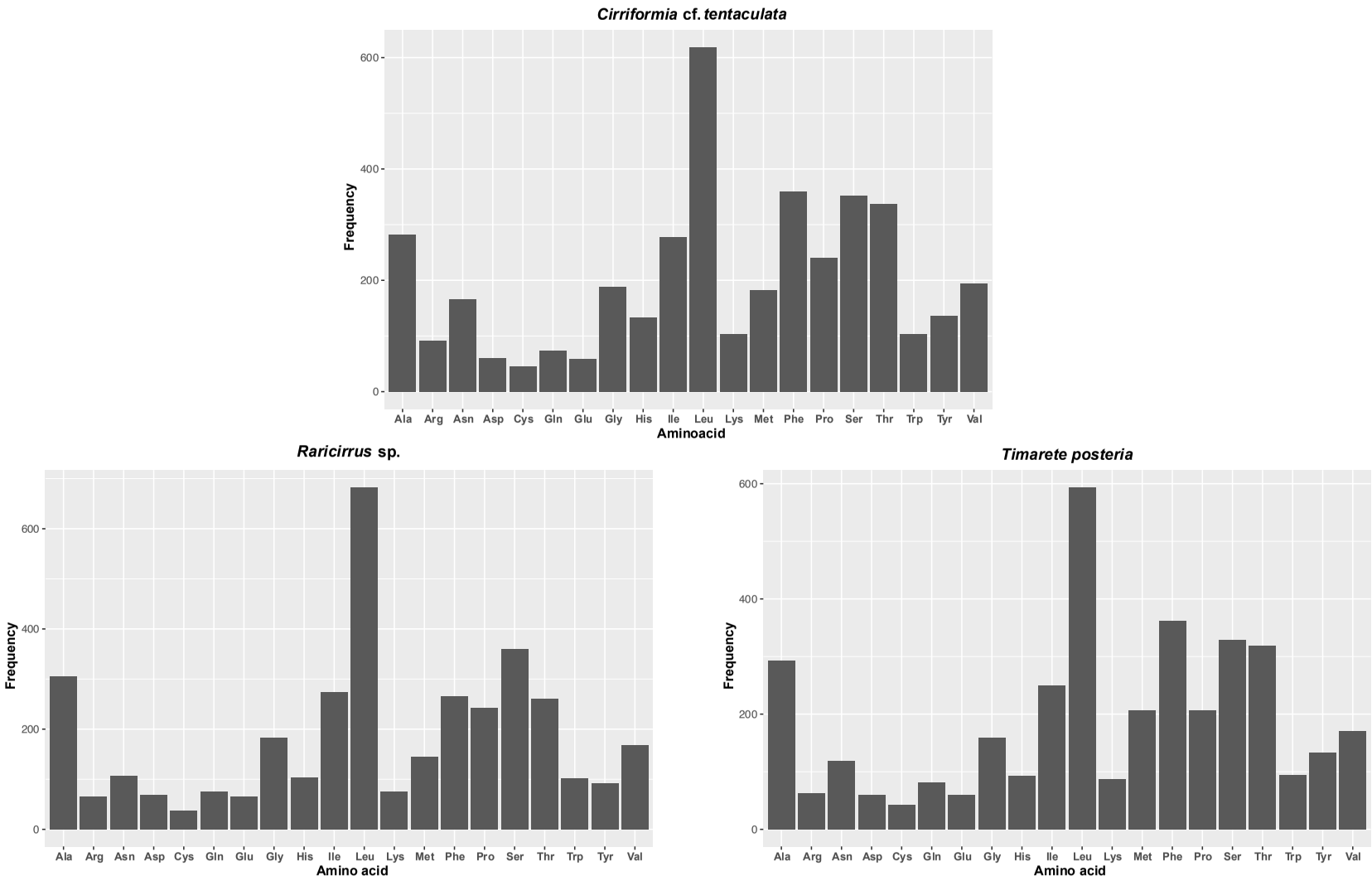

Figure 2.21: Amino acid frequencies in *Cirriformia* cf. *tentaculata*, *Raricirrus* sp., and *Timarete posteria*.

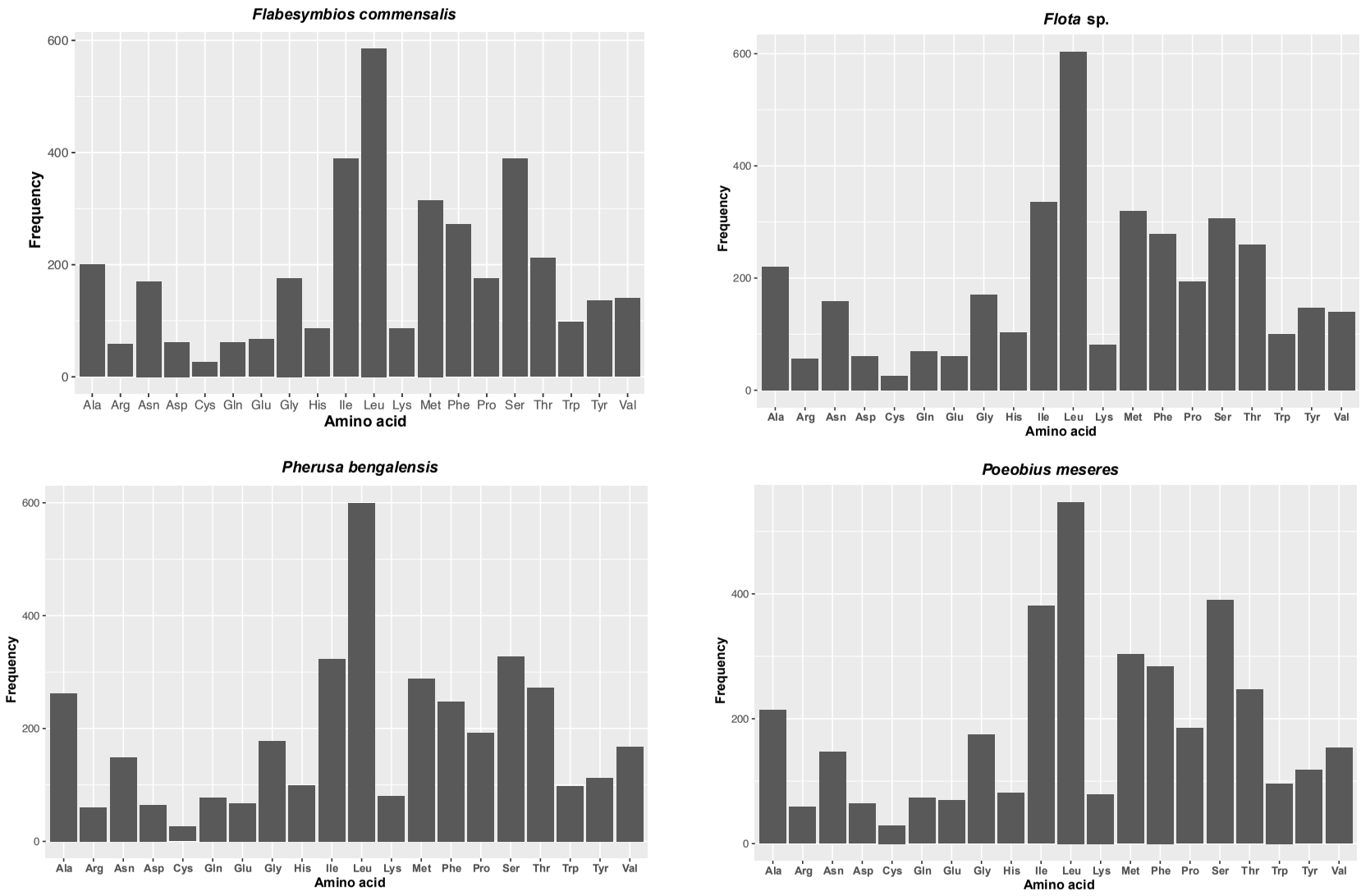

Figure 2.22: Amino acid frequencies in *Flabesymbios commensalis, Flota* sp., *Pherusa bengalensis*, and *Poeobius meseres*.

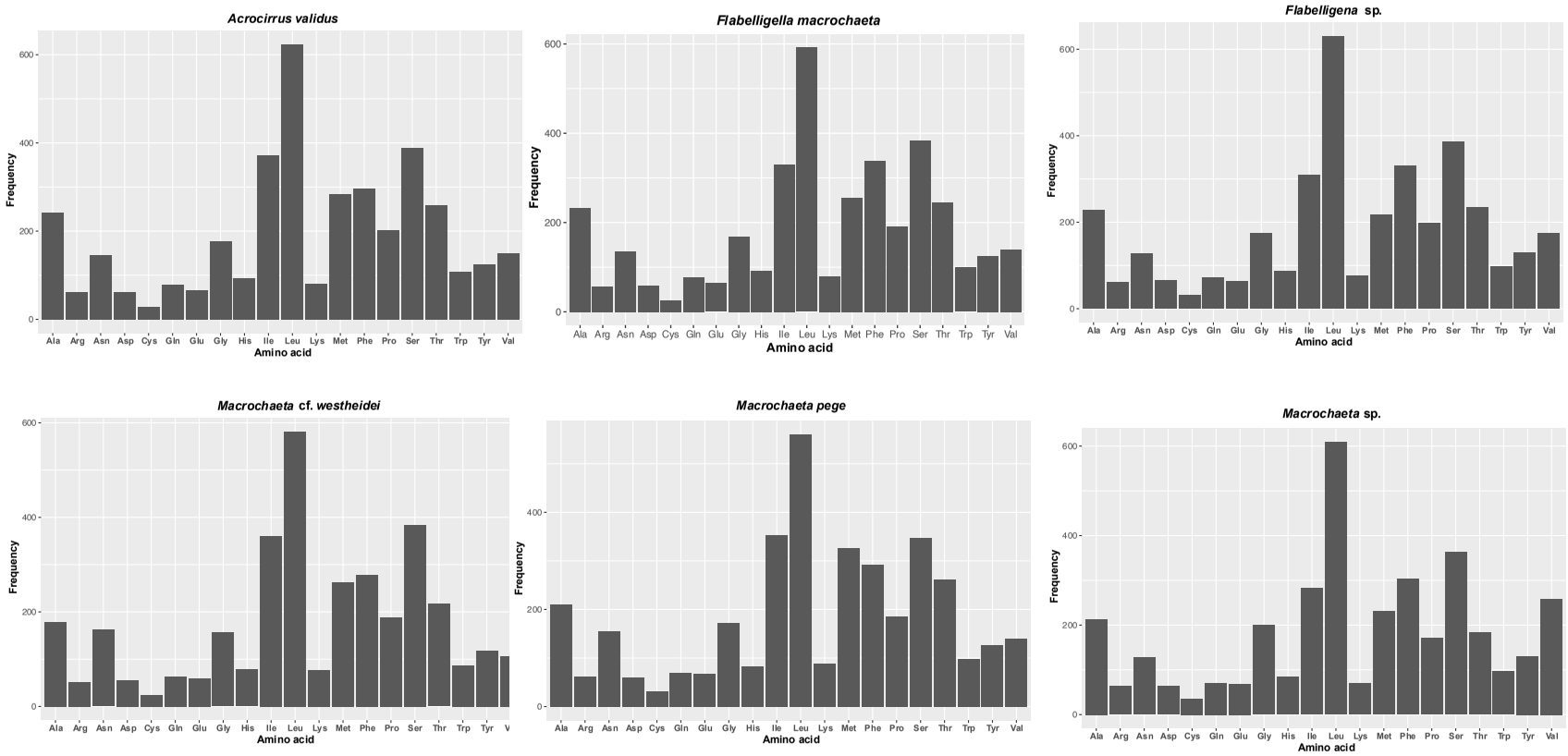

Figure 2.23: Amino acid frequencies in *Acrocirrus validus*, *Flabelligella macrochaeta, Flabelligena* sp., *Macrochaeta* cf. *westheidei*, *Macrochaeta pege*, and *Macrochaeta* sp.

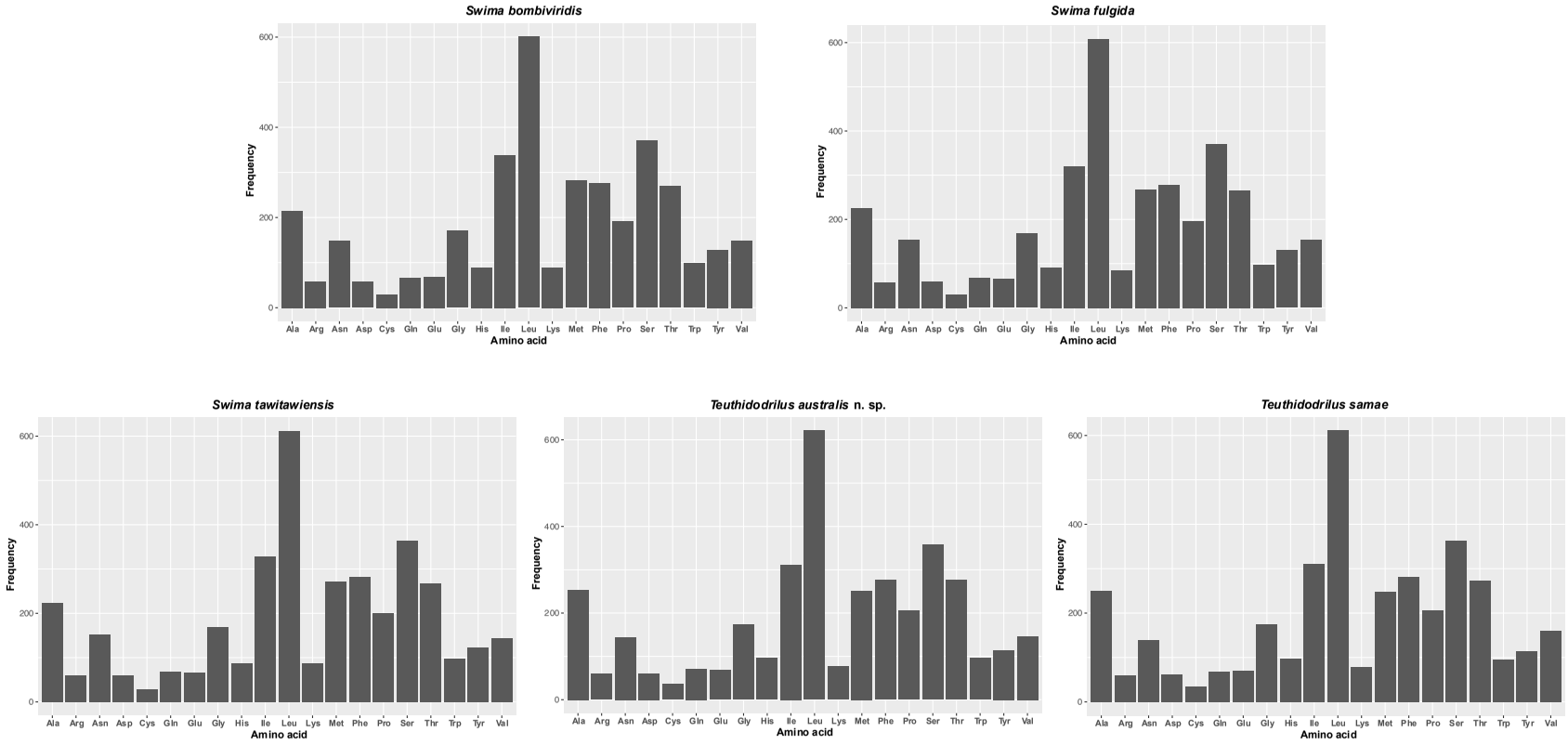

Figure 2.24: Amino acid frequencies in *Swima bombiviridis*, *Swima fulgida*, *Swima tawitawiensis*, *Teuthidodrilus australis* n. sp., and *Teuthidodrilus samae.*

Acknowledgments

Chapter 2 is currently being prepared for submission for publication of the material. Proctor, Paul P.; Hiley, Avery S.; Rouse, Greg W. The thesis author was the primary investigator and author of this material.

REFERENCES

Adobe Inc. (2019). Adobe Illustrator. Retrieved from https://adobe.com/products/illustrator.

Allio, Rémi, Alex Schomaker-Bastos, Jonathan Romiguier, Francisco Prosdocimi, Benoit Nabholz, and Frédéric Delsuc. 2020. "MitoFinder: Efficient Automated Large-Scale Extraction of Mitogenomic Data in Target Enrichment Phylogenomics." *Molecular Ecology Resources* 20(4): 892–905.

Altschul, S.F., W. Gish, W. Miller, E. W. Myers, and D. J. Lipman. 1990. "Basic local alignment search tool." *J. Mol. Biol.* 215: 403-410. doi: 10.1016/S0022-2836(05)80360-2.

Averincev, V.G. 1980. "*Chauvinelia arctica*, sp. n. (Acrocirridae, Polychaeta) from the Canadian plain." *Issledovaniya fauny morei*. *Zoologicheskii Institut Akademii Nauk USSR* 25(33): 57– 62.

Banse, Karl. 1969. "Acrocirridae n.fam. (Polychaeta Sedentaria)." *Journal of the Fisheries Research Board of Canada* 26(10): 2595–2620. doi.org/10.1139/f69-25.

Bernt, M., A. Donath, F. Jühling, F. Externbrink, C. Florentz, G. Fritzsch, J. Pütz, M. Middendorf, and P. F. Stadler. 2013a. "MITOS: Improved de novo metazoan mitochondrial genome annotation. Molecular Phylogenetics and Evolution." 69(2): 313–319. doi.org/10.1016/j.ympev.2012.08.023.

Bernt, Matthias, Christoph Bleidorn, Anke Braband, Johannes Dambach, Alexander Donath, Guido Fritzsch, Anja Golombek, Heike Hadrys, Frank Jühling, Karen Meusemann, Martin Middendorf, Bernhard Misof, Marleen Perseke, Lars Podsiadlowski, Björn von Reumont, Bernd Schierwater, Martin Schlegel, Michael Schrödl, Sabrina Simon, Peter F. Stadler, Isabella Stöger, and Torsten H. Struck. 2013b. "A Comprehensive Analysis of Bilaterian Mitochondrial Genomes and Phylogeny." *Molecular Phylogenetics and Evolution* 69(2): 352–64.

Bernt M., D. Merkle, K. Ramsch, G. Fritzsch, M. Perseke, D. Bernhard, M. Schlegel, P. Stadler, M. Middendorf. 2007. "CREx: inferring genomic rearrangements based on common intervals." *Bioinformatics* 23: 2957–2958.

Bolger, Anthony M., Marc Lohse, and Bjoern Usadel. 2014. "Trimmomatic: A Flexible Trimmer for Illumina Sequence Data." *Bioinformatics (Oxford, England)* 30(15): 2114–20.

Burnette, A. B., T. H. Struck, and K. M. Halanych. 2005. "Holopelagic *Poeobius meseres* ('Poeobiidae,' Annelida) is derived from benthic flabelligerid worms. *Biological Bulletin* 208: 213-220.

Carr, Christina M., Sarah M. Hardy, Tanya M. Brown, Tara A. Macdonald, and Paul D. N. Hebert. 2011. "A Tri-Oceanic Perspective: DNA Barcoding Reveals Geographic

Structure and Cryptic Diversity in Canadian Polychaetes." *PLoS ONE* 6(7). doi: 10.1371/journal.pone.0022232.

Castellana, S., S. Vicario, and C. Saccone. 2011. "Evolutionary Patterns of the Mitochondrial Genome in Metazoa: Exploring the Role of Mutation and Selection in Mitochondrial Protein Coding Genes." *Genome Biology and Evolution* 3: 1067–79.

Cejb, B., A. Ravara, and M. T. Aguado. 2022. "First mitochondrial genomes of Chrysopetalidae (Annelida) from shallow-water and deep-sea chemosynthetic environments." *Gene* 815: 146149.

Clement, Mark, David Posada, and Keith A. Crandall. 2000. "TCS: A Computer Program to Estimate Gene Genealogies." *Molecular Ecology* 9(10): 1657–59. doi: 10.1046/j.1365-294X.2000.01020.x.

Danecek, Petr, James K. Bonfield, Jennifer Liddle, John Marshall, Valeriu Ohan, Martin O. Pollard, Andrew Whitwham, Thomas Keane, Shane A. McCarthy, Robert M. Davies, and Heng Li. 2021. "Twelve years of SAMtools and BCFtools." *GigaScience* 10(2). doi.org/10.1093/gigascience/giab008.

Darriba, Diego, David Posada, Alexey M. Kozlov, Alexandros Stamatakis, Benoit Morel, and Tomas Flouri. 2020. "ModelTest-NG: A New and Scalable Tool for the Selection of DNA and Protein Evolutionary Models*." Molecular Biology and Evolution* 37(1):291–94. doi:10.1093/molbev/msz189.

Darriba D., G. L. Taboada, R. Doallo, D. Posada. 2012. "jModelTest 2: more models, new heuristics and parallel computing." *Nature Methods* 9(8):772.

Edgar, Robert C. 2004. "MUSCLE: multiple sequence alignment with high accuracy and high throughput." *Nucleic Acids Research* 32(5):1792–1797. doi.org/10.1093/nar/gkh340.

Edler, D., J. Klein, A. Antonelli, and D. Silvestro. 2020. "raxmlGUI 2.0: A graphical interface and toolkit for phylogenetic analyses using RAxML." *Methods in Ecology and Evolution* 12: 373–377. dx.doi.org/https://doi.org/10.1111/2041-210X.13512.

Farias, Savio T. de, Thaís G. do Rêgo, and Marco V. José. 2014. "Evolution of Transfer RNA and the Origin of the Translation System." *Frontiers in Genetics* 5: 303.

Folmer, O., M. Black, W. Hoeh, R. Lutz, and Robert C. Vrijenhoek. 1994. "DNA Primers for Amplification of Mitochondrial Cytochrome c Oxidase Subunit I from Diverse Metazoan Invertebrates." *Australian Journal of Zoology* 3(5):294–99. doi: 10.1071/ZO9660275.

Fuiman, Lee A. 1997. "What Can Flatfish Ontogenies Tell Us about Pelagic and Benthic Lifestyles?" *Journal of Sea Research* 37(3–4): 257–67.

Gillet, P. 2001. "*Flabelligena amoureuxi* new genus, new species (Polychaeta: Acrocirridae) from Crozet Island (Indian Ocean)." *Bulletin of Marine Science* 68(1): 125–131.

Giribet, Gonzalo, Salvador Carranza, Jaume Baguñà, Marta Riutort, and Carles Ribera. 1996. "First Molecular Evidence for the Existence of a Tardigrada + Arthropoda Clade." *Molecular Biology and Evolution* 13(1): 76–84. doi: 10.1093/oxfordjournals.molbev.a025573.

Gissi, C., F. Iannelli, and G. Pesole. 2008. "Evolution of the mitochondrial genome of Metazoa as exemplified by comparison of congeneric species." *Heredity* 101: 301-320.

Glasby, C. J. and K. Fauchald. 1991. "Redescription of *Helmetophorus rankini* Hartman, 1978 (Polychaeta: Helmetophoridae) and its transfer to the Flabelligeridae." *Proceedings of the Biological Society of Washington* 104(4): 684–687.

Gonzalez, Brett C., Alejandro Martínez, Katrine Worsaae, and Karen J. Osborn. 2021. "Morphological Convergence and Adaptation in Cave and Pelagic Scale Worms (Polynoidae, Annelida)." *Scientific Reports* 11(1): 10718.

Grube, Adolf Eduard. 1850. "Die Familien der Anneliden." *Archiv für Naturgeschichte, Berlin.* 16(1): 249-364.

Grube, A.E. 1873. "Die Familie der Cirratuliden." *Jahres-Bericht der Schlesischen Gesellschaft für vaterländische Cultur, Breslau.* 50: 59-66.

Guindon S. and O. Gascuel. 2003. "A simple, fast and accurate method to estimate large phylogenies by maximum-likelihood". *Systematic Biology* 52: 696-704.

Hahn, C., Lutz Bachmann, and Bastien Chevreux. 2013. "Reconstructing mitochondrial genomes directly from genomic next-generation sequencing reads - A baiting and iterative mapping approach." *Nucleic Acids Research* 41(13): e129. doi.org/10.1093/nar/gkt371.

Halanych, Kenneth M., L. Nicole Cox, and Torsten H. Struck. 2007. "A Brief Review of Holopelagic Annelids." *Integrative and Comparative Biology* 47(6): 872–79.

Hartman, Olga. 1965. "Deep-water benthic polychaetous annelids off New England to Bermuda and other North Atlantic areas." *Occasional Papers of the Allan Hancock Foundation.* 28: 1-384.

Hartman, Olga. 1978. "Polychaeta from the Weddell Sea quadrant, Antarctica." *Antarctic Research Series.* 26(4): 125-223.

Hollingsworth Jr, Phillip R., Andrew M. Simons, James A. Fordyce, and C. Darrin Hulsey. 2013. "Explosive Diversification Following a Benthic to Pelagic Shift in Freshwater Fishes." *BMC Evolutionary Biology* 13(1): 272.

Jimi, Naoto, Shinta Fujimoto, and Satoshi Imura. 2020. “A New Interstitial Genus and Species of Acrocirridae from Okinawa-Jima Island, Japan.” *Zoosymposia* 19(1): 164–72. doi.org/10.11646/zoosymposia.19.1.17.

Katoh, Kazutaka and Daron M. Standley. 2013. “MAFFT Multiple Sequence Alignment Software Version 7: Improvements in Performance and Usability.” *Molecular Biology and Evolution* 30(4): 772–780. doi.org/10.1093/molbev/mst010.

Kearse, M., R. Moir, A. Wilson, S. Stones-Havas, M. Cheung, S. Sturrock, S. Buxton, A. Cooper, S. Markowitz, C. Duran, T. Thierer, B. Ashton, P. Meintjes, and A. Drummond. 2012. “Geneious Basic: an integrated and extendable desktop software platform for the organization and analysis of sequence data.” *Bioinformatics* 28(12): 1647-1649. doi: 10.1093/bioinformatics/bts199.

Kirkegaard, J.B., 1982. New records of abyssal benthic polychaetes from the Polar Sea. *Steenstrupia* 8: 253–260.

Kozlov, Alexey M., Diego Darriba, Tomáš Flouri, Benoit Morel, and Alexandros Stamatakis. 2019. “RAxML-NG: A fast, scalable, and user-friendly tool for maximum likelihood phylogenetic inference.” *Bioinformatics* 35(21): 4453-4455. doi:10.1093/bioinformatics/btz305.

Lamarck, J.B. 1818. “Histoire naturelle des Animaux sans Vertèbres, présentant les caractères généraux et particuliers de ces animaux, leur distribution, leurs classes, leurs familles, leurs genres, et la citation des principales espèces qui s'y rapportent; precedes d'une Introduction offrant la determination des caracteres essentiels de l'Animal, sa distinction du vegetal et desautres corps naturels, enfin, l'Exposition des Principes fondamentaux de la Zoologie.” *Paris, Deterville.* 5: 612: biodiversitylibrary.org/page/12886879.

Laslett, D. and B. Canbäck. 2008. “ARWEN: A program to detect tRNA genes in metazoan mitochondrial nucleotide sequences.” *Bioinformatics* 24(2): 172–175. doi.org/10.1093/bioinformatics/btm573.

Laubier, L. 1974. “*Chauvinelia biscayensis* gen. sp. nov., un Flabelligeridae (annélide polychète sédentaire) aberrant de l'étage abyssal du Golfe de Gascogne.” *Bulletin de la Société Zoologique de France.* 99(3): 391-399.

Lei, Lei, and Zachary F. Burton. 2020. “Evolution of Life on Earth: TRNA, Aminoacyl-TRNA Synthetases and the Genetic Code.” *Life (Basel)* 10(3): 21.

Leigh, Jessica W. and David Bryant. 2015. “POPART: Full-Feature Software for Haplotype Network Construction.” *Methods in Ecology and Evolution* 6(9): 1110–1116. doi: 10.1111/2041-210X.12410.

Li, D., R. Luo, C. M. Liu, C. M. Leung, H. F. Ting, K. Sadakane, H. Yamashita, and T. W. Lam. (2016). “MEGAHIT v1.0: A fast and scalable metagenome assembler driven by

advanced methodologies and community practices." *In Methods* 102: 3–11. doi.org/10.1016/j.ymeth.2016.02.020.

Li, H. 2018. "Minimap2: Pairwise alignment for nucleotide sequences." *Bioinformatics* 34(18): 3094–3100. doi.org/10.1093/bioinformatics/bty191.

Lindgren, Annie R., Molly S. Pankey, Frederick G. Hochberg, and Todd H. Oakley. 2012. "A Multi-Gene Phylogeny of Cephalopoda Supports Convergent Morphological Evolution in Association with Multiple Habitat Shifts in the Marine Environment." *BMC Evolutionary Biology* 12: 129.

Maddison, W. P. and D. R. Maddison. 2023. "Mesquite: a modular system for evolutionary analysis." Version 3.80. http://www.mesquiteproject.org.

Orensanz, J. M. 1974. "Poliquetos de la provincia biogeografica Argentina. X. Acrocirridae." *Neotropica.* 20(63): 113– 118.

Osborn, K. J. and G. W. Rouse. 2008. "Multiple Origins of Pelagicism within Flabelligeridae (Annelida)." *Molecular Phylogenetics and Evolution* 49(1): 386–92.

Osborn, K. J. and G. W. Rouse. 2011. "Phylogenetics of Acrocirridae and Flabelligeridae (Cirratuliformia, Annelida)." *Zoologica Scripta* 40(2): 204– 219. doi.org/10.1111/j.1463-6409.2010.00460.x.

Osborn, K. J., S. H. D. Haddock, F. Pleijel, L. P, Madin, G. W. Rouse. 2009. "Deep-sea, swimming worms with luminescent 'bombs'." *Science* 325: 964. doi.org/10.1126/science.1172488.

Osborn, K. J., L. P. Madin, & G. W. Rouse. 2011a. "The remarkable Squidworm is an example of discoveries that await in deep, pelagic habitats." *Biology Letters* 7:449– 453. doi.org/10.1098/rsbl.2010.0923.

Osborn, K. J., S. H. D. Haddock, & G. W. Rouse. 2011b. "*Swima* (Annelida, Acrocirridae), holopelagic worms from the deep Pacific." *Zoological Journal of the Linnean Society* 163(3): 663-678. doi.org/10.1111/j.1096-3642.2011.00727.x.

Palumbi, Stephen R. 1996. "Nucleic Acids II: The Polymerase Chain Reaction." Pp. 205–247 in *Molecular Systematics*, edited by D. M. Hillis, C. Moritz, and B. K. Mable. Sunderland: Sinauer & Associates Inc.

Pante, Eric and Benoit Simon-Bouhet. 2013. "marmap: A package for importing, plotting and analyzing bathymetric and topographic data in R." *PLOS One* 8(9). doi.org/10.1371/journal.pone.0073051.

Perna, Nicole T. and T. D. Kocher. 1995. “Patterns of nucleotide composition at fourfold degenerate sites of animal mitochondrial genomes.” *Journal of Molecular Evolution* 41: 353-358.

Rambaut, A. 2009. “FigTree: Tree Figure Drawing Tool.” Available at: http://tree.bio.ed.ac.uk/software/figtree/.

Rambaut, Andrew, Alexei J. Drummond, Dong Xie, Guy Baele, and Marc A. Suchard. 2018. “Posterior Summarization in Bayesian Phylogenetics Using Tracer 1.7.” *Systematic Biology* 67 (5): 901–4. doi.org/10.1093/sysbio/syy032.

Ronquist, Fredrik, Maxim Teslenko, Paul van der Mark, Daniel L. Ayres, Aaron Darling, Sebastian Höhna, Bret Larget, Liang Liu, Marc A. Suchard, and John P. Huelsenbeck. 2012. “MrBayes 3.2: Efficient Bayesian Phylogenetic Inference and Model Choice across a Large Model Space.” *Systematic Biology* 61(3): 539–42. doi.org/10.1093/sysbio/sys029.

Rouse, G. W. 2022. Chapter 60. *Acrocirridae*. In *Annelida*. G. W. Rouse, F. Pleijel, & E. Tilic. Oxford University Press, Oxford, New York. Pages: 253-257. In print.

Rouse, G. W. and F. Pleijel. 2001. *Polychaetes*. Oxford University Press. In print.

Rouse, Greg W., and Fredrik Pleijel. 2003. “Problems in Polychaete Systematics.” *Hydrobiologia* 496(1–3): 175–89.

Ryckholt, Philippe de (Baron). (1851). “Mélanges paléontologiques. Part 1.” *Memoires Couronnes et Memoires des Savants Etrangers de l'Academie Royale des Sciences, des Lettres et des Beaux-Arts de Belgique.* 24: 1-176.

Saint-Joseph, A. de, 1894. “Les annélides polychètes des côtes de Dinard, troisième partie (Nephtydiens–Serpuliens).” *Annales des Sciences Naturelles, Zoologie, 8ème Série,* 17: 1–395.

Salazar-Vallejo, Sergio I., Patrick Gillet, and Luis F. Carrera-Parra. 2007. “Revision of *Chauvinelia*, Redescriptions of *Flabelliseta incrusta*, and *Helmetophorus rankini*, and Their Recognition as Acrocirrids (Polychaeta: Acrocirridae).” *Journal of the Marine Biological Association of the United Kingdom* 87(2):465–477. doi.org/10.1017/S0025315407054501.

Salazar-Vallejo, Sergio I. and A. E. Zhadan. 2007. “Revision of *Buskiella* McIntosh, 1885 (including *Flota* Hartman, 1967), and description of its trifid organ (Polychaeta: Flotidae).” *Invertebrate Zoology* 4(1): 65-82.

Sahyoun, Abdullah H., Matthias Bernt, Peter F. Stadler, and Kifah Tout. 2014. “GC Skew and Mitochondrial Origins of Replication.” *Mitochondrion* 17: 56–66.

Shen, Xuejuan, Zhiqing Pu, Xiao Chen, Robert W. Murphy, and Yongyi Shen. 2019. "Convergent Evolution of Mitochondrial Genes in Deep-Sea Fishes." *Frontiers in Genetics* 10: 925.

Struck, Torsten H., Anja Golombek, Christoph Hoesel, Dimitar Dimitrov, and Asmaa Haris Elgetany. 2023. "Mitochondrial Genome Evolution in Annelida - A Systematic Study on Conservative and Variable Gene Orders and the Factors Influencing Its Evolution." *Systematic Biology*. https://doi.org/10.1093/sysbio/syad023.

Struck, Torsten H., Günter Purschke, and Kenneth M. Halanych. 2006. "Phylogeny of Eunicida (Annelida) and Exploring Data Congruence Using a Partition Addition Bootstrap Alteration (PABA) Approach." *Systematic Biology* 55(1): 1-20. doi.org/10.1080/10635150500354910.

Swofford, David L. 2002. "Phylogenetic Analysis Using Parsimony." *Options* 42(2):294–307.

Vaidya, G., D. J. Lohman, and R. Meier. 2011. "SequenceMatrix: concatenation software for the fast assembly of multi-gene datasets with character set and codon information." *Cladistics* 27(2): 171–180. doi.org/10.1111/j.1096-0031.2010.00329.x.

Weigert, Anne, Anja Golombek, Michael Gerth, Francine Schwarz, Torsten H. Struck, and Christoph Bleidorn. 2016. "Evolution of mitochondrial gene order in Annelida." *Molecular Phylogenetics and Evolution* 94: 196-206.

Weigert, A. and C. Bleidorn. 2016. "Current status of annelid phylogeny." *Organisms Diversity & Evolution* 16: 345-362.

Whiting, Michael F., James C. Carpenter, Quentin D. Wheeler, and Ward C. Wheeler. 1997. "The Stresiptera Problem: Phylogeny of the Holometabolous Insect Orders Inferred from 18S and 28S Ribosomal DNA Sequences and Morphology." *Systematic Biology* 46(1): 1. doi: 10.2307/2413635.

Wiens, J. J. 2004. "The Role of Morphological Data in Phylogeny Reconstruction." *Systematic Biology* 53(4): 653-661.

Yang, Mei, Lin Gong, Jixing Sui, and Xinzheng Li. 2019. "The Complete Mitochondrial Genome of *Calyptogena Marissinica* (Heterodonta: Veneroida: Vesicomyidae): Insight into the Deep-Sea Adaptive Evolution of Vesicomyids." *PloS One* 14(9): e0217952.

Yu, Yan-Qin, Xiao-Li Liu, Hua-Wei Li, Bo Lu, Yu-Peng Fan, and Jin-Shu Yang. 2016. "The Complete Mitogenome of the Atlantic Hydrothermal Vent Shrimp *Rimicaris Exoculata* Williams & Rona 1986 (Crustacea: Decapoda: Alvinocarididae)." *Mitochondrial DNA. Part A, DNA Mapping, Sequencing, and Analysis* 27(5): 3115–17.

Zhang, Bo, Yan-Hong Zhang, Xin Wang, Hui-Xian Zhang, and Qiang Lin. 2017. "The Mitochondrial Genome of a Sea Anemone *Bolocera* sp. Exhibits Novel Genetic

Structures Potentially Involved in Adaptation to the Deep-Sea Environment." *Ecology and Evolution* 7(13): 4951–62.

Zhang, Yanjie, Jin Sun, Greg W. Rouse, Helena Wiklund, Fredrik Pleijel, Hiromi K. Watanabe, Chong Chen, Pei-Yuan Qian, and Jian-Wen Qiu. 2018. "Phylogeny, Evolution and Mitochondrial Gene Order Rearrangement in Scale Worms (Aphroditiformia, Annelida)." *Molecular Phylogenetics and Evolution* 125: 220–31.